

# Performance Evaluation of Coordinated Beamforming in LTE-Advanced Systems

Von der Fakultät für Elektrotechnik und Informationstechnik der Rheinisch-Westfälischen Technischen Hochschule Aachen zur Erlangung des akademischen Grades eines Doktors der Ingenieurwissenschaften genehmigte Dissertation

vorgelegt von

Diplom-Ingenieur  
Benedikt Martin Wolz

aus Landshut

Berichter: Universitätsprofessor Dr.-Ing. Bernhard Walke  
Universitätsprofessor Dr.-Ing. Christian Wietfeld

Tag der mündlichen Prüfung 06.02.2014



# Abstract

---

In telecommunications, new application areas in social, private and business sector are developing, such as eHealth, Connected Car, Mobile Payment, Smart Energy, Cloud Media, Maschine-2-Maschine communication. The new services will demand the Internet to be available everywhere and will contribute to the current exponential growth in data traffic. In wireless communication systems such as IMT-Advanced systems, key features to increase mean spectral efficiencies are integrating multi antenna techniques and mitigating inter-cell interference by coordination. On the one hand, beamforming is the most promising MIMO technique in macro cell scenarios since it allows for both increased system capacity and extended cell range. On the other hand, coordination of neighbour cells can further improve beamforming by overcoming the so called *flash light* effect and mitigating inter-cell interference by avoiding harmful beam combinations. In this thesis, a beam coordination algorithm is designed called "Synchronised Cycles of Coordinated Beams" which aims to achieve ubiquitous high rate coverage by reducing interference, especially at the cell edge. Several coordinated beamforming schemes are discussed and evaluated such as the coordination of cells of the same base station, the coordination in systems with adaptive beamforming using multiple beams (SDMA), and region coordination. Beam coordination schemes are quantitatively analytically evaluated on system level in cellular scenario in the framework of the ITU-R evaluation guidelines, the LTE-Advanced standard and detailed models of beamforming techniques. The evaluation model comprises a detailed antenna and channel model and considers MAC and PHY layer functions, such as link adaptation, error recovery, and protocol overhead. Important parameters of system configurations are identified and their impact on the performance of beam coordination is studied, such as the scheduling strategy,

## Abstract

frequency reuse scheme, and number of available beams. The results can assist operators and manufacturers to decide under which circumstances beam coordination schemes can be employed most beneficially in terms of cell spectral efficiency and cell edge user spectral efficiency.

# Kurzfassung

---

In der Telekommunikation, entstehen neue Dienstleistungen im sozialen, privaten und geschäftlichen Bereich, wie elektronische Gesundheit, verbundene Fahrzeuge, mobiles Bezahlen, intelligente Energieversorgung, Medien aus der Wolke, oder Kommunikation zwischen Maschinen. Die neuen Anwendungen benötigen ein überall verfügbares Internet und werden zum aktuellen exponentiellen Wachstum des Datenverkehrs beitragen. Der Schlüssel zu höherer benötigter spektraler Effizienz in Funksystemen wie IMT-Advanced ist die Integration von Mehrfachantennen-Techniken und Reduzierung der Interzell-Interferenz durch Koordination von benachbarten Basisstationen. Auf der einen Seite ist Strahlformung, sogenanntes Beamforming, die vielversprechendste MIMO-Technik in Makrozell-Szenarien, da erhöhte Systemkapazität und erweiterte Funkzellen ermöglicht werden. Auf der anderen Seite kann die Koordinierung von Nachbarzellen die Leistungsfähigkeit von Strahlformungstechniken weiter verbessern indem schädliche Strahlkombination in Nachbarzellen, der sogenannte Flash-Light-Effect, vermieden und die Interzell-Interferenz reduziert wird. In dieser Arbeit, wird ein Algorithmus mit dem Namen "Synchron Cycles of Coordinated Beams" für die Strahlen-Koordinierung entworfen. Dieser ermöglicht eine allgegenwärtige hohe Datenrate durch Verringerung von Interferenz, vor allem am Zellerand. Weitere Methoden der Strahlen-Koordinierung in Mobilfunknetzen werden entwickelt und bewertet: wie die Strahlen - Koordinierung von Zellen einer Basisstation, die adaptive Strahlen-Koordinierung mit parallel übertragenen Datenströmen (SDMA) einschließlich der Strahlen-Koordinierung unter Berücksichtigung von Regionen. Methoden der Strahlen-Koordinierung werden quantitativ auf Systemebene in zellularen Szenarien analytisch bewertet unter Berücksichtigung der ITU-R Bewertungsrichtlinien, des LTE-Advanced-

## Kurzfassung

Standards und detaillierter Modelle von Strahlen-Techniken. Das zur Auswertung verwendete Modell beinhaltet ein detailliertes Antennen- und Kanalmodell und berücksichtigt MAC und PHY-Schicht-Funktionen wie Ratenanpassung, Fehlerkorrektur und Protokolloverhead. Wichtige Parameter der Systemkonfiguration werden bestimmt und ihre Auswirkungen auf die Leistung der Strahlen-Koordinierung untersucht, wie die Strategie der Ressourcenvergabe, der Art der Frequenzwiederverwendung und die Anzahl der verfügbaren Strahlen. Die gezeigten Ergebnisse können Betreibern und Hersteller helfen zu entscheiden, unter welchen Umständen Strahlen-Koordination am vorteilhaftesten eingesetzt werden kann um die mittlere spektrale Effizienz und die am Zellrand zu steigern.

# Contents

---

Abstract .....	3
Kurzfassung.....	5
Contents .....	7
1 Introduction .....	13
1.1 Motivation .....	13
1.2 Objectives .....	14
1.3 Contributions of This Thesis.....	14
1.4 Outline .....	15
2 LTE / LTE-Advanced Radio Access.....	17
2.1 Introduction .....	17
2.1.1 Previous Generation of Mobile Communication.....	17
2.1.2 The Mobile Radio Landscape .....	18
2.1.3 3GPP Standardisation.....	19
2.1.4 IMT-Advanced .....	20
2.2 Architecture Overview .....	21
2.2.1 The Core Network (CN) - EPC.....	22
2.2.2 The Access Network (E-UTRAN) .....	24
2.3 Radio Access Protocol Architecture.....	24
2.3.1 Radio Resource Control (RRC).....	26
2.3.2 The Packet Data Convergence Protocol (PDCP).....	27
2.3.3 Radio Link Control (RLC).....	27

# Contents

2.3.4	Logical Channels .....	28
2.3.5	Medium Access Control (MAC).....	29
2.3.6	Transport Channels.....	32
2.3.7	Physical Layer (PHY).....	33
2.3.8	Physical Channels.....	38
2.4	Quality of Service and EPS Bearers .....	40
2.5	Components introduced by LTE-Advanced .....	40
2.6	Load and Interference Management Over X2 E-UTRAN Network Interface .....	41
2.6.1	Inter-Cell Interference Coordination Signalling in Downlink .....	42
2.6.2	Inter-Cell Interference Coordination Signalling in Uplink	43
2.6.3	Enhanced Inter-Cell Interference Coordination in LTE- Advanced.....	43
2.7	Coordinated Multipoint (CoMP) Transmission in LTE- Advanced .....	44
3	MIMO Techniques.....	47
3.1	Introduction.....	47
3.2	Comments and Technique Choice.....	48
3.3	Model of Beamformer According to Godara 1997 .....	50
3.3.1	Conventional Beamformer .....	53
3.3.2	Zero Forcing Beamformer .....	53
3.3.3	Optimal Beamformer .....	54
3.3.4	Optimal Beamformer with Reference Signal .....	56
3.3.5	Spatial Filtering for Interference Reduction.....	57
3.3.6	Spatial Division Multiple Access (SDMA).....	58

3.4	Fixed Beamforming.....	59
3.5	Open- versus Closed-Loop MIMO.....	60
4	The Model of the Analytical Evaluation and the IMT-Advanced Channel .....	61
4.1	Introduction .....	61
4.2	ITU-R Evaluation Guidelines.....	62
4.2.1	Deployment Scenarios.....	63
4.2.2	Antenna Model.....	65
4.2.3	Antenna Model with Beamforming.....	67
4.3	Radio Channel Model.....	68
4.3.1	Pathloss Model .....	68
4.3.2	Line-of-sight Propagation Probability.....	69
4.3.3	Overview of the System Level Evaluation Model .....	70
4.3.4	Receive Power and Signal to Interference Plus Noise Ratio .....	72
4.3.5	Link Permutation Probability .....	73
4.3.6	Beam Permutation Probability .....	74
4.3.7	Mean SINR and Probability of SINR.....	76
4.4	Channel Model Validation.....	78
4.5	Link-to-System Model .....	80
4.5.1	Link-to-System-Level Mapping .....	80
4.5.2	Mean Data Rate and Probability of Data Rate .....	83
4.5.3	Distribution of Number of MSs per Cell.....	84
4.5.4	Scheduling Strategies and Probability of MS Throughput.....	85
4.5.5	Cell Spectral Efficiency (CSE).....	86
4.5.6	Cell Edge - User Spectral Efficiency (CE-USE) .....	87

## Contents

4.6	LTE-Advanced System-Level Validation .....	87
5	Inter-cell Interference Coordination.....	89
5.1	Frequency Reuse Schemes .....	90
5.2	Coordinated Beamforming Schemes.....	92
5.3	Coordination for Adaptive Beamforming with SDMA .....	95
5.3.1	Coordination for Adaptive Beamforming with SDMA - Scheme I.....	96
5.3.2	Region Coordination for Adaptive Beamforming with SDMA - Schemes II and III .....	101
5.4	Synchronised Cycles of Coordinated Beams (CyBeamCo)..	106
5.4.1	Cell Type Specific Beam Coordination.....	107
5.4.2	Algorithm for Seeking Beneficial Fixed Beam Combinations .....	109
5.4.3	Beam Coordination under SFR.....	112
5.4.4	Beam Coordination of Cells of the Same Site .....	112
5.4.5	Fair Evaluation of the Coordination Algorithm.....	113
5.4.6	Creation of a Coordination Matrix in a Real System .....	114
5.4.7	Dynamic Beam Coordination – An Outlook.....	115
6	Analytical Performance Evaluation .....	117
6.1	Beam Coordination Performance versus other System Types	118
6.2	Impact of Scheduling Strategies on Beam Coordination Performance.....	123
6.3	SFR - Derivation of an Operating Point .....	126
6.3.1	Different Scheduling Strategies Operated under SFR.....	126
6.3.2	Different System Types Operated under SFR.....	128
6.4	Impact of Frequency Reuse Schemes on Beam Coordination Performance.....	130

6.5	Impact of the Codebook Size on Beam Coordination Performance .....	134
7	Conclusion and Outlook .....	139
A	Additional Results .....	141
A.1	Example Coordination Matrices.....	144
B	Performance Evaluation of CB for adaptive BF with SDMA (Scheme I) - Assumptions and Results.....	147
B.1	Simulation Scenario .....	147
B.1.1	Simulator and Traffic Model .....	148
B.1.2	Link Adaptation and Error Modelling.....	149
B.1.3	WiMAX Frame Structure and Overhead .....	149
B.1.4	Other Simulation Parameters .....	150
B.2	Simulation Results.....	151
B.3	Conclusion.....	154
C	Performance Evaluation of Region Coordination for Adaptive BF with SDMA (Scheme II and III) - Assumptions and Results .....	157
C.1	Simulation Results.....	157
C.1.1	Constant Bit Rate Downlink Traffic with 30 MSs.....	157
C.1.2	Variable Bit Rate Uplink Traffic .....	160
C.2	Conclusion.....	162
	List of Figures.....	165
	List of Tables.....	171
	List of Abbreviations .....	173
	Bibliography .....	177
	Acknowledgement.....	185



# CHAPTER 1

---

## Introduction

Integrating mobile Internet into everybody's life is not a vision but it is partly reality today. Statistically every second person in Europe and the US has a smart phone, with increasing tendency. Future mobile communication networks are required to enable the Internet to be accessible from everywhere, as the all-encompassing communications platform enabling ubiquitous computer based applications. The performance of upcoming radio networks will enable new application areas in social, private and business sector, such as eHealth, Connected Car, Mobile Payment, Smart Energy, Cloud Media, Maschine-2-Maschine communication. These services will further increase the need for a higher bit rate in wireless systems.

### 1.1 Motivation

Latest wireless communication systems such as IMT<sup>1</sup>-Advanced systems promise to provide a data rate of 100Mbps with a peak data rate of 1Gbps. Besides a higher rate, providing homogeneous high rate coverage is equally important as it guarantees constant user experience over the served area and is a key enabler to an increased average spectral efficiency of a system. A higher data rate in cellular networks can be achieved by three measures, (1) enlarging system bandwidth, (2) increasing mean cell density, and (3) improving spectral efficiency. This work focuses on two questions: how can inter-cell coordinated beamforming increase spectral efficiency and achieve ubiquitous high rate coverage? Hence, beam coordination schemes are studied in an

---

<sup>1</sup> International Mobil Telecommunications

LTE<sup>2</sup>-Advanced deployment, which is the prevailing technology for IMT-Advanced systems.

## 1.2 Objectives

In this thesis, coordination schemes are designed in order to improve ordinary beamforming techniques by overcoming the so called *flash light* effect and mitigated inter-cell interference by coordinating neighbour cells. Potential performance improvements are shown based on analytical evaluations on system level in a quantitative manner in the framework of the ITU-R<sup>3</sup> evaluation guidelines and the LTE-Advanced standard. Reproducibility of the results and intelligibility of the model are provided by presenting surveys of Multiple Input Multiple Output (MIMO) techniques, evaluation guidelines and the 3GPP<sup>4</sup> standard, the latter with focus on the support of beamforming and coordination techniques where possible. The results should help operators and manufactures to decide under which circumstances beam coordination schemes can be employed most beneficially in terms of cell capacity and coverage.

## 1.3 Contributions of This Thesis

The key contribution of the work is the development of a beam coordination schemes for interference mitigation and it's quantitative analytical evaluation on system level in terms of system capacity and cell edge coverage in cellular scenarios. Therefore an evaluation tool has been implemented which comprises detailed antenna and channel models and deployment scenarios according to the ITU-R evaluation guidelines for IMT-Advanced systems. The tool considers Medium Access Control (MAC) and Physical layer (PHY) functions, such as link adaptation, error control, and protocol overhead according to the LTE-

---

<sup>2</sup> Long Term Evolution

<sup>3</sup> The International Telecommunication Union – Radio Communication Sector

<sup>4</sup> The Third Generation Partnership

Advanced standard. Results gained by the tool are compared to results provided by an event driven stochastic system-level simulator and are found to match each other well.

The work provides an outline of the state of the art of beamforming coordination schemes and summarizes the LTE-Advanced standard, with a focus on beamforming and coordination support and parts relevant for the evaluation. An overview of MIMO techniques is given. Scenarios are identified where beamforming and beamforming coordination are superior to other MIMO-techniques. A qualitative comparison is provided between the characteristics and advantages of a fixed beam coordination method developed in this work and coordination schemes using multiple beams (SDMA) and adaptive beamforming. For an initially developed semi-static coordination scheme, an extension is outlined which dynamically adapts to bursty traffic and non-uniformly distributed user positions.

Additional important parameters of the system configuration are identified and their impact on the beam coordination performance is studied. The evaluation results confirm that beam coordination schemes significantly outperform ordinary beamforming for all studied parameters such as scheduling strategy, reuse scheme, and number of beams, independent of whether all cells in a multi-site scenario or cells only of one site are coordinated. Results reveal that scheduling strategies and reuse schemes trade fairness against cell capacity, whereas beam coordination improves both at the same time. Findings show in detail the limitations of the current standards in supporting MIMO-techniques and especially Coordinated Multi Point (CoMP)-schemes since they lack measures for transforming increased Signal-to-Interference plus Noise Ratio (SINR) into a higher data rate. Studies of the Soft Frequency Reuse (SFR) scheme derive an optimal operating point in terms of effective reuse factor and expose its dependency on other parameters such as the scheduling strategy.

## **1.4 Outline**

This thesis is organized as follows:

## 1 Introduction

Chapter 2 summarizes the 3GPP standard LTE (Release 8 and 9) and new features of LTE-Advanced (Release 10). An architecture overview is given by drawing the functional line between core network (EPC) and the access network (E-UTRAN). The radio access protocol stack is sketched with focus on parts relevant for this work. The description of how the standard supports MIMO-schemes, coordination interfaces and CoMP-schemes ends the chapter.

Chapter 3 gives a brief survey of MIMO techniques before the model and algorithms of beamforming are explained including required channel state feedback. It also reasons the choice of the studied beamforming techniques.

Chapter 4 describes the analytical evaluation tool and the IMT-Advanced channel model. The evaluation procedure is described as well as how the different models of antenna characteristic, path loss, link-to-system-level mapping, signalling overhead, etc. are integrated to the system under study. A validation of the channel model is provided as well as a validation on system level.

Chapter 5 discusses the coordination of inter-cell interference and first defines frequency reuse schemes (i.e., *reuse one*, *reuse three* and SFR) as their simplest representation. Second, beamforming coordination schemes are put in the context of CoMP transmission and reception schemes. Coordination schemes for adaptive beamforming allowing for multiple streams are discussed. The developed scheme of synchronised cycles of coordinated beams is introduced. It is shown how fixed beams of the 3GPP precoding codebook are employed and how the scheme targets to mitigate interference especially at the cell edge. The designed scheme is shown to be applicable for coordination of cells of the same site, too.

Chapter 6 presents the analytical results generated by the evaluation tool. Results of coordination enabled systems are compared to results of two reference systems under different system configurations such as scheduling strategy, frequency reuse schemes, and number of beams.

Chapter 7 provides a summary of main findings and major results and proposes work to be done in the future.

## CHAPTER 2

---

# LTE / LTE-Advanced Radio Access

## 2.1 Introduction

This Chapter outlines the 3GPP system proposal *LTE-Advanced*. LTE-Advanced is initiated by 3GPP Release 10 which bases on LTE defined by 3GPP Release 8 and 9. In the following, LTE is described and the amendments of Release 10 are sketched. Release 8 and 9 meets many of the requirements set by the ITU-R for IMT-Advanced systems. Release 10 matches all ITU-R requirements and surpasses them in several aspects. LTE has been designed to purely support packet-switched services different from the 3G systems which also support circuit-switched service. LTE provides seamless Internet Protocol (IP) connectivity between User Equipment (UE) and the Packet Data Network (PDN), without any disruption to end users' mobile applications.

Before LTE and LTE-Advanced standards are outlined, the next Subsection highlights history, landscape, and standardisation process, as well as the IMT-Advanced framework.

### 2.1.1 Previous Generation of Mobile Communication

LTE-Advanced (i.e. 3GPP Release 10 and 11) also called fourth generation of mobile radio networks, is the latest technological step in a rather evolutionary development of mobile telecommunication standards. Despite new features introduced by Release 10 and 11 several technologies are inherited from previous generations.

Commercial wireless phone calls were enabled by the first generation (1G) of analogue mobile radio networks. Different technologies were

regionally deployed starting from the 1980s. Exemplary technologies are EIA-553 AMPS (Advanced Mobile Phone System) used in North America and Australia, C-450 in West Germany, Australia, Portugal and South Africa. The Second Generation (2G) of mobile radio networks was the first full digital system also providing SMS and data services. Among different techniques used in 2G systems, GSM was the only one globally deployed starting from the 1990s, using Time Division Multiple Access (TDMA) and Frequency Division Multiple Access (FDMA). With *General Packet Radio Service* (GPRS), a packet switched service was introduced in 2001 to GSM and link adaptation in 2005 called *Enhanced Data Rates for GSM Evolution* (EDGE) providing internet access with adaptable data rate up to 284 kbit/s. *Universal Mobile Telecommunications System* (UMTS) is the most prominent 3G system, deployed from 2005 on, utilizing Code Division Multiple Access (CDMA). Peak data rates have been successively improved from 384 kbit/s to 28 Mbit/s with HSPA (3.75G). Nevertheless, CDMA based systems were found to be unable to further increase mobile data rate. Long Term Evolution (LTE), sometimes referred to as 3.9G, bases on OFDMA and multi antenna support. It achieves a data rate up to 300 Mbit/s in downlink. LTE was firstly deployed around 2010. LTE-Advanced being the first purely packet switched system supports carrier aggregation, enhanced multi antenna support, relaying, and advanced inter-cell interference coordination and targets a peak downlink data rate of 1 Gbit/s. A first LTE-Advanced system was deployed in 2013 in Moscow. [Sesia, 2010]

### 2.1.2 The Mobile Radio Landscape

Figure 2.1 depicts the approximate timeline of mobile communications standards. The figure also shows the 3GPP release number corresponding to technology name and to the generation of mobile communication standards. Exemplarily, LTE-Advanced inhabits Releases 10 and 11 and is of fourth generation (4G). Other standards like the ones shown of IEEE and 3GPP2 stopped evolution from 2007 on or converged to 3GPP standardization.

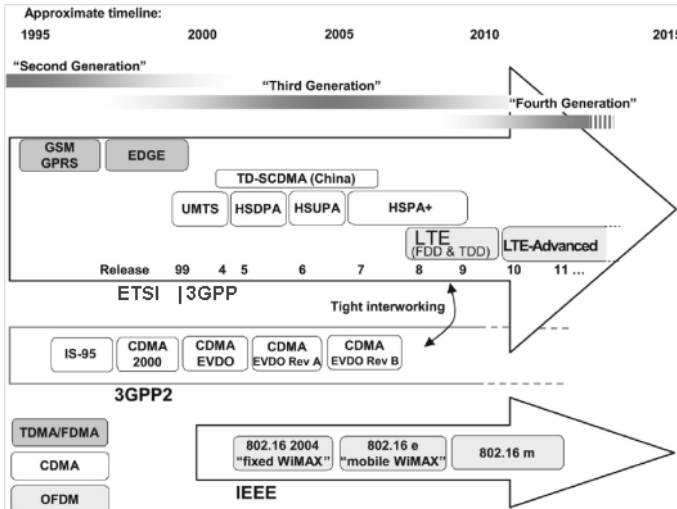


Figure 2.1: approximated timeline of mobile communication standards [Sesia, 2010]

### 2.1.3 3GPP Standardisation

The 3GPP founded in 1999 unites telecommunications standard organizations from China, Europe, Japan, Korea, and North America and aims for generating global standards for mobile telecommunication systems. The 3GPP specification work is done in four *Technical Specification Groups* (TSGs): *Radio Access Networks* (RAN), *Service & Systems Aspects* (SA), *Core Network & Terminals* (CT) and *GSM EDGE Radio Access Networks* (GERAN). A TSG comprises a set of Working Groups (WGs) responsible for specific aspects as shown in Figure 2.2. These WGs make decisions only by consensus without a dissident vote. Besides the quest for a technically optimal solution (for example in terms of simplicity, efficiency, robustness, low CAPEX and OPEX), 3GPP participating companies try to include own IPR in the standards aiming for license business.

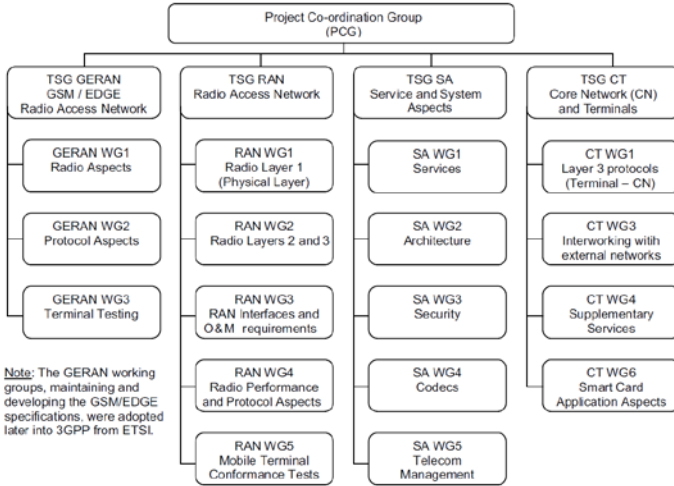


Figure 2.2: 3GPP working group structure

### 2.1.4 IMT-Advanced

The ITU-R beside others synchronise worldwide spectrum allocation for IMT-Advanced systems and define requirements [ITU-R M.2134] for candidate technologies instead of dedicating spectrum to a specific technology as applied in the past before the IMT-2000 initiative. The ITU define detailed guidelines [ITU-R M.2135] and a spatial channel model for evaluating IMT-Advanced compliant technologies. The guidelines serve as de facto framework for future standards which were followed by both 3GPP and IEEE standardization bodies with their individual members during their self evaluation. More details about the guidelines and the channel model are presented in Section 4.2 and Section 4.3, respectively. The 3GPP system proposal accepted as IMT-Advanced systems is outlined in the next Sections.

IMT-Advanced systems are mobile systems which provide access to a wide range of telecommunication services, support low to high mobility applications, and a wide range of data rates according to user and service demands in multiple user environments. Requirements of IMT-Advanced system target supporting high-quality multimedia

applications and providing a significant improvement in performance and quality of service compared to 3G systems. In order to support advanced services and applications, peak data rates of 100 Mbit/s for high and 1 Gbit/s for low mobility users were established as targets for research.

## 2.2 Architecture Overview

While the term ‘LTE’ describes the evolution of the radio access through the Evolved-UTRAN (E-UTRAN<sup>5</sup>), it is accompanied by an evolution of the non-radio aspects under the term ‘System Architecture Evolution’ (SAE) which includes the Evolved Packet Core (EPC) network. Together LTE and SAE comprise the Evolved Packet System (EPS). EPS provides the user with IP connectivity to a PDN for accessing the Internet, as well as for running services such as VoIP. An EPS bearer is typically associated with a QoS class. Multiple bearers can be established for a user in order to provide different QoS streams or connectivity to different PDNs. The network must also provide sufficient security and privacy for the user and protection for the network against fraudulent use.

Figure 2.3 shows the overall network architecture including network elements and standardized interfaces. All these features are supported by means of several EPS network elements with different roles. At a high level, the network comprises the core network (CN) (i.e. EPC) and the access network (i.e. E-UTRAN). While the CN consists of many logical nodes, the access network is made up of essentially one node type, the evolved NodeB<sup>6</sup> (eNB), which connects the UEs. Each of these network elements is inter-connected by means of standardized interfaces in order to allow multivendor interoperability. The functional split between the EPC and E-UTRAN is shown in

---

<sup>5</sup> Universal Terrestrial Radio Access Network (UTRAN)

<sup>6</sup> In the following, instead of the 3GPP terms *eNB* and *UE* the terms *Base Station* (BS) and *Mobile Station* (MS) are also used, respectively, according to IMT-Advanced terminology.

Figure 2.3. More Details can be found in the standard documents [3GPP 36.300] and for example in [Dahlmann, 2011].

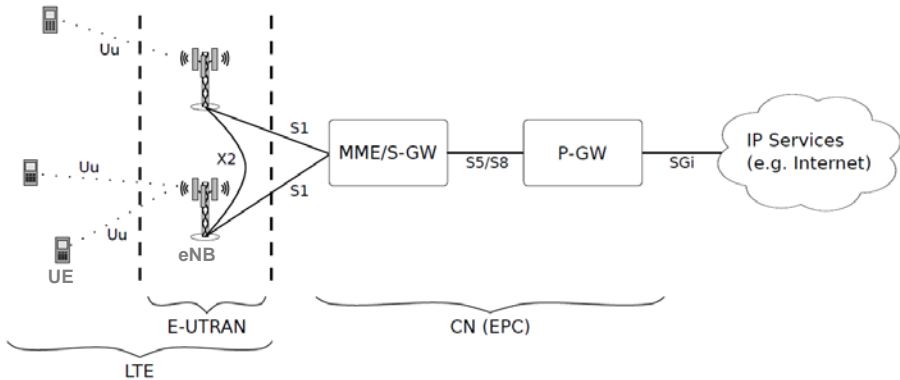


Figure 2.3: functional split between E-UTRAN and EPC; and the EPS network elements relevant for radio evaluation [3GPP 36.300]

## 2.2.1 The Core Network (CN) - EPC

Figure 2.3 shows the nodes of the CN relevant for the evaluation in Chapter 6 of the radio access coordination schemes. The nodes are the *Packet Data Network Gateway* (P-GW), the *Service-Gateway* (S-GW), and the *Mobility Management Entity* (MME) see below [3GPP 36.300], [Dahlmann, 2011].

**Packet Data Network Gateway (P-GW)** is responsible for IP address allocation for the UE, as well as QoS implementation and flow-based charging according to rules from the Policy Control and Charging Rules Function (PCRF). The P-GW is responsible for the filtering of downlink user IP packets into the different QoS-based bearers. The P-GW performs QoS enforcement for Guaranteed Bit Rate (GBR) bearers.

**Service-Gateway (S-GW).** All user IP packets are transferred through the S-GW, which serves as the local mobility anchor for the data bearers when the UE moves between eNBs. It also retains the information about the bearers when the UE is in idle state and temporarily buffers downlink data while the MME initiates paging of the UE to re-establish the bearers. In addition, the S-GW performs some administrative functions in the visited network, such as collecting information for charging (e.g. the volume of data sent to or received from the user). It also serves as the mobility anchor for inter-working with other 3GPP technologies such as GPRS and UMTS.

**Mobility Management Entity (MME)** is the control node which processes the signalling between UE and CN. The protocols running between UE and CN are known as the *Non-Access Stratum* (NAS) protocols. The main functions supported by MME are classified as:

- Functions related to bearer management. This includes establishment, maintenance and release of bearers, and is handled by the session management layer in the NAS protocol.
- Functions related to connection management. This includes the establishment of the connection and security between the network and UE, and is handled by the connection or mobility management layer in the NAS protocol layer.
- Functions related to inter-working with other networks. This includes handover of voice calls to legacy networks

In addition to these nodes, the EPC also includes other logical nodes and functions such as the Gateway Mobile Location Centre (GMLC), the Home Subscriber Server (HSS) and the Policy Control and Charging Rules Function (PCRF). Since the EPS only provides a bearer path of a certain QoS, control of multimedia applications such as VoIP is provided by the IMS which is considered to be outside the EPS itself. When a user is roaming outside his home country network, the user's P-GW, GMLC and IMS domain may be located in either the home network or the visited network.

### 2.2.2 The Access Network (E-UTRAN)

The access network of LTE, E-UTRAN, simply consists of a network of eNBs, as illustrated in Figure 2.3; the E-UTRAN architecture is flat without any centralized controller besides eNBs. The eNBs are usually inter-connected with each other by means of an interface known as X2, and connected to the EPC by means of the S1 interface – more specifically, to the MME by means of the S1-MME interface and to the S-GW by means of the S1-U interface. The protocols which run between the eNBs and the UE are known as the *Access Stratum* (AS) protocols. The E-UTRAN is responsible for all radio-related functions, which can be summarized as:

- Radio Resource Management. This covers all functions related to the radio bearers, such as radio bearer control, radio admission control, radio mobility control, scheduling and dynamic allocation of resources to UEs in both uplink and downlink
- Header Compression. Headers from upper layers are transmitted only once across a bearer and then attached to the following received packets transmitted without the higher layer header
- Security. Data sent over the radio interface is encrypted
- Positioning. The E-UTRAN assists the Evolved Serving Mobile Location Centre (E-SMLC) in finding the UE position
- Connectivity to the EPC. Signalling towards the MME and maintaining the bearer path to the S-GW

On the network side, above functions reside in eNB. An eNB manages multiple radio cells. If the UE leaves the service area of an eNB, the network transfers all UE related information, i.e., the UE context and any buffered data, from one eNB to another. The Packet Data Convergence Protocol (PDCP) avoids data loss during handover. For further details see [3GPP 36.300].

## 2.3 Radio Access Protocol Architecture

This Section outlines the radio access protocol architecture of E-UTRAN, which is structured in the User Plane and the Control Plane .

**User Plane:** the E-UTRAN user plane protocol stack, shown in Figure 2.4, comprises Packet Data Convergence Protocol (PDCP), Radio Link Control (RLC), Medium Access Control (MAC) sublayers of layer-2 and PHY (layer-1) running between UE and eNB.

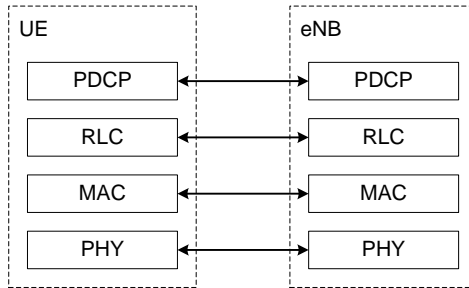


Figure 2.4: user plane protocol stack [3GPP TS 36.300]

**Control Plane:** Figure 2.5 depicts the Control Plane which also handles radio specific functionalities of the AS. The applicable AS-related procedures depend on the Radio Resource Control (RRC) state of the UE, which can be either IDLE or CONNECTED, see Section 2.3.1. The lower layers, PDCP to PHY, perform the same functions as for the user plane but no header compression.

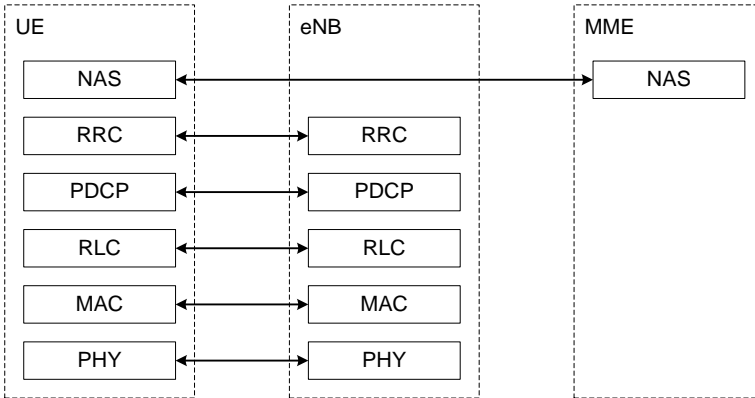


Figure 2.5: control plane protocol stack [3GPP TS 36.300]

In the following the layers and interfaces of the User and Control Plane of the Radio Access Protocol are described.

### 2.3.1 Radio Resource Control (RRC)

RRC protocol is known as ‘Layer 3’ in the AS protocol stack and is the main controlling function in the AS. It is responsible for establishing the radio bearers and configuring all the lower layers using RRC signalling between the eNB and the UE. The RRC protocol supports the transfer of NAS information and additionally supports notification of incoming calls (via paging) for UEs in idle state. The RRC protocol provides, see [3GPP TS 36.331] and [Sesia, 2010]:

- 1) Broadcast of system information,
- 2) Connection control including
  - a. Connection mobility including e.g. intra-frequency and inter-frequency handover
  - b. QoS control service type and its configuration
- 3) Inter-RAT mobility
- 4) Measurements configuration and reporting
- 5) Others including support of self-configuration and self-optimisation

### 2.3.2 The Packet Data Convergence Protocol (PDCP)

This layer processes RRC messages in the control plane and IP packets in the user plane [3GPP TS 36.323]. Depending on the radio bearer, the main functions of the PDCP layer are header compression, security (integrity protection and ciphering), support for reordering and retransmission during handover, and discarding user plane data due to timeouts or duplicates. For radio bearers which are configured to use the PDCP layer, there is one PDCP entity per radio bearer. PDCP uses the services provided by the RLC sublayer. PDCP is used for Signalling Radio Bearer (SRB) and Data Radio Bearer (DRB) mapped on Dedicated Control CHannel (DCCH) and Dedicated Traffic CHannel (DTCH) type of logical channels, see Section 2.3.4. PDCP is not used for any other type of logical channels.

### 2.3.3 Radio Link Control (RLC)

The main functions of the RLC layer are concatenation, segmentation and reassembly of upper layer packets in order to adapt the size of the transmitted packet [3GPP TS 36.322]. An RLC entity can be configured to perform data transfer in one of the following three modes: Transparent Mode (TM), Unacknowledged Mode (UM) or Acknowledged Mode (AM). The mode of data transfer that the RLC entity is configured defines its functionality. One RLC entity exists per radio bearer.

**Transparent Mode:** the TM RLC entity performs no functions and does not add any overhead but the entity is transparent to the Protocol Data Units (PDUs) that are transferred. In the RLC, a Service Data Unit (SDU) is directly mapped to a PDU and vice versa. TM RLC is not used for user plane data and used in a restricted manner for RRC messages such as broadcast System Information (SI) messages, paging messages which do not need RLC configuration.

**Unacknowledged Mode:** the UM RLC entity provides a unidirectional data transfer service and is mainly used by delay-sensitive and error-tolerant real-time applications and especially VoIP. The main functions are:

- Segmentation and concatenation and reassembly of RLC SDUs

- Reordering and duplicate detection of RLC PDUs

**Acknowledged Mode:** an AM RLC entity provides a bidirectional data transfer service and hence can perform error correction through ARQ retransmissions. This mode is mainly utilized by error-sensitive and delay-tolerant non-realtime applications such as web browsing, file downloading and streaming services (if required delay is not too small). RRC messages in the control plane typically use this reliable transmission mode due to the RLC acknowledgements and retransmissions. AM RLC performs the functions of UM RLC and its additional main functions are:

- Retransmission of RLC Data PDUs
- Re-segmentation of retransmitted RLC Data PDUs
- Polling, status reporting, status prohibit

### 2.3.4 Logical Channels

Two types of logical channels are distinguished: control channels which transport RLC messages and traffic channels which carry user plane data. Logical control channels are associated in the RLC layer with an AM RLC entity if not stated differently. Logical channels used by the MAC are (see Figure 2.6):

- **Logical control channel:**

**Broadcast Control Channel (BCCH)** is a downlink channel which is used to broadcast System Information (SI) and any Public Warning System (PWS) messages.

**Paging Control Channel (PCCH)** is a downlink channel used to activate idle UEs, e.g., in the case of an incoming call.

**Common Control Channel (CCCH)** is used to send control information during connection establishment in uplink and downlink if confirmed association between a UE and the eNB does not exist.

**Dedicated Control Channel (DCCH)** is used to transmit dedicated control information to a specific UE, in uplink and downlink if a UE has an RRC connection with an eNB (associated with an AM RLC entity).

**Multicast Control Channel (MCCH)** is a downlink channel which is used to transmit control information related to the reception of MBMS services (associated with an UM RLC entity)

- **Logical traffic channels:**

**Dedicated Traffic Channel (DTCH)** is used to transmit dedicated user data in uplink and downlink (associated with an UM or AM RLC entity)

**Multicast Traffic Channel (MTCH)** is used to transmit user data for Multimedia Broadcast/Multicast Service (MBMS) services in the downlink (associated with a UM RLC entity)

### 2.3.5 Medium Access Control (MAC)

The Medium Access Control (MAC) sublayer performs radio resource allocation as a main function and resides below the RLC and above the Physical Layer [3GPP TS 36.321]. MAC entities communicate with each other over transport channels provided by the PHY. RLC entities communicate via logical channels provided by the MAC layer. The coordination functionality studied in this work resides in the MAC layer. The following functions are supported by MAC sublayer, see Figure 2.6:

1. Mapping between logical channels and transport channels;
2. Multiplexing of MAC SDUs from one or different logical channels onto transport blocks (TB) to be delivered to the physical layer on transport channels
3. Demultiplexing of transport blocks delivered from the physical layer on transport channels and reconstructing MAC SDUs dedicated to one or different logical channels
4. Error correction through Hybrid Automatic Repeat reQuest (HARQ). The transmit HARQ entity transmits and retransmits TBs, as well as receives and processes ACK/NACK signalling. The receive HARQ entity receives TBs, combines the received data and generates ACK/NACK signalling. Up to eight HARQ processes in parallel are used to support multiprocess 'Stop-And-Wait' HARQ operation.

5. Transport format selection, i.e., link adaptation including the transport block size, service specific rate matching, convolutional channel coding and interleaving, and any service-specific rate matching, error protection scheme (i.e. turbo coding, rate is 1/3, size of CRC is 24 bits).
6. Priority handling between UEs by means of dynamic scheduling
7. Priority handling between logical channels of one UE. The logical channel prioritization entity prioritizes the data from the logical channels to decide how much data and from which logical channels should be included in each MAC PDU and delivers the decision to the multiplexing and demultiplexing entity.
8. Scheduling information reporting

[3GPP TS 36.321] defines two MAC entities, one in the UE and one in the eNB with partly different functions. The above mentioned functions (5.) and (6.) are only performed by the eNB MAC entity whereas the function (8.) resides in the UE only. Other functions are performed in both entities either in uplink, in downlink, or both. Figure 2.6 sketches the structure for the UE side MAC entity.

## 2.3 Radio Access Protocol Architecture

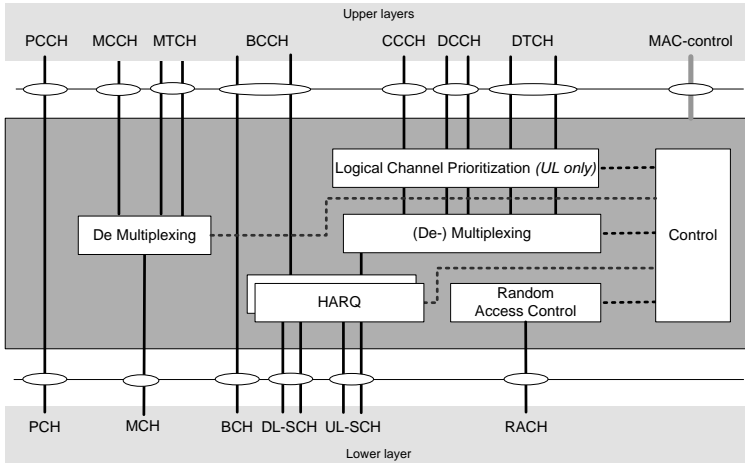


Figure 2.6: MAC structure overview, UE side [3GPP TS 36.321]

The MAC layer provides a HARQ entity, a multiplexing/demultiplexing entity, a logical channel prioritization entity, a random access control entity, and a controller which performs various control functions such as Discontinuous Reception (DRX), the Data Scheduling procedure, and for maintaining the uplink timing alignment.

A logical channel is mapped to a transport channel as described in Figure 2.7 (a) for the downlink and (b) for the uplink. The mapping of logical channels on transport channels depends on the multiplexing configured by RRC. In the downlink, the DL-SCH transfers the information from all logical channels except MTCH, MCCH, and PCCH. In the uplink, the UL-SCH transports the information from all the logical channels.

## 2 LTE / LTE-Advanced Radio Access

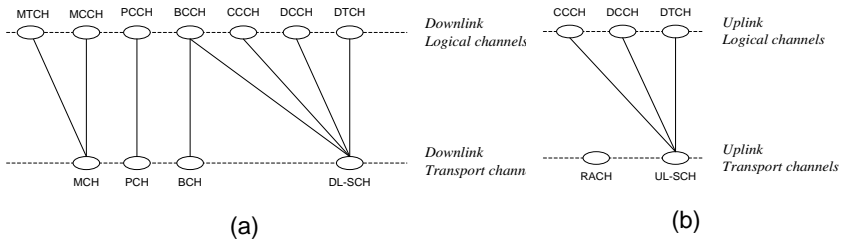


Figure 2.7: channel mapping (a) in downlink (b) in uplink [3GPP TS 36.321]

### 2.3.6 Transport Channels

Transport channels provided to the MAC by the PHY-layer are the following:

- **Downlink Transport Channels:**

**Broadcast Channel (BCH)** transports parts of the System Information (SI) which is important for accessing the Downlink Shared Channel (DL-SCH). The transport format is fixed and the capacity is limited.

**Downlink Shared Channel (DL-SCH)** transports downlink user data or control messages. The remaining parts of the SI not transported on BCH are transported on the DL-SCH

**Paging Channel (PCH)** transports paging information to UEs, and updates of the SI and PWS

**Multicast Channel (MCH)** transports MBMS user data or control messages that require Multimedia Broadcast Single Frequency Network (MBSFN) combining

- **Uplink Transport channels**

**Uplink Shared Channel (UL-SCH)** transports uplink user data or control messages

**Random Access CHannel (RACH)** provides access to the network if the UE is not associated yet or is not allocated to uplink transmission resources

### 2.3.7 Physical Layer (PHY)

The next three Subsections outline functions of the PHY, Orthogonal Frequency Division Multiple Access (OFDMA), and the frame structure used in the PHY.

#### 2.3.7.1 Physical Layer Functions

Figure 2.8 shows the processing structure for data transport channels to physical channels. Data arrives to the coding unit in the form of transport blocks which are processed in the following coding steps [3GPP TS 36.211]:

- A 24-bit Cyclic Redundancy Check (CRC) is attached to each TB which is used at the receiver to verify correct reception and to generate the HARQ ACK/NACK feedback.
- TB (of arbitrary size) are segmented into 'code blocks' aiming for minimum number of filler bits and CRC is attached to the code blocks (in the same manner as to the TB).
- Information bits are first channel-coded with a turbo code of a mother code rate of 1/3 with a contention-free quadratic permutation polynomial (QPP) interleaver.
- Rate matching of the coded bit stream to a suitable final code rate via puncturing and/or repetition.
- Code block concatenation sequentially joins different code blocks which each corresponds to one TB and results in one codeword

Figure 2.9 depicts the general structure for processing physical channels to baseband signals, applicable to more than one physical channel. Processing of the downlink physical channel is defined by the following steps:

- **Scrambling** of coded bits in each of the codewords to be transmitted on a physical channel by a length-31 Gold code.

- **Modulation** in order to generate complex-valued modulation symbols from the scrambled bits supporting the modulation schemes QPSK, 16QAM and 64QAM
- **Layer mapping** allocates modulation symbols onto one or several transmission layers in case of transmission in SDMA or spatial multiplexing mode
- **Precoding** applies complex weights to modulation symbols on each layer for each antenna port
- **Resource element mapping** allocates symbols for each antenna port to resource elements
- **Signal generation** of complex-valued time-domain OFDM (or time-domain SC-FDMA in uplink) for each antenna port

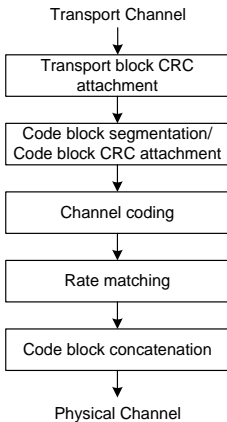


Figure 2.8: Transport Channel processing for DL-SCH, PCH and MCH.

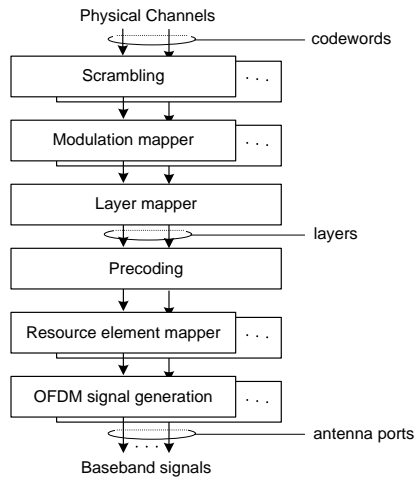


Figure 2.9: Physical Channel processing

The PHY distinguishes the following Transmission Modes which support different MIMO techniques and corresponding signalling:

- Mode 1: transmission from a single eNodeB antenna port
- Mode 2: transmit diversity
- Mode 3: open-loop spatial multiplexing
- Mode 4: closed-loop spatial multiplexing
- Mode 5: Multi-User Multiple-Input Multiple-Output (MU-MIMO)
- Mode 6: closed-loop rank-1 precoding
- Mode 7: transmission using UE-specific Reference Signals (RSs) with a single spatial layer
- Mode 8: transmission using UE-specific RSs with up to two spatial layers
- Mode 9: transmission using UE-specific RSs with up to eight spatial layers.

### 2.3.7.2 Orthogonal Frequency Division Multiple Access (OFDMA)

Orthogonal Frequency Division Multiplexing (OFDM) exploits the spectrum efficiently by subdividing the channel bandwidth into multiple subcarriers without spectrum-wasting guard bands. In this manner subcarriers overlap and are orthogonal in the frequency domain. This technique, for example employed in Digital Video Broadcasting (DVB) and Wireless Local Area Network (WLAN), requires relatively cheap and simple receivers. The transmitter is more complex and expensive as highly linear power amplifiers are required to cope with a drawback of OFDM that is the high Peak to Average Power Ratio. LTE-Advanced using OFDM can be deployed in different channel bandwidths in a straight forward manner due to the fixed subcarrier spacing. Inter Symbol Interference (ISI) caused by multipath propagation is cancelled by adding to OFDM symbols a Cyclic Prefix (CP) with a suitable length which should be longer than the highest delay spread. The CP is a copy of the last fragment of the radio signal appended at the beginning of each symbol. OFDM is sensitive in terms of Bit Error Rate (BER) to Doppler shift or other carrier frequency offsets between transmitter and receiver if the subcarrier spacing is too small because orthogonality between subcarriers is removed then. OFDMA is an access method to an OFDM channel, instead of dedicating all subcarriers to a single user simultaneously, in OFDMA, subcarriers are

grouped to subchannels<sup>7</sup> in a manner that a number of subchannels exist in parallel. A radio resource allocated to a MS can comprise one or more subchannels for a given time duration. The flexibility and smaller granularity of radio resource assignment in OFDMA increase overhead for specifying MS allocations subchannel- or even subcarrier-wise. OFDMA allows also for frequency-selective scheduling resulting in gains if actual channel conditions from each MS and subchannel are known. More Details about OFDMA can be found in [Einhaus, 2009] and [Dahlmann, 2011].

In the uplink of LTE and LTE-Advanced, Single Carrier Frequency Division Multiple Access (SC-FDMA) is employed which is similar to OFDMA but has much smaller Peak to Average Power Ratio. In contrast to OFDM, where a data symbol directly modulates each subcarrier independently (each signal of a subcarrier at a given time is defined by a constellation point of the digital modulation scheme), in SC-FDMA the signal modulated onto a given subcarrier is a linear combination of all the data symbols transmitted at the same time. In other words in a symbol period, all the transmitted subcarriers carry a component of each modulated data symbol. For more details see [Myung, 2006]. From MAC layer perspective, the differences of the two PHY technologies can be neglected.

### 2.3.7.3 OFDMA Frame Structure and Overhead

Figure 2.10 shows the OFDMA resource grid of LTE, which is used to transmit a transport block formed by the payload of an IP-packet. The size of the transport block depends on the number of Physical Resource Blocks<sup>8</sup> (PRB) dedicated to a user and the employed Modulation and Coding Scheme (MCS). A scheduler allocates PRB to a MS and within the *link adaptation* procedure a MCS is selected for a MS. The transport block is segmented to the code block length and the encoded bits are mapped to RE during the rate matching.

---

<sup>7</sup> Subchannel is a Physical Resource Block (PRB), see Section 2.3.7.3

<sup>8</sup> A PRB is also called subchannel

## 2.3 Radio Access Protocol Architecture

A MAC frame with length of 10 ms consists of 10 consecutive subframes with the length of 1 ms, also called Transmission Time Intervals (TTIs), each comprising 2 slots or PRBs, [3GPP TS 36.211]. One subframe consists of a number of PRB in the frequency domain depending on the channel bandwidth, e.g. 50 PRB per subframe for 10 MHz bandwidth, as assumed throughout in this work. A PRB consists of 12 subcarriers (with a total bandwidth of  $12 \times 15 \text{ kHz} = 180 \text{ kHz}$ ) and 7 OFDMA-symbols ( $\approx 71 \mu\text{s}$  with normal cyclic prefix), which results in 84 Resource Elements per PRB. A Resource Element (RE) is a modulation symbol carrying 2, 4, or 6 bits for Quadrature Phase Shift Keying (QPSK), 16-Quadrature Amplitude Modulation (16-QAM), or 64-QAM, respectively. In each subframe the first 3 of 14 symbols are occupied by the control region in the downlink as shown in Figure 2.10. Additionally 6 RE per PRB are occupied by reference symbols. The bits of each RE are mapped to the constellation diagram yielding the phase and amplitude shift of each subcarrier.

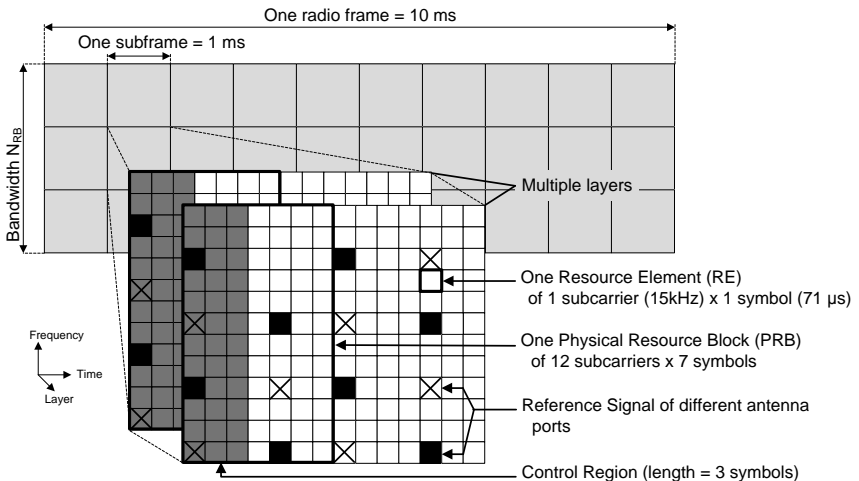


Figure 2.10: frame structure and downlink resource grid (normal cyclic prefix) [3GPP TS 36.211]

Two radio frame structures are supported: Type 1, applicable to FDD, and Type 2, applicable to TDD. For FDD, uplink and downlink transmissions are separated in the frequency domain and hence the entire frame is dedicated to one direction. For TDD, the frame is split up between down and uplink according to the supported configurations given in Table 2.1 where “D” refers to a downlink subframe, “U” to an uplink subframe, and “S” denotes a special subframe that carries three fields: the Downlink Pilot Time Slot, the Guard Period (GP) and the Uplink Pilot Time Slot.

Table 2.1: TDD uplink-downlink configurations.

Uplink-downlink configuration	Downlink-to-Uplink Switch-point periodicity	Subframe number									
		0	1	2	3	4	5	6	7	8	9
0	5 ms	D	S	U	U	U	D	S	U	U	U
1	5 ms	D	S	U	U	D	D	S	U	U	D
2	5 ms	D	S	U	D	D	D	S	U	D	D
3	10 ms	D	S	U	U	U	D	D	D	D	D
4	10 ms	D	S	U	U	D	D	D	D	D	D
5	10 ms	D	S	U	D	D	D	D	D	D	D
6	5 ms	D	S	U	U	U	D	S	U	U	D

### 2.3.8 Physical Channels

Transport channels, see Figure 2.7, are mapped to physical channels which can be control or data channels. Control channels carry physical layer messages which cannot be carried efficiently or quickly by data channels considering conflicting requirements such as coverage, robustness, flexibility, low overhead and complexity.

The following **physical control channels** are distinguished:

- **Physical Control Format Indicator Channel (PCFICH)** indicates the number of OFDM symbols (i.e. normally one, two or three) which are used for control channel information in each subframe.

- **Physical Downlink Control Channel (PDCCH)** carries a Downlink Control Information (DCI) message, which includes resource assignments and other control information for a UE.
- **Physical Hybrid ARQ Indicator Channel (PHICH)** transports HARQ ACKs/NACKs, which indicate correctly received data by the eNB on PUSCH.
- **Physical Uplink Control Channel (PUCCH)** carries feedback control messages for downlink transmissions such as Channel Quality Indicators (CQIs) to support link adaptation, and MIMO feedback such as Rank Indicators (RIs) and Precoding Matrix Indicators (PMIs).
- **Physical Random Access Channel (PRACH)** is used for initial network access, for uplink time synchronization and it allows to send a Scheduling Request (SR) if a UE is not allocated to another uplink resource.

Following **physical data channels** are provided by the physical layer to the MAC layer:

- **Physical Downlink Shared Channel (PDSCH)** carries all user data in downlink and broadcast system information which is not carried on the PBCH, and paging information.
- **Physical Broadcast Channel (PBCH)** bears one part of the basic system information, i.e. the 'Master Information Block', which essential for initial access to the cell.
- **Physical Multicast Channel (PMCH)** carries Multimedia Broadcast and Multicast Services (MBMS) data. It can only be present in specific Multimedia Broadcast Single Frequency Network (MBSFN) subframes.
- **Physical Uplink Shared Channel (PUSCH)** carries data from the Uplink Shared Channel (UL-SCH) transport channel which consists of user data and higher layer control data.

The transport Paging CHannel (PCH) is mapped to Physical Downlink Shared Channel (PDSCH), otherwise the mapping in the physical layer of transport channels to physical channels (and vice versa) is explicit and obvious by their naming. For example messages of the transport

Random Access CHannel (RACH) are mapped to the Physical Random Access Channel (PRACH).

### 2.4 Quality of Service and EPS Bearers

Applications with different QoS requirements can run in a UE simultaneously. Services such as VoIP and web browsing are supported by specific bearers within the EPS per UE. Two type of bearers can generally be distinguished the minimum granted bit rate (GBR) bearer and the non-GBR bearer. The first type is typically established for VoIP sessions whereas the second one is for example suitable for FTP sessions. During the association procedure of a UE to the network, the UE is assigned an IP address by the P-GW and at least one bearer is permanently established, called the default bearer, which provides the UE with always-on IP connectivity during a connection. Additional bearers or dedicated bearers can be established at any time during or after the association of the UE and can be of both types either GBR or non-GBR. Dedicated bearers can be established by the network, for example triggered by the IP Multimedia Subsystem (IMS) domain, or requested by the UE.

The eNB is responsible to provide the necessary QoS of a given bearer over the radio interface. Each bearer has an associated QoS Class Identifier (QCI), and an Allocation and Retention Priority (ARP). The QCI is described by priority, packet delay budget and acceptable packet loss rate. Hence, the QCI label for a bearer determines how the scheduler processes packets in the MAC layer, e.g., in terms of policies regarding scheduling, queue management, and rate shaping. For more details on bearers and QCIs see [3GPP TS 23.203].

### 2.5 Components introduced by LTE-Advanced

The main components of Release 10 that upgrade LTE to LTE-Advanced are:

**Carrier aggregation** allows for exploiting system bandwidth of up to 100 MHz even if not contiguously available. LTE-Advanced supports multiple Component Carriers (CCs) aggregation of up to five 20 MHz CCs. In a flexible manner fragmented spectrum can be

## 2.6 Load and Interference Management Over X2 E-UTRAN Network Interface

efficiently used by employing aggregated CCs of the same or different bandwidths, adjacent or non-adjacent in the same or in different frequency bands.

**Enhanced multiple antenna transmission.** Release 10 introduces enhancements to multi-antenna operation for the purpose of a higher peak data rate and spectral efficiency. The supported number of antennas is increased from 2 to 4 antenna elements at the UE and from 4 to 8 at the eNB. The corresponding signalling is supported by new reference signals for CSI estimation and data demodulation, enhanced UE feedback by the use of transmit diversity, and enhanced feedback for improved CSI accuracy with low overhead. The sophisticated CSI feedback mechanism especially improves Multi User MIMO (MU-MIMO) techniques. The same type of feedback is utilized, namely Channel Quality Indicator (CQI), Precoding Matrix Indicator (PMI), and Rank Indicator (RI). A new PDSCH Transmission Mode 9, is introduced for the support of CoMP schemes such as Joint Transmission (JT).

**Relaying.** A newly introduced Relay Node operates as a kind of eNB, with a wireless backhaul link. Relaying can offer cost advantages for operators and depending on the deployment scenario allowing for coverage extension, capacity enhancement, or both.

**Heterogeneous network deployments.** A diverse set of base stations (BSs) (relays, picos, and femtos) can be deployed to improve spectral efficiency per unit area and release a macro cell by shifting data service to smaller cell type. The operation of heterogeneous network deployments is enabled by the capability of carrier aggregation and enhanced Inter Cell Interference Coordination (eICIC), see Section 5.

## 2.6 Load and Interference Management Over X2 E-UTRAN Network Interface

The X2 interface shown in

Figure 2.3 inter-connects two neighbour eNBs in order to exchange signalling information. Two types of information can be exchanged over the X2 interface: load or interference related information and handover

related information [3GPP TS 36.420], [3GPP TS 36.423], [Sesia, 2010]. If an X2 interface is not established between two adjacent eNBs, a handover is processed over the S1 interface. X2 interface is initialized by identification of a suitable neighbour eNB. A suitable neighbour eNB can be defined by configuration or by information received from the network. An eNB can provide information about all its cells to a neighbour eNB, such as the cell's physical identity, the frequency band, and the tracking area identity. Load and Interference Management Over X2: in contrast to UMTS with the entity of a Radio Network Controller, LTE(-Advanced) does not have a central Radio Resource Management (RRM) entity and hence the exchange of load information between eNBs is essential in the flat LTE(-Advanced) network architecture. Load information can be exchanged for **load balancing** between neighbouring cells with low frequency in the order of seconds or for **interference coordination** and inter site RRM with frequently information exchange in the order of tens of milliseconds.

### 2.6.1 Inter-Cell Interference Coordination Signalling in Downlink

In downlink, a bitmap called the Relative Narrowband Transmit Power (RNTP) indicator can be exchanged between eNBs over the X2 interface. Each bit of the RNTP indicator corresponds to one RB in the frequency domain and is used to inform neighbouring eNBs if a cell is planning to keep the transmit power for the RB below a certain upper threshold or not. The value of this upper threshold and the period of time for which the indicator is valid are configurable. This enables the neighbouring cells to take into account the expected level of interference in each RB when scheduling UEs in their own cells. The reaction of the eNB in case of receiving an indication of high transmit power for a RB in a neighbouring cell is not standardized as the scheduling algorithm is out of the scope of the standard. A typical response could be to avoid scheduling cell-edge UEs in such RBs. In the definition of the RNTP indicator, the transmit power per antenna port is normalized by the maximum output power of a BS or cell. The reason for this is that a cell with a smaller maximum output power, corresponding to smaller cell size (and hence a reduced distance to neighbour cells), can create as

much higher interference as a cell with a larger maximum output power corresponding to a larger cell size.

### 2.6.2 Inter-Cell Interference Coordination Signalling in Uplink

For uplink transmissions, two messages can be exchanged over the X2 interface between eNBs to coordinate their transmit powers and scheduling of users: a reactive indicator, known as the 'Overload Indicator' (OI), and a proactive indicator, known as the 'High Interference Indicator' (HII). The OI can be exchanged to indicate physical layer measurements of the average uplink interference plus thermal noise for each RB. The OI can take three values, expressing low, medium, and high level of interference plus noise. An excessive signalling load is avoided by limiting the minimal updated period to 20 ms. The HII can also be sent by an eNB to its neighbour eNBs to inform them that it will in the near future schedule uplink transmissions by one or more cell-edge UEs in certain parts of the bandwidth, and therefore that high interference might occur in those frequency regions. Neighbour cells can consider this information in scheduling their own users to limit the interference impact. This can be achieved either by not scheduling own cell-edge UEs in that resources but centre-cell users (requiring less transmission power), or by not scheduling any user at all in the relevant RBs. The HII consists of a bitmap with one bit per RB and, like the OI, is not sent more often than every 20 ms. The HII bitmap is addressed to specific neighbour eNBs. By setting the uplink transmission power of an UE, the serving eNB can trade off the throughput of own cell-edge UEs against the amount of emitted inter-cell interference.

### 2.6.3 Enhanced Inter-Cell Interference Coordination in LTE-Advanced

eICIC is an important feature of LTE-Advanced for operating heterogeneous network deployments. The eICIC extends the ICIC by the time domain and allows for interference mitigation of the control channels by muting certain subframes of one layer of cells in order to reduce the interference to the other layer. These muted subframes are called Almost Blank Subframes (ABS).

## 2.7 Coordinated Multipoint (CoMP) Transmission in LTE-Advanced

CoMP transmission and reception is a concept in LTE-Advanced for improving cell edge throughput and the entire cell capacity. A subset of CoMP schemes are already defined for the purpose of ICIC in the 3GPP standard for LTE. Especially, CoMP transmission schemes coordinating radio resource assignment of cells of one eNB can be simply implemented by manufacturer proprietary algorithms. In LTE-Advanced a new framework is provided supporting CoMP schemes relying on increased backhaul capacity and MIMO techniques with up to eight antenna elements at the BS and up to four at the MS. The 3GPP classifies CoMP schemes into these categories: Joint Transmission (JT), Dynamic Point Selection (DPS) also called muting, and Coordinated Scheduling/ Beamforming (CS/CB), [3GPP TR 36.819].

With *JT*, also known as ‘network MIMO’, multiple eNBs simultaneously transmit data packets to the same MS. The resulting signals are combined to a desired signal at the receiving MS. JT requires low latency and high bandwidth of the backhaul connectivity between adjacent BS in order to enable CoMP to be beneficial. Especially coherent JT (in contrast to non-coherent JT) has to meet substantial synchronization constraints to realize theoretical gains. Theoretical gains of JT have not been shown to be feasible in real systems.

With *DPS* (including dynamic cell selection (DCS)) one BS, e.g. with the best SINR reported by MS, transmits the signal. The transmitting BS can change from subframe to subframe and hence user data has to be available at multiple BSs. Neighbour BSs can remain silent to increase the SINR of the receiving MS.

In *CS* enhanced systems, neighbour BSs can cooperate by mutually reducing transmission power on sets of time-frequency resources for the benefit of users in participating cells. One example of coordinated scheduling is by SFR where the transmit power level used on different radio resources is exchanged between BSs via the X2 interface.

*Coordinated Beamforming* (CB) adds a spatial dimension to ICIC and demands for multi-antenna equipped BSs. With CB, MSs experience a reduced interference level because beamforming weights can be appropriately selected at the BSs in order to steer the interference away from interference victim MSs. Data for an MS is only available at one BS but scheduling decisions and beamforming weight selection are coordinated among the BSs forming a CoMP cooperating set.

The 3GPP defines another hybrid category using both JT and CS/CB, where for example some BSs perform JT while others of the cooperating set perform CS/CB. An overview of CoMP techniques, objectives, and potential gains is given in [Lee, 2012], [3GPP TR 36.819], and [Seisa, 2011].

CoMP transmission or reception schemes can be distinguished by the complexity and signalling requirements on the backhaul connecting BSs. In general, CoMP trade increased capacity against low signalling demand in terms of data rate and packet delay requirements. JT (or network MIMO) such as dirty paper coding [Lee, 2007], promise high capacity gains but demand extensive backhaul capacity scaling with the utilized radio bandwidth. With these CoMP schemes, user data must be present at several BSs connected via high speed links; otherwise JT techniques are infeasible. In any case, JT techniques face severe synchronization problems in real test application [Marsch, 2010] and require extensive MAC-layer support. If only very limited information can be exchanged between BSs, only coordinated scheduling can reduce inter-cell interference and still yield capacity gains as shown in Section 5.3 and 5.4. Since CB/CS is already generally supported by LTE /LTE-Advanced, this work focuses on coordinated beamforming.



## CHAPTER 3

---

# MIMO Techniques

### 3.1 Introduction

Multi antenna techniques are one of the most promising means for higher spectral efficiency in future wireless communication systems. Besides utilizing increased bandwidth, multi antenna techniques became essential in meeting required data rates as defined by ITU-R<sup>9</sup>. The theoretically achievable spectral efficiency linearly scales with the minimum of the number of transmit and receive antennas employed [Sesia, 2011]. Multi antenna algorithms exploit the spatial dimension and aim for improving the link performance in terms of one or more possible metrics such as the error rate, communication data rate, coverage area and the spectral efficiency. Figure 3.1 depicts the fundamental principles of multi antenna techniques.

- **Diversity gain** allows for an improved robustness of a signal transmission by mitigation of multipath fading, through transmitting or receiving over multiple antennas at which fading is sufficiently uncorrelated.
- **Spatial multiplexing gain** is achieved by transmitting multiple data streams to a single user on multiple low correlated spatial channels which are created by combining available antennas.
- **Array gain** arises by focusing the transmitted or received energy in one or more given directions via precoding or beamforming. In this manner, multiple users located in different directions can be served

---

<sup>9</sup> The International Telecommunication Union – Radiocommunication Sector

### 3 MIMO Techniques

simultaneously which is called Spatial Division Multiple Access (SDMA) and is also known as multi-user MIMO in 3GPP standard documents.

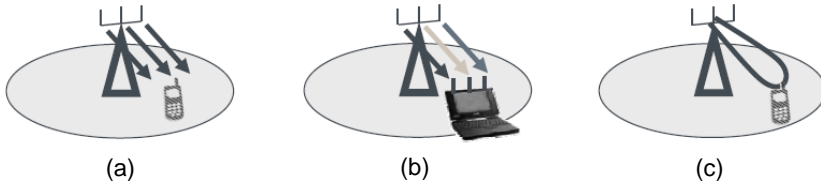


Figure 3.1: fundamental benefits of multiple antennas:

(a) diversity gain; (b) spatial multiplexing gain; (c) array gain [Sesia, 2011]

Techniques utilizing diversity or spatial multiplexing gain rely on low mutual correlation between channels experienced at the different antennas and hence are more feasible in rich multipath scattering environments such as indoor- or urban micro cell scenarios. Beamforming techniques usually rely on high mutual correlation and hence are more beneficial in sparse multipath scenarios such as urban macro or rural macro scenarios with increased cell size and high Line-of-Sight (LOS) probability.

## 3.2 Comments and Technique Choice

The required degree of mutual channel correlation impacts the size of the desired antenna array because uncorrelated fading<sup>10</sup> is implied by relatively far distanced antenna elements whereas very similar instantaneous fading or correlated fading is perceived at relatively narrow spaced elements of an array. The absolute distance depends on the wavelength ( $\lambda$ ) of the signal and its propagation environment. Multi-path reflections causing fading mainly occur in the near-zone

---

<sup>10</sup> For sake of simplicity in the following text, the terms “uncorrelated” and “correlated” are used and mostly refer to the more precise terms “low mutually correlated” and “high mutually correlated” in the context of fading perceived at different antennas elements of one array.

around the MS (or around a micro-cell Base Station (BS) below roof top) which result in a high angular spread of the multiple paths. Under these circumstances, a relatively small antenna elements distance of  $\lambda/2$  (or  $< 3*\lambda$  for BSs) is considered sufficient to achieve uncorrelated fading. In contrast, for a macro-cell BS antenna mounted above roof top to serve large cells, a distance of approximately  $10 \lambda$  between antenna elements is required to achieve uncorrelated fading [Dahlmann, 2011]. Low mutual fading correlation is also achieved at co-located antenna elements mounted in a cross polarization manner. Nevertheless, an macro cell antenna array suitable for transmit diversity or spatial multiplexing with eight elements and cross polarization still needs four spatially separated antenna elements, resulting in an array width of  $30 \lambda$  that is 11 m with a carrier frequency of 800 MHz. The dimension of the antenna shrinks by a factor of 20 to 40 if the array is designed for beamforming only. As mentioned, the choice of the employed MIMO technique should also depend on the type of environment and its multipath propagation characteristics. Differences between the techniques can be identified in the required deployment and during operation.

Although MIMO techniques based on spatial multiplexing and diversity gain are capable to increase capacity or robustness of a link, they have unsustainable drawbacks. Either the peak data rate of users served with high SINR is improved (e.g., by spatial multiplexing gain) or the bit error rate of cell edge users is increased (e.g., by diversity gain). Multiple antennas are required at the transmitter and the receiver and the performance heavily depends on a precise and thereby costly estimation of the current channel state at least for those techniques providing significant gain.

Beamforming techniques provide both coverage extension and improve cell capacity. The achieved array gain significantly enhances signal quality at the cell edge, which results in extended coverage. In good SINR regions of a cell, SDMA allows for simultaneous data streams, which increases system capacity. Multiple antennas are only required at the BS resulting in simple and cheap user devices. The size of the antenna array at the BS can be kept relatively small down to a fraction

of the wave length. As a downside, an SDMA enabled cell generates less predictable interference than a conventional cell without beamforming, because a variable number of MSs send uplink data in parallel and downlink streams are transmitted by the BS with changing direction and power per beam. Thereby SINR estimations tends to be less precise and the link adaptation sub optimal.

In this thesis, beamforming techniques and beamforming coordination promising to avoid these drawbacks are studied. Sections 3.3 to 3.3.4 describe the signal model with beamforming for which a narrow angular spread at the receive and transmit antenna, correlated antenna elements, and a narrowband signal<sup>11</sup> are assumed according to [Godara, 1997]. This model is applicable to OFDM systems such as LTE since under beamforming weights are applied to narrow band signals transmitted either on single subcarriers or on a group of continuous subcarriers.

### 3.3 Model of Beamformer According to Godara 1997

This Section outlines the signal model of the beamformer according to [Godara, 1997]. Figure 3.2 and Figure 3.3 show a linear array consisting of  $L$  equidistant omnidirectional elements in the far field of  $M$  uncorrelated sinusoidal point sources transmitting at the frequency  $f_0$ . The origin of the coordinate system is taken as a time reference. Thus the plane wave from the  $i^{\text{th}}$  source in direction  $(\phi_i, \theta_i)$  arrives at the  $l^{\text{th}}$  element at time  $\tau_l$  given by Eq. (3.1) if the first element resides in the origin, where  $d$  is the element spacing and  $c$  is the propagation speed of the wave front.

$$\tau_l(\phi_i, \theta_i) = \frac{d}{c} l \cos(\phi_i) \sin(\theta_i) \quad (3.1)$$

---

<sup>11</sup> The model is applied in Section 4.3.4 to calculate the SINR for LTE-Advanced systems. The subcarrier bandwidth of LTE(-Advanced) is 15 kHz and is assumed to be sufficiently “narrow” so that Godara’s model can be applied.

The signal induced at the reference element due to the  $i^{\text{th}}$  source can be expressed in complex notation as  $m_i(t)e^{j2\pi f_0 t}$  where  $m_i(t)$  denotes a complex modulation function. The delayed complex signal at the  $l^{\text{th}}$  element can accordingly be expressed as  $m_i(t)e^{j2\pi f_0(t-\tau_l(\phi_i, \theta_i))}$ . This expression is valid for the narrow-band assumption for signal array processing which approximates the modulation function as almost constant during  $\tau_l$  seconds, i.e.,  $m_i(t) \cong m_i(t + \tau_l(\phi_i, \theta_i))$ . The total signal received at the  $l^{\text{th}}$  element from all  $M$  sources and the background noise is given by Eq. (3.2) where  $n_l(t)$  is a random noise component on the  $l^{\text{th}}$  element including background and electronic noise on the  $l^{\text{th}}$  channel.

$$x_l(t) = \sum_{i=1}^M m_i(t)e^{j2\pi f_0(t-\tau_l(\phi_i, \theta_i))} + n_l(t) \quad (3.2)$$

Noise is assumed to be temporarily white with zero mean and variance  $\sigma_n^2$ . The array output is the complex weighted sum of the signals from each element given by Eq. (3.3) where  $( )^*$  stands for the complex conjugate. If  $\vec{w}$  are the weights of the beamformer and  $\vec{x}(t)$  are the received signals on all elements, the output of the beamformer is given in Eq. (3.4) where  $( )^H$  denotes complex conjugate transpose of a vector.

$$y(t) = \sum_{l=1}^L w_l^* x_l(t) \quad (3.3)$$

$$y(t) = \vec{w}^H \vec{x}(t) \quad (3.4)$$

with  $\vec{w} = [w_1, w_2, \dots, w_L]^T$  and  $\vec{x}(t) = [x_1(t), x_2(t), \dots, x_L(t)]^T$

If the components of  $\vec{x}(t)$  can be modeled as zero mean stationary processes, then for a given  $\vec{w}$  the mean output power of the beamformer is given by Eq. (3.5) where  $E[\cdot]$  represents the expectation operator and  $R$  is the correlation matrix defined by Eq. (3.7). Equation (3.7) also shows the compact matrix notation where the columns of the  $L$  by  $M$  matrix  $A$  are made up of the steering vectors, according to Eq. (3.6), and the  $M$  by  $M$  matrix  $S_{ij}$  represents the source correlation which is a diagonal matrix for uncorrelated sources. Figure 4.3 shows a beam pattern derived from the output power calculated by Eq. (3.5).

$$P(\vec{w}) = E[y(t) y^*(t)] = \vec{w}^H R \vec{w} \tag{3.5}$$

$$\vec{s}_i = [e^{j2\pi f_0 \tau_1(\phi_i, \theta_i)}, e^{j2\pi f_0 \tau_2(\phi_i, \theta_i)}, \dots, e^{j2\pi f_0 \tau_L(\phi_i, \theta_i)}]^T \tag{3.6}$$

$$R = E[\vec{x}(t) \vec{x}^H(t)] = A S A^H + \sigma_n^2 I \tag{3.7}$$

with  $A = [\vec{s}_1, \vec{s}_2, \dots, \vec{s}_M]$  and  $S_{ij} = \{p_i \text{ if } i = j, 0 \text{ if } i \neq j\}$

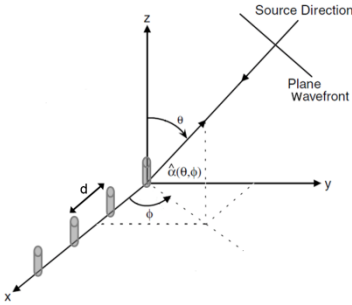


Figure 3.2: definition of coordinate system

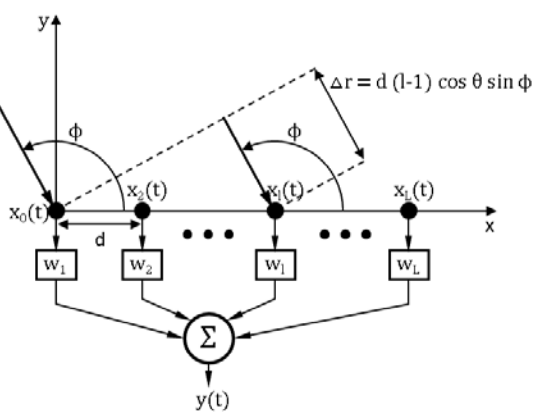


Figure 3.3: linear array with plane wave incident [Mailloux, 2005]

The matrix  $R$  can be expressed by its eigenvalues  $\lambda$  and their corresponding eigenvectors  $\vec{U}_l$ . The eigenvalues, in the case of uncorrelated directional sources and uncorrelated noise, can be divided in two sets. Eigenvalues of one set are equal and correspond to the variance of the white noise. The eigenvalues of the other set depend on the transmit power and the direction of the sources. The number of the eigenvalues equals to the number of the sources and each eigenvalue is associated to a source. In Eq. (3.8)  $R$  is represented by its  $L$  eigenvalues  $\lambda_l$  and their associated unit-norm eigenvectors  $\vec{U}_l$  for  $l = 1, \dots, L$  where the diagonal matrix is defined in Eq. (3.9) and the eigenvector matrix is given by Eq. (3.10). The  $L$  eigenvalues consist of  $M$  signal eigenvalues and  $L-M$  noise eigenvalues.

$$R = \Sigma \Lambda \Sigma^H \quad (3.8)$$

$$\Lambda = \begin{bmatrix} \lambda_1 & & 0 \\ & \ddots & \\ & & \lambda_l \\ 0 & & & \ddots \\ & & & & \lambda_L \end{bmatrix} \quad (3.9)$$

$$\Sigma = [\vec{U}_1, \vec{U}_2, \dots, \vec{U}_L] \quad (3.10)$$

### 3.3.1 Conventional Beamformer

A conventional beamformer applies complex weights of the same amplitude at all antenna elements. The weights' phases are selected in a manner that the array is steered to the desired look direction  $(\phi_i, \theta_i)$ . If  $\vec{s}_0$  is the look direction according to Eq. (3.6), the weight vector is given by Eq. (3.11). An array with such weights has unity response in the look direction. Hence, the output power of the weighted array caused by the source in look direction is the same as the source power. In an environment with uncorrelated noise and without directional interference the beamformer yields maximum SNR. For uncorrelated noise the noise correlation matrix is defined by  $R_N = \sigma^2 I$  and the output noise power of beamformer is given by (3.12).

$$\vec{w}_c = \frac{1}{L} \vec{s}_0 \quad (3.11)$$

$$P_N = \vec{w}_c^H R_N \vec{w}_c = \frac{\sigma_n^2}{L} \quad (3.12)$$

The noise power at the array output is reduced  $L$  times compared to the noise power perceived at one element. Hence the array gain, which is the ratio between output  $SNR = p_s L / \sigma^2$  and input  $SNR = p_s / \sigma^2$ , is equal to  $L$  the number of receive antennas. The beamformer cannot be effective in the presence of directional interferers received in side lobes.

### 3.3.2 Zero Forcing Beamformer

A Zero-Forcing beamformer cancels a signal arriving from a known direction. A beam with unity response in a desired direction and zero

response towards interferers has the constraints given by Eq. (3.13) where  $\vec{s}_0$  is the steering vector towards the desired source and  $\vec{s}_i$  represents  $k$  steering vectors towards the  $k$  interferers. The simultaneous equations are given in matrix notations by Eq. (3.14) where  $A$  is a matrix whose columns are the steering vectors towards the sources including the look direction and  $\vec{e}_1^T$  is a vector of zeros except the first element that is a one [Godara, 1997].

$$\vec{w}^H \vec{s}_0 = 1, \quad \vec{w}^H \vec{s}_i = 0, \quad \text{with } i = 1, \dots, k \quad (3.13)$$

$$\vec{w}^H A = \vec{e}_1^T, \quad \text{with } A = [\vec{s}_0, \vec{s}_1, \dots, \vec{s}_k] \quad \text{and} \quad \vec{e}_1^T = [1, 0, \dots, 0]^T \quad (3.14)$$

The weight vector is calculated by Eq. (3.15) if  $k = L - 1$  and the inverse of  $A$  exists. If the inverse of  $A$  does not exist, the pseudo inverse of  $A$  can be used instead. The solution for weight vector is given by Eq. (3.16) if the number of required zeros is less than  $L-1$ . This beamformer is able to cancel the interference of directional jammers but does not minimize the uncorrelated noise at the beamformer output.

$$\vec{w}^H = \vec{e}_1^T A^{-1} \quad (3.15)$$

$$\vec{w}^H = \vec{e}_1^T A^H (A A^H)^{-1} \Rightarrow \vec{w}^H = \vec{e}_1^T A^{-1} \quad (3.16)$$

#### 3.3.3 Optimal Beamformer

The Zero-Forcing beamformer described in the Section 3.3.2 needs to know the directions of interferers and does not maximise the output SNR of the array. The optimal beamformer also known as Minimum Variance Distortionless Response (MVDR) beamformer, overcomes these limitations [Godara, 1997]. It optimizes the output SNR by only knowing the direction of the desired signal.

Let Eq. (3.17) represent the weight vector of an optimal beamformer which optimizes the output SNR with  $R_N$  being the array correlation matrix of the noise only which does not contain any signal from the look direction and  $\mu_0$  is a constant. With unity response in look direction this constant is given by Eq. (3.18) resulting in Eq. (3.19) representing the weight vector. It is also known as the Maximum Likelihood (ML) filter

because it finds the ML estimate of the power of the signal source while assuming signals of other sources as interference.

$$\vec{w} = \mu_0 R_N^{-1} \vec{s}_0 \quad (3.17)$$

$$\mu_0 = \frac{1}{\vec{s}_0^H R_N^{-1} \vec{s}_0} \quad (3.18)$$

$$\vec{w} = \frac{R_N^{-1} \vec{s}_0}{\vec{s}_0^H R_N^{-1} \vec{s}_0} \quad (3.19)$$

In a real system, if an estimate of the noise alone matrix  $R_N$  is not available, the total correlation matrix  $R$  including signal plus noise is used to estimate the weight vector. Note, both approaches perform identically and find the same weight vector [Godara, 1997]. The weights are a solution of the constraints given in Eq. (3.21). The beamformer weights are chosen by minimizing the mean output power of the array while maintaining unity response in the look direction. Eq. (3.21) ensures that the output signal power is the same as the power of the source in look direction. Hence, SINR is maximized by minimizing the noise which includes the interference and the uncorrelated noise. The output signal power of the optimal beamformer is given by Eq. (3.22) [Godara, 1997].

$$\vec{w} = \frac{R^{-1} \vec{s}_0}{\vec{s}_0^H R^{-1} \vec{s}_0} \quad (3.20)$$

$$\underset{\vec{w}}{\text{minimize}} \quad \vec{w}^H R \vec{w}, \quad \text{subject to} \quad \vec{w}^H \vec{s}_0 = 1 \quad (3.21)$$

$$\alpha = p_s \vec{s}_0^H R_N^{-1} \vec{s}_0 \quad (3.22)$$

The optimal beamformer applied to an array with  $L$  elements performs as described above in maximizing SINR by cancelling all interferers, if the number of interferers is less or equal to  $L - 2$ , because such an array has  $L - 1$  degrees of freedom and one degree is spend for the signal in look direction. In the presence of multipath propagation, the optimal beamformer might not be able to maximize SINR by cancelling all interferences. Still, by only partially suppressing inference, the output

SINR is usually significantly improved compared to a conventional beamformer.

### 3.3.4 Optimal Beamformer with Reference Signal

The optimal beamformer described in the Section 3.3.3 requires the knowledge of the direction of the desired signal in order to be able to maximize the output SINR. Figure 3.4 shows the structure of a beamformer which uses a reference signal instead of the knowledge of the direction of the desired signal in order to estimate the weight vector. An error signal is calculated by subtracting the array output from the reference signal:  $\varepsilon(t) = r(t) - \bar{w}^H \vec{x}(t)$ . The calculated error is used to control the weights in a manner that the Mean Squared Error (MSE) between the array output and the reference signal is minimized. The MSE is calculated by Eq. (3.23) where  $\vec{z}$  is the correlation between the reference signal and the array signal vector  $\vec{x}(t)$ . From Eq. (3.23) it can be derived [Godara, 1997] that the optimal weights are given by the well known Wiener-Hoff equation in Eq. (3.24). These weights are used by the Minimum Mean Square Error (MMSE) processor, also known as Wiener filter, which is given by Eq. (3.25). In general, the Wiener-filter provides higher output SINR than the ML filter, see previous Section, if the signal source is weak. If the power of the input signal becomes larger compared to the background noise, the two beamformers yield equal results. Note, that the MMSE scheme (Wiener filter) is a closed-loop method whereas the MVDR scheme (the ML filter) is an open-loop method, see Section 3.5.

$$MSE = E[|\varepsilon(t)|^2] = E[|\varepsilon(t)|^2] + \bar{w}^H R \bar{w} - 2 \bar{w}^H \vec{z} \quad (3.23)$$

$$\text{with } \vec{z} = E[\vec{x}(t)r(t)]$$

$$\bar{w}_{MSE} = R^{-1} \vec{z} \quad (3.24)$$

$$MMSE = E[|r(t)|^2] - \vec{z}^H R^{-1} \vec{z} \quad (3.25)$$

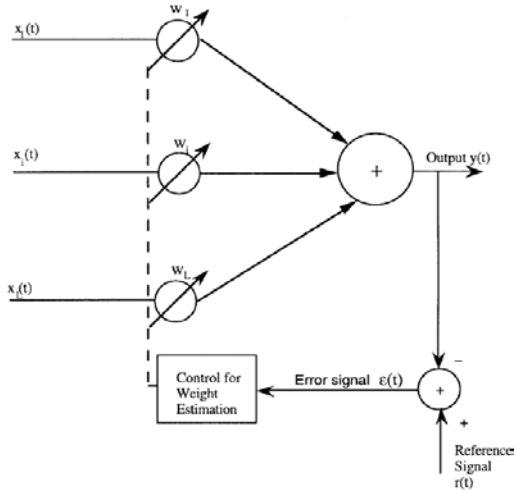


Figure 3.4: structure of a narrow-band beamformer using a reference signal [Godara, 1997]

### 3.3.5 Spatial Filtering for Interference Reduction

As described in the preceding Sections, multi antennas at the BS are able to reduce inter-cell interference in a system by forming one beam and transmitting or receiving one signal at any time. Figure 3.5 (a) shows the pattern of a sector antenna (dashed blue line) and two example fixed beam pattern (solid lines in green and red), always with the same total transmit power. The beam pattern focuses the transmitted energy towards a desired direction compared to the sector pattern which radiates the energy over a broad sector. The beam pattern in downlink decreases inter-cell interference while increasing the signal towards the intended user. In uplink, the applied beam pattern reduces received interference at the BS from undesired directions while keeping the signal strength in look direction. Hence, beams at the BS improve mean SINR of both transmitted and received signals. This type of beamforming is called Spatial Filtering for Interference Reduction [Hoymann, 2008]. The sector pattern in Figure 3.5 (a) is generated by a reflector behind the antenna element. Multiple such elements assembled in an antenna array generate a specific beam by applying phase shifts

[3G Americas, 2010]. Hence a beam pattern, as shown in Figure 3.5, is created by an original symmetrical beam pattern of a linear array superposed by the sector pattern. Note, that the interference towards the back side of the antenna array is also increased in several directions compared to the sector antenna without beamforming. Figure 3.5 (b) shows the beams defined by the codebook in [IEEE 802.16m], which are less narrow than 3GPP beams but have the advantage of lower interference towards the back side of the cell.

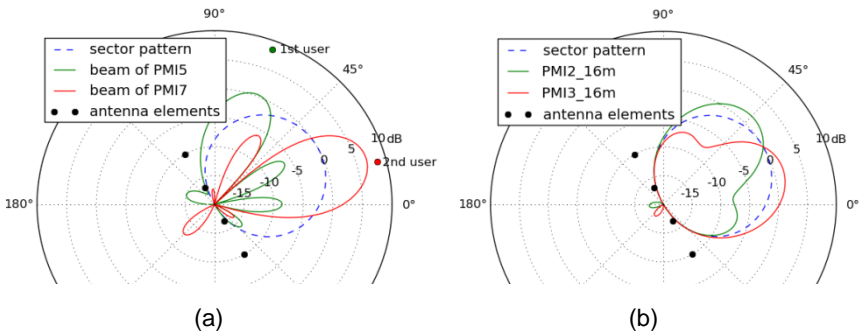


Figure 3.5: sector pattern and example beam patterns defined by the Precoding Matrix Index (PMI) from codebook of (a) [3GPP TS36.211]  $\lambda/2$  and (b) [IEEE802.16m]  $\lambda/4$ ; both with antenna array of four elements with  $30^\circ$ boresight

#### 3.3.6 Spatial Division Multiple Access (SDMA)

SDMA allows for serving multiple users on the same frequency and time resource. Figure 3.6 depicts a beamforming antenna which can transmit different signals into desired directions, simultaneously, by applying individual weight vectors  $(\vec{w}_1, \vec{w}_2, \dots, \vec{w}_3)$  to each signal. In this manner each signal is transmitted by its beam pattern as exemplarily shown in Figure 3.5. Each pattern has a high gain to the desired user and preferably a zero gain towards the other user. Occasionally, a signal cannot be entirely suppressed towards the undesired direction and thus

intra-cell interference occurs. In the receive case joint transmissions allow for concurrent reception of signals from different directions.

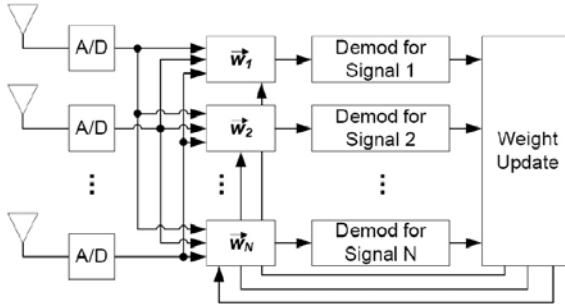


Figure 3.6: beamforming system supporting  $N$  parallel beams [Liberti and Rappaport, 1999]

### 3.4 Fixed Beamforming

Fixed beam pattern usually rely on a codebook providing a limited number of predefined weight vectors. The size of the codebook depends on the number of employed elements and is a trade-off between the number of signalling bits required to address a particular matrix in the codebook and the suitability of the resulting transmitted beam direction. In this manner due to the limited number of beams, the overhead of measuring and signalling the channel state is significantly reduced versus adaptive beamforming, especially in FDD. Only a few bits are needed for the Precoding Matrix Index (PMI) to signal a preferred beam. The techniques SFIR (Section 3.3.5) and SDMA (Section 3.3.6) can be conducted with fixed beamforming although the gain is degraded due to the suboptimal beams applied. Scheduling of radio resources is simpler especially with multiple beams (i.e., SDMA) since adaptive beamforming requires advanced grouping algorithms selecting simultaneously served MSs [Hoymann, 2007]. The limited number of beams under fixed beamforming enables analytical performance evaluation on system level, which is not possible owing to the infinite number of beams under adaptive beamforming. To the best

knowledge of the author, no analytical model of adaptive beamforming is known suitable for system level performance evaluation. In current 3GPP standards and corresponding products, fixed beamforming transmission is applied but adaptive beamforming transmission is not applied due to its sophistication.

### **3.5 Open- versus Closed-Loop MIMO**

In Open-Loop MIMO, the assumption is that the transmitter only knows the channel statistics but not its actual realization (hence “open-loop”). The transmitter transmits equal power ( $P/M$ ) from each antenna element. The receiver perfectly knows the channel. In Closed-Loop MIMO the channel is assumed known at both the transmitter and receiver and the transmitter therefore can coherently weight the signals on each antenna element.

## CHAPTER 4

---

# The Model of the Analytical Evaluation and the IMT-Advanced Channel Model

### 4.1 Introduction

Channel models allow performance evaluation of wireless systems by means of computer simulation. ‘Simulation of wireless systems such as LTE-Advanced are essential in the research and standardization phase when the technology is still being developed. At this stage, prototypes are often not available and testing different candidate features in the field would be too expensive and time consuming. In comparison, simulations can be set up easily and deliver quick results. For relevant simulation results the radio channels as well as the investigated wireless system have to be modelled accurately enough’ [Ellenbeck, 2012c]. The International Telecommunication Union (ITU) adopted a well established spatial channel model developed by the WINNER project [WINNER II D 1.1.2, 2008] when it defined the “Guidelines for evaluation of radio interface technologies for IMT-Advanced” [ITU-R M.2135].

These guidelines are presented in Section 4.2 and the channel model in Section 4.3. Both are considered as de facto standards followed by both 3GPP and IEEE standardization bodies during self evaluation of their respective system concepts proposed, as well as by independent IMT-Advanced evaluation groups. Section 4.3.3 introduces the analytical tool for evaluation of SINR, data rate, throughput and cell spectral efficiency distributions. Section 4.4 presents the metrics used to validate the channel model implementations and give example validation results. To

## 4 The Model of the Analytical Evaluation and the IMT-Advanced Channel

be able to evaluate a wireless system by system-level simulation, a so-called link-to-system model is typically employed to reduce simulation complexity while preserving the main performance characteristics of the wireless links. In Section 4.5, commonly applied link-to-system mapping techniques are introduced. Building on that in Section 0, simulation results of an LTE system are shown that base on the channel model and the link-to-system mapping techniques chosen. Finally, the results of the IMT-Advanced system level tool are calibrated against the *IMTaphy*<sup>12</sup> which is a well calibrated IMT-Advanced system level simulator.

This work particularly extends the evaluation tool basing on [Buelmann, 2010] by beamforming and beam coordination capabilities (see Section 4.2.3, 4.3.6, 5.4), metrics based on probability distributions (see Section 4.3.7, 4.5.2, and 4.5.4), scheduling strategies using the probability of number of MSs per cell (see Section 4.5.3 and 4.5.4), and by validation results of the channel model and the LTE-Advanced system (see Section 4.4 and 0).

### 4.2 ITU-R Evaluation Guidelines

The ITU-R guidelines [ITU-R M.2135-1] define a general procedure of evaluation, performance metrics, test environments, scenarios, and equivalent channels models. The document specifies test environments which span the range of possible operating environments of IMT-Advanced systems and allow for well comparable evaluation results. Three evaluation procedures are proposed: simulation, analysis and inspection. Several performance metrics such as Cell Spectral Efficiency (CSE) and VoIP capacity are supposed to be evaluated by system level simulations considering multiple layers of the protocol stack of a cellular system operating many communication links in multiple cells at the same time. Modelling all links allows to consider mutual interference which is an important factor limiting system performance.

---

<sup>12</sup> The IMTaphy has been released as an open-source project on the Internet [Ellenbeck, 2012a] [Ellenbeck, 2012b] using the framework of the openWNS [Buelmann, 2009].

In contrast to link level simulation, focusing only on a single communication link, in this work a system level model is employed that also takes link-to-system simulation results in to account.

#### 4.2.1 Deployment Scenarios

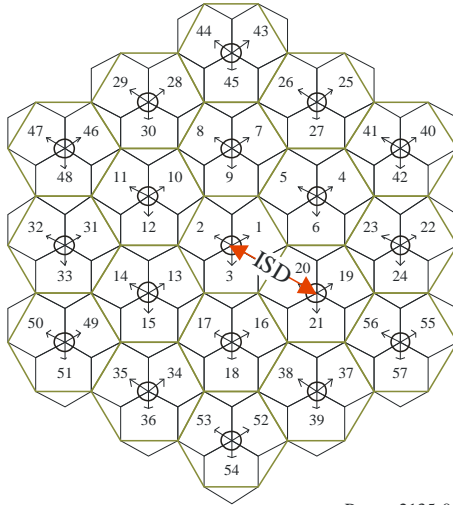
Table 4.1 lists the deployment scenarios and the corresponding test environments and channel models as defined in [ITU-R M.2135] used for evaluating performance metrics. In this work, only parameter sets of cellular scenarios for the Urban Macro-cell (UMa) scenario are studied, summerized in Table 4.2 as defined in the ITU guidelines [ITU-R M.2135] and [ITU-R M.2134]. Several parameters such as the BS antenna downtilt are not specified by the ITU and are parameterised by the 3GPP's specifications for system-level simulations as described in the annex of [3GPP TR 36.814].

Table 4.1: deployment scenarios and related channel models  
[ITU-R M.2135, Table A1-1]

Deployment scenario	Indoor hotspot	Urban micro-cell	Urban macro-cell	Rural macro-cell
Test environment	Indoor	Microcellular	Base coverage urban	High speed
Channel model	InH	UMi	UMa	RMa

Figure 4.1 shows a model of a cellular deployment with 19 sites used to study UMa scenarios. At each site, one BSs is equipped with three sectorised antennas each serving a hexagonal cell. The deployment scenario comprises 57 cells (= 19 sites x 3 cells). Inter-site distance is 500m for UMa scenario. Cellular systems in the real world cover large areas with hundreds of cells potentially interfering. Their capacity is inter-cell interference limited. In modelling cellular systems, a good trade-off between low complexity and an accurate representation of interference is achieved by the wrap around scenario of 19 sites shown in Figure 4.1.

## 4 The Model of the Analytical Evaluation and the IMT-Advanced Channel



Report 2135-01

Figure 4.1: hexagonal cell layout, Figure 1 in [ITU-R M.2135]

In the analysis (sketched in Table 4.3) wrap around is neglected and hence only metrics of cells of the centre site are evaluated that are surrounded by two tiers of interfering sites. This modified scenario is proven to yield correct results, see the validation results in Section 4.4.

Pathloss and SINR calculation are conducted for each intersection point of an equidistant grid placed over the scenario area. The number of MSs served per cell is considered as described in Section 4.5.3. MSs are associated to the BS with the strongest Reference Signal Received Power (RSRP). The effect of handover hysteresis of 1dB handover margin which keeps a MS associated to its previous BS while another is already stronger is considered in the analysis, as assumed in [3GPP TR 36.814].

Several parameters of the channel model presented in Section 4.3 depend for example on distance between BS and MS. As a simplification, all distances are measured in the xy-plane in two dimensions only without taking BS or MS heights into account. However, antenna field patterns are modelled in three dimensions (see Section 4.2.2) so that the elevation angle between MS and BS is

computed, correctly. MSs are assumed to be outside the small circular area around a site shown in Figure 4.1 with a radius defined in Table 4.2 as the minimum distance between BS and MS [ITU-R M.2135].

Table 4.2: UMa scenario and configuration parameters

<b>Deployment scenario</b>	<b>Urban macro-cell</b>
Parameter	
Channel model	UMa
BS height	25 m
Min. BS-MS distance	25 m
Carrier frequency	2 GHz
Antenna downtilt [3GPP TR 36.814]	12°
Inter-site distance	500 m
User distribution	Vehicles, Uniform
UT speeds	30 km/h
Total BS transmit power for 20 MHz	49 dBm
Max. UT transmit power	24 dBm
BS noise figure	5 dB
UT noise figure	7 dB
BS antenna gain (boresight)	17 dBi
UT antenna gain	0 dBi
Thermal noise level	-174 dBm/Hz
Number of users per cell	10

### 4.2.2 Antenna Model

The IMT-Advanced evaluation guidelines [ITU-R M.2135] only specify simple antenna patterns with vertical polarization. The mobile antenna is assumed to be omnidirectional with 0 dBi gain. The BS antenna for the hexagonal scenarios in Figure 4.1 is defined as a three-dimensional pattern with azimuth and elevation power gain patterns as shown in Figure 4.2.

#### 4 The Model of the Analytical Evaluation and the IMT-Advanced Channel

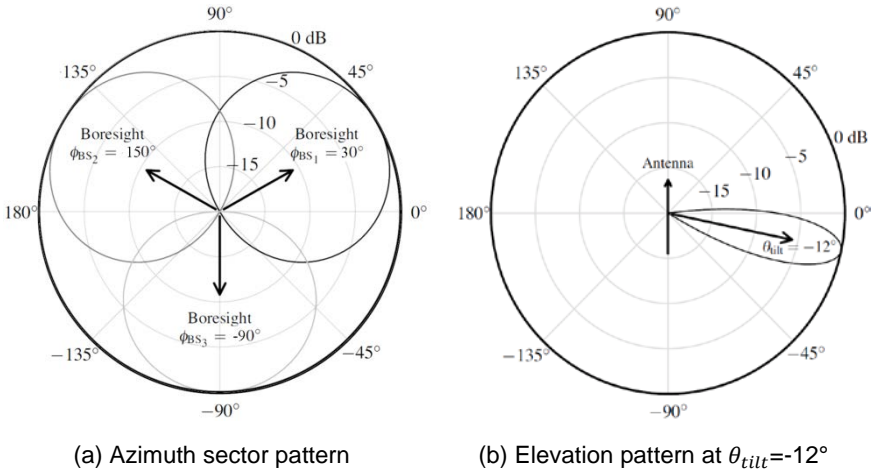


Figure 4.2: antenna gain pattern<sup>13</sup>

The horizontal antenna pattern used for each sector is specified by Eq. (4.1), where  $A_a(\phi)$  is the relative azimuth antenna gain (in the xy-plane) and  $\min[.]$  denotes the minimum function,  $\phi_{3dB}$  is the 3 dB beamwidth (corresponding to  $\phi_{3dB} = 70^\circ$ ), and  $A_{min} = 20 \text{ dB}$  is the maximum attenuation. Figure 4.2 (a) shows the antenna pattern of the BS for a site with three cells, which are defined relative to the azimuth angle of the antenna array boreside direction  $\phi_{BS}$ .

The elevation antenna pattern is given by Eq. (4.2) where  $A_e(\theta)$  is the relative elevation antenna gain (upwards angle from the xy-plane),  $\theta_{3dB}$  is the elevation 3 dB value, and it is assumed to be  $15^\circ$ . The patterns are defined relative to the downtilt angle  $\theta_{tilt}$  of the antenna array. Downtilt angle  $\theta_{tilt}$  is not defined by ITU and hence the 3GPP default value of  $-12^\circ$  is taken as defined by [3GPP TR 36.814]. The combined antenna pattern at angles off the cardinal axes is computed in Eq. (4.3).

<sup>13</sup> Antenna gain of 17 dBi is to be added, i.e., the omnidirectional antenna gain

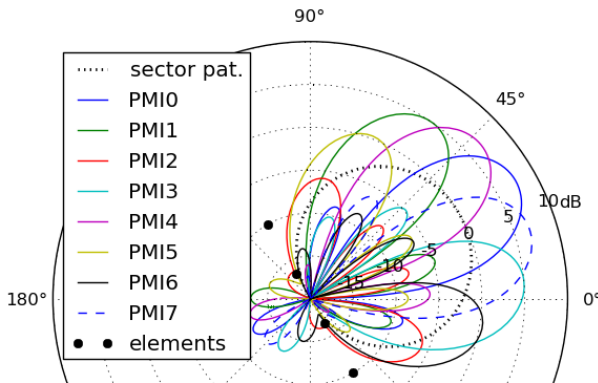
$$A_a(\phi) = -\min \left[ 12 \left( \frac{\phi - \phi_{BS}}{\phi_{3dB}} \right)^2, A_{min} \right] \text{ in dB}, -180 \leq \phi - \phi_{rot} \leq 180 \quad (4.1)$$

$$A_e(\theta) = -\min \left[ 12 \left( \frac{\theta - \theta_{tilt}}{\theta_{3dB}} \right)^2, A_{min} \right] \text{ in dB}, -90 \leq \theta - \theta_{tilt} \leq 90 \quad (4.2)$$

$$A(\theta, \phi) = -\min \left[ -(A_a(\phi) + A_e(\theta)), A_{min} \right] \text{ in dB} \quad (4.3)$$

### 4.2.3 Antenna Model with Beamforming

Figure 4.3 shows example beam patterns according to the precoding matrices of the codebook in [3GPP TS 36.211] for four antenna elements. A Precoding Matrix Index (PMI) is used to indicate a beam pattern. The weight vectors given by the codebook are applied according to Eq. (3.5). The sector pattern is generated by a reflector behind the antenna element. Multiple such elements assemble an antenna array which generates a specific beam by employing the appropriate phase shifts [3G Americas]. Hence a beam pattern, as shown in Figure 4.3, is created by an original symmetrical beam pattern of a linear antenna array superposed by the sector pattern of Figure 4.2.



## 4 The Model of the Analytical Evaluation and the IMT-Advanced Channel

Figure 4.3: beam pattern of codebook in [3GPP TS 36.211] for four antenna elements, calculated by Eq. (3.5). Sector antenna characteristic (see Figure 4.2 (a)) is already included in the diagram.

### 4.3 Radio Channel Model

#### 4.3.1 Pathloss Model

The pathloss in UMa scenario consists of a distance component plus a vehicle penetration loss component which is lognormal distributed with mean of 9 dB and standard deviation of  $\sigma = 5$  dB as defined in [ITU-R M.2135] and [Finland].

$$PL(d) = PL_b(d) + PL_{veh} \text{ in dB, with } PL_{veh} \sim \ln \mathcal{N}(9\text{dB}, 5\text{dB}) \quad (4.4)$$

Note that the vehicle penetration loss  $PL_{veh}$  is specific to each user, i.e., the same loss from one vehicle to all BSs is assumed. The models for the basic pathloss  $PL_b(d)$  for various deployment scenarios are derived from channel models of the IST-WINNER II project. The models are valid in the frequency range of 2-6 GHz in the UMa scenario. The pathloss of a LOS link characteristic is modelled by a two slope model with a higher path-loss exponent for distances beyond a break point  $d_{BP}$ . The model for the basic path-loss allows for variable parameters such as street width, average building heights, height of BS and MS as well as centre frequency. Assuming the standard parameter set given in Table 4.2 and [ITU-R M.2135], a simplified form of pathloss equations is given by Eq. (4.5) - (4.6) for scenarios UMa. The break point distance is calculated as  $d_{BP} = 2\pi h'_{BS} h'_{MS} f_c / c$  where  $h'_{BS}$  and  $h'_{MS}$  are the height of the BS and MS (minus one meter), respectively,  $f_c$  is the centre frequency and  $c$  is the speed of light.

In the UMa scenario with  $h_{BS} = 25m$ ,  $h_{MS} = 1.5m$  and  $f_c = 2GHz$ , the break point distance is  $d_{BP} = 320m$ . The basic pathloss in the UMa scenario is given by Eq. (4.5) for LOS and by Eq. (4.6) for Non-LOS (NLOS) link characteristic, as shown in Figure 4.4 versus distance.

$$PL_{b,LOS} = \begin{cases} 22 \log_{10}(d) + 34.02 \text{ in dB, if } 10m < d < 320m \\ 40 \log_{10}(d) - 11.02 \text{ in dB, if } 320m < d < 5000m \end{cases} \quad (4.5)$$

$$PL_{b,NLOS} = 39.09 \cdot \log_{10}(d) + 19.57 \text{ in dB} \quad (4.6)$$

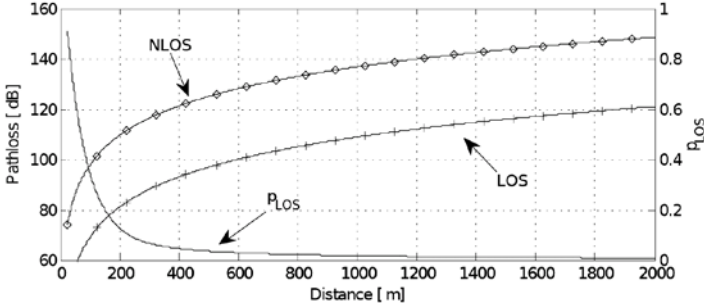


Figure 4.4: pathloss and LOS probability in UMA

### 4.3.2 Line-of-sight Propagation Probability

[ITU-R M.2135] suggests after defining positions of MS in a given deployment scenario, the first step for initializing the channel model is randomly classifying each link (of BS to MS) to have LOS or NLOS characteristic. The LOS probability  $Pr(d)$  as a function of the distance  $d$  in the xy-plane is given in Eq. (4.7) for UMA. Obviously, the closer a MS is to a site the more likely the corresponding link has LOS propagation condition, see Figure 4.4. Note that the propagation condition is defined on a per-site basis so that a user experiences identical propagation conditions to co-located antenna (arrays) at a site.

$$Pr_{UMa,LOS} = \begin{cases} (1 - e^{-d/63}) + e^{-d/63} & \text{if } d \leq 18 \\ 18/d \cdot (1 - e^{-d/63}) + e^{-d/63} & \text{if } d > 18 \end{cases} \quad (4.7)$$

The probability of a NLOS propagation condition is:

$$P_{rNLOS} = 1 - P_{rLOS} \quad (4.8)$$

### 4.3.3 Overview of the System Level Evaluation Model

The analytical approach presented in this Section using the previous models and scenarios calculates performance metrics on system level for downlink considering inter-cell interference. A separate link-to-system model is employed in order to enable the use of link adaptation.

In contrast to stochastic event driven simulation using the *drop concept* [ITU-R M.2135], the presented analytical tool takes the approach of *permutations* [Bueltmann, 2010] which can be described by considering an infinite number of drops. In the drop concept a realization of a random variable such as the position of a MS in the cell is defined once for the duration of a simulation so that the randomly chosen instance of the path loss to serving and interfering BS is fixed. A *permutation instance* is a set of link realizations concerning LOS or NLOS link characteristic of all BSs involved. By considering all permutations (i.e. all combinations of link characteristics in terms of NLOS/LOS), the model used within this work is equivalent to a model with an infinite number of drops as shown in [Bueltmann, 2010] providing an exact mean throughput, see Section 4.3.6. In contrast, an event driven simulator such as the IMTAphy [Ellenbeck, 2012a&b] calculates performance metrics for a sufficient number of drops targeting to converge the mean value, such as the mean throughput<sup>14</sup>, with a predefined statistical confidence level. During a *drop*, users are randomly dropped into the scenario and for each BS to MS link a specific channel characteristic (LOS or NLOS) is independently assumed.

As the focus is on evaluating the performance of the beam coordination process which is supposed to happen on a longer time scale (seconds and longer), small scale effects like fast fading are not modelled. The small-scale component of shadowing is also neglected in this model because it can be considered as random processes with zero mean and hence does not affect the calculated mean values.

---

<sup>14</sup> Other metrics than *throughput* are for example SINR, packet delay, distributions of random variables.

Table 4.3 presents the structure of the system model as pseudo code which is commented in the following. While iterating over all link permutations (as discussed in Section 4.3.5, and, if beamforming is enabled, also over all beam permutations (as presented in Section 4.3.6), in each iteration the path loss is calculated at each grid point to all BSs. The pathloss calculation comprises the antenna model of Section 4.2.2 and channel model of Section 4.3. Depending on path loss values, a grid point is associated to the best serving BS which receives signals from other BS as interferences. SINR at the MS is calculated and the best suited data rate is derived by considering the overhead of the LTE feedback and control channels (see Section 2.3.7.3) and the link-level model (see Section 4.5.1). The data rates achieved at grid points in the evaluation area are weighted by their local permutation probabilities (see Section 4.3.5) and stored in a histogram common for all permutation instance. From the resulting data rate distribution (such as in Figure 6.2) a distribution of the mean user throughput is derived (as shown in Figure 4.15) by considering a scheduling strategy (see Section 4.5.4) and probabilities of different numbers of users (as in Section 4.5.3). A full buffer traffic model according to [ITU-R M.2135, Annex 2] is assumed for each MS. The Cell Spectral Efficiency (CSE) and the Cell Edge User Spectral Efficiency (CE-USE) are derived as the mean and the 5<sup>th</sup> percentile of the mean user throughput distribution, respectively (see Section 4.5.4). Instead of a histogram (in line eight), a map can be calculated (as in Figure 4.7) showing the dependency of the metric on the position.

## 4 The Model of the Analytical Evaluation and the IMT-Advanced Channel

Table 4.3: analytical system model in pseudo code

```

1  for all link_permutations:
2      for all beam_permutations: #if beamforming
3          for grid_point in evaluation_area:
4              calculatePathLoss() #for each link
5              associate2servingBS() #with sector pattern
6              calculateSINR()
7              calculateDataRate() #by means of link-level model
8              histogram.put(rate) #weight by local permutation probability
9  deriveMeanUserThroughputDistribution() #by considering #users & scheduling
10 calculateMean() #i.e. CSE
11 calculate5thPercentile() #i.e. CE-USE

```

### 4.3.4 Receive Power and Signal to Interference Plus Noise Ratio

The received power at the position of a MS,  $P_{Rx}$ , is:

$$P_{Rx}(x, y) = P_{Tx} \cdot G_{MT}(\theta, \phi) \cdot G_{BS}(\theta, \phi) \cdot L_{PL}(d) \text{ in } W \quad (4.9)$$

where  $P_{Tx}$  is the total power emitted at the transmitter,  $G_{MT}$  and  $G_{BS}$  is the directional antenna gain at the MS and BS, respectively and  $L_{PL}$  is the path loss depending on the distance  $d$  between transmitter and receiver. If beamforming technology is applied, the directional antenna gain  $G_{BS}(\theta, \phi)$  of a BS depends on a given beam pattern (e.g., as depicted in Figure 4.3).

In Eq. (4.10), the downlink SINR is calculated by the power of the desired signal from transmitter  $m$  divided by the sum of the interfering signals from transmitter  $l \in M$  with  $l \neq m$  plus the thermal noise level including the MS's noise figure  $n$ . Each permutation  $j \in J$  is build according to Section 4.3.5, where  $J$  is the set of all link permutations.

$$SINR_{m,j} = \frac{P_{Rx}(d_m)}{\sum_{\substack{l \in M \\ l \neq m}} P_{Rx}(d_l) + n}, \text{ in dB} \quad (4.10)$$

The term  $SINR_{m,j}$  is in the following also referred to by the term  $SINR_j(\vec{x})$ , because the position  $\vec{x}$  and the permutation instance  $j$  uniquely defines all distances  $d_l$  to the transmitter and interferers.

### 4.3.5 Link Permutation Probability

The ITU report M.2135 suggests for system level simulation that MSs are placed in a scenario and randomly assigned to LOS and NLOS channel condition for each MS to BS link<sup>15</sup>. The probability for one link condition at a position is given by Eqs. (4.7) and (4.9). One combination of allocated link characteristics (in terms of LOS/NLOS) between a MS and all sites is called *permutation instance*, Figure 4.5. A permutation instance can be described by a binominal word with a bit length equal to the number of sites in the scenario, where '1' stands for LOS and '0' for NLOS condition. A bit in the word represents a link between a MS and a specific site. Over the permutations, the serving BS of a MS at a given position can vary assuming an association to the strongest RSRP. This can occur for example because in several permutations, the strongest RSRP is originated from a more distant BS via a link with LOS condition, if links from close BSs have NLOS characteristic. With the number  $M$  of cells, the number of sites in the scenario is  $M/3$ . Accordingly,  $2^{(M/3)}$  possible combinations of link characteristics or *permutation instances* can occur for a given MS. The probability of a permutation instance is calculated in Eq. (4.11) by multiplying the site specific individual link probabilities. Where  $I$  is the set of LOS links and  $I^*$  is the set of NLOS links.

$$p_{perm,j} = \prod_{i \in I} p_{LOS,i} \prod_{i^* \in I^*} (1 - p_{LOS,i^*}), \forall j \quad (4.11)$$

---

<sup>15</sup> LOS or NLOS link characteristics are identical between a MS and BS co-located at the same site.

## 4 The Model of the Analytical Evaluation and the IMT-Advanced Channel

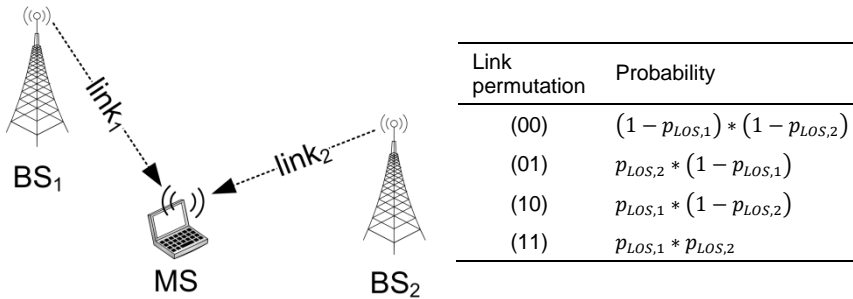


Figure 4.5: link permutation instances of two BSs as binominal words, where  $i^{\text{th}}$  bit defines  $i^{\text{th}}$  link characteristic, with 1 = LOS, 0 = NLOS

### 4.3.6 Beam Permutation Probability

This Section explains how fixed beams, as discussed in Section 4.2.3, are considered in the model. A number of beams  $n_{beams}$  is available from a specific codebook or a subset thereof and can be applied at each BS. Only one beam at a time per BS is assumed, as SDMA is out of scope of this model. The possible combination of applied beams, one per BS, is called *beam permutation instance* in the following. The number of possible beam permutation instances is the number of available beams  $n_{beams}$  (e.g. = 7) to the power of the number of cells  $n_{cells}$  in the scenario, i.e.,  $n_{beams}^{n_{cells}}$ . Figure 4.6 shows the areas where preferably different beams are applied for the examples of seven beams. As the areas covered by a beam are approximated to be of the same size<sup>16</sup>, the mean amount of radio resources allocated to a beam is almost the same. Accordingly, the probability of operating a beam is approximated to be the same. From

<sup>16</sup> The initial areas covered by each of the seven beams are close to a 7<sup>th</sup> part (14.3%) of the cell area except the outer beams initially covering only 7%. Equalizing areas served by a beam can be reached by using an offset in the beam association process in a way that smaller areas are advantaged. The resulting beam association has only marginal lower cell spectral efficiency than the one shown in Figure 4.6 because SINR reductions are small and results either in the same data rate (MCS) or in marginally lower data rate, see Figure 4.12.

this assumption, the probability for one beam permutation instance can be derived as being equal to the inverse of the number of beam permutation instances.

$$p_{beam\ perm} = 1/(n_{beams}^{n_{cells}}) \quad (4.12)$$

If beam coordination is conducted, all beam permutations are generated for each link permutation instance and potentially contribute to the SINR at a grid point. The association of a MS to a cell is conducted with sector antenna patterns as the broadcast control channel does not support beamforming. Then of the chosen cell, the best serving beam is selected at each position as shown in Figure 4.6. Only permutation instances considering the selected beam of the serving BS contributes to the SINR computation at a given position. In this manner, the considered number of beam permutations per grid point (for each link permutation<sup>17</sup>) is reduced by  $n_{beams}$  to  $n_{beams}^{n_{cells}-1}$ . The probability for a beam permutation instance under coordination has to be corrected to:

$$p_{beam\ perm} = 1/(n_{beams}^{n_{cells}-1}) \quad (4.13)$$

The number of beam permutation instances calculated for each link permutation is computer runtime limited. Hence, the number of link permuted sites is reduced to the first tier of sites and the number of beam permuted BSs is limited to the first tier of cells, yielding  $n_{beams}^6$  beam permutations and  $2^7$  link permutations. Assuming a beamforming system with 7 beams, this scenario still requires calculations of more than 15 million permutations and results in computer runtimes in the order of days for one given parameter set.

---

<sup>17</sup> This specific serving pair per position (of serving cell and beam) alters in different link permutations.

## 4 The Model of the Analytical Evaluation and the IMT-Advanced Channel

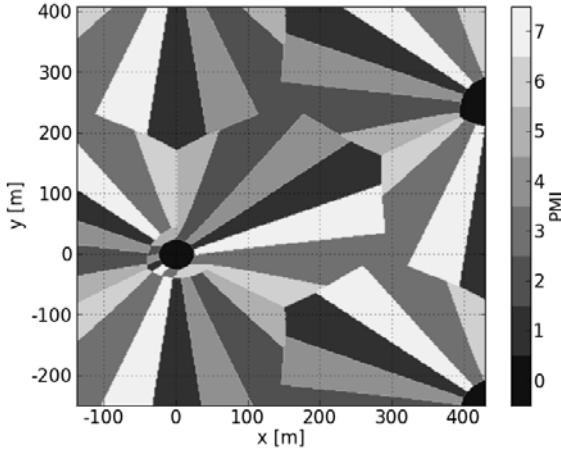


Figure 4.6: map of most likely applied beams; identified by Precoding Matrix Index (PMI), UMa scenario with LOS; centre site in origin (0m,0m)

### 4.3.7 Mean SINR and Probability of SINR

In Eq. (4.14), mean SINR ( $\overline{SINR}(\vec{x})$ ) is calculated for a position by summing SINR values (see Eq. (4.10)) of each permutation instance  $j$ , weighted by the probability  $p_{perm,j}$ . (see Eq. (4.11))

$$\overline{SINR}(\vec{x}) = \sum_{j \in J} p_{perm,j} SINR_j(\vec{x}) \quad , \text{ in dB} \quad (4.14)$$

Where  $J$  is the set of all possible link permutations. This mean SINR ( $\overline{SINR}(\vec{x})$ ) is computed for all positions<sup>18</sup> in the cellular system and plotted in the xy-plane in Figure 4.7.

---

<sup>18</sup> *All positions* refers to all intersections of an equidistant grid. The chosen distance between neighbor points of the grid depends on scenario and is for example 5 m in an Urban Macro-cell scenario.

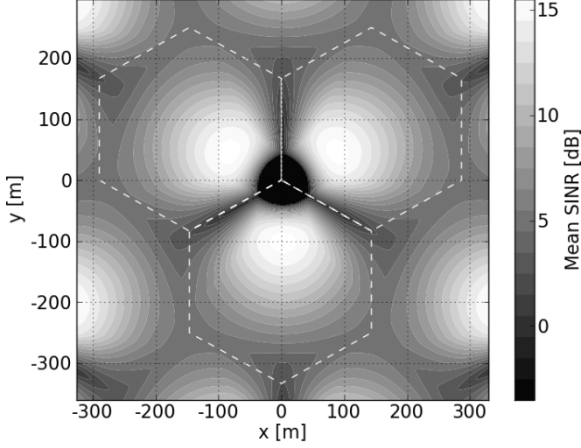


Figure 4.7: example of mean SINR topography [dB]; UMA scenario with sectorised antennas

Eq. (4.15) formally defines the probability of the SINR (see Eq.(4.10)) at position  $\vec{x}$  for the permutation instance  $j$  to be used to calculate the SINR probability of the entire cell given by Eq. (4.16). Eq. (4.16) integrates over the evaluated cell area  $A_{cell}$ , consisting of  $n_A$  number of grid points, and over all link permutation instances ( $j \in J$ ).

$$P_{j,\vec{x}}(SINR) = 1, \text{ if } SINR = SINR_j(\vec{x}) \quad (4.15)$$

$$P_{cell}(SINR) = \frac{1}{n_A} \sum_{\vec{x} \in A_{cell}} \sum_{j \in J} p_{perm,j} P_{j,\vec{x}}(SINR) \quad (4.16)$$

Exemplarily, the probability of SINR (see Eq.(4.16)) is shown by Figure 4.9 in an UMA scenario. With beamforming, mean SINR and its probability are calculated in Eq. (4.17) to (4.19) by also considering beam permutation instances ( $k \in K$ ) and their probabilities ( $p_{beam\ perm,k}$ ), see Eq.(4.12) or (4.13):

$$\overline{SINR}(\vec{x}) = \sum_{j \in J} p_{perm,j} \sum_{k \in K} p_{beam\ perm,k} SINR_{j,k}(\vec{x}) \quad (4.17)$$

$$P_{j,k,\vec{x}}(SINR) = 1, \text{ if } SINR = SINR_{j,k}(\vec{x}) \quad (4.18)$$

## 4 The Model of the Analytical Evaluation and the IMT-Advanced Channel

$$P_{cell}(SINR) = \frac{1}{n_A} \sum_{\vec{x} \in A_{eval}} \sum_{j \in J} p_{perm,j} \sum_{k \in K} p_{beam perm,k} P_{j,k,\vec{x}}(SINR) \quad (4.19)$$

Where  $K$  is the set of all possible beam permutations.

### 4.4 Channel Model Validation

The IMT-Advanced evaluation guidelines and channel model are implemented in simulation tools owned by different entities involved in the IMT-Advanced evaluation process. Simulation results gained by different tools usually differ due to a great many of parameters and the complexity of system-level simulators and channel model implementations. Several reasons exist for a potential deviation of simulation results such as

- specifications of the fully standardized LTE system have still many freely selectable parameters,
- several algorithms are not specified such as the scheduling of data packets and radio resources,
- in detail defined models and guidelines still leave room for interpretation.

3GPP and independent evaluation groups such as the project WINNER+ conducted calibration campaigns in order to align simulation results. Sources of errors have been reduced by defining a detailed specification of simulation parameters and algorithm assumptions. In the calibration process, evaluations have been conducted such as comparing distributions of certain metrics instead of mean values. The IMTaphy tool is well calibrated against 3GPP evaluation group member's results and is utilized for the validation of the analytical tool.

For the large-scale calibration which neglects multipath effects, two metrics are presented here: the feeder pathgain CDF and the wideband SINR CDF. Feeder pathgain is the mean difference between MS received and BS transmitted power disregarding fast-fading. It's components are the feeder loss, the pathloss of the feeder link, shadowing, outdoor to vehicle penetration loss, and the transmitter and receiver antenna patterns with their respective gains. Figure 4.8 shows the feeder

pathgain CDF from Eq. (4.9) of the analytical tool (Table 4.3) and of the IMTaphy [Ellenbeck, 2012a&b]. This comparison validates the channel model implementation of the analytical tool including association of MSs to BSs, placement of MSs in the cells, the classification of links in LOS/NLOS. Figure 4.9 depicts the mean downlink SINR CDF in a reuse one UMa scenario. Again, results obtained with the permutation based analytical tool and results obtained by the calibrated IMTaphy simulator match very well.

Simulation with the IMTaphy tool are conducted for the scenario of Figure 4.1 with the same parameter set used by the analytical tool: fast fading and random shadowing are disregarded and vehicle penetration loss is modelled by a constant value ( $9 \text{ dB}$ ) instead of a log-normal distributed loss ( $\mathcal{N}(9; 5)$  in  $\text{dB}$ ). The analytical tool evaluates the area of cells at the central site only, whereas the IMTaphy evaluates the entire scenario with wraparound technique. The result comparison confirms that correct results are gained by evaluating only the area of cells at the central site.

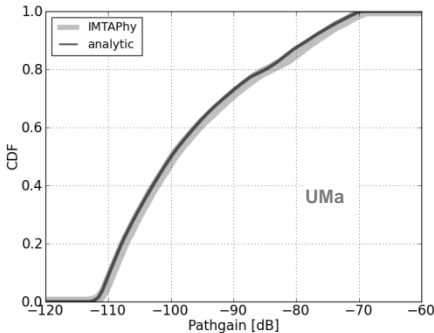


Figure 4.8: Feeder Pathgain CDF

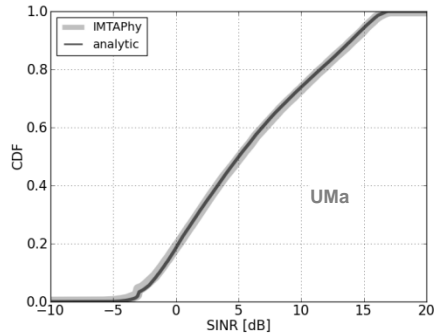


Figure 4.9: Wideband SINR CDF

## 4.5 Link-to-System Model

### 4.5.1 Link-to-System-Level Mapping

SINR during a transmission of a PRB and a chosen MCS results in a certain Block Error Rate (BLER). If a target maximum BLER is given, Figure 4.11 shows which MCS has to be chosen depending on SINR, assuming a transport block length of 50 PRB. If several PRBs with different SINR values are transmitted in a transport block, their mean Mutual Information per Bit (MIB) value is calculated over all PRBs instead and mapped to an *effective SINR* value by means of the graphs in Figure 4.10. With this effective SINR value, a BLER is derived by means of the look-up-table in Figure 4.11. This manner of deriving a BLER from multiple MIs is called MI Effective SINR Metric (MIESM).

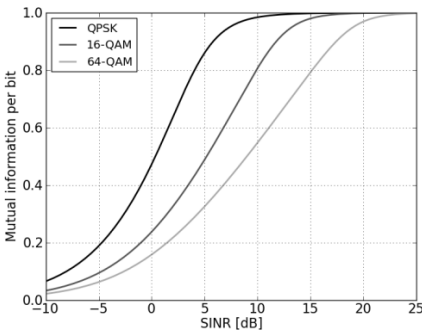


Figure 4.10: Mutual Information per bit depending on the SINR and the modulation [Schoenen, 2007]

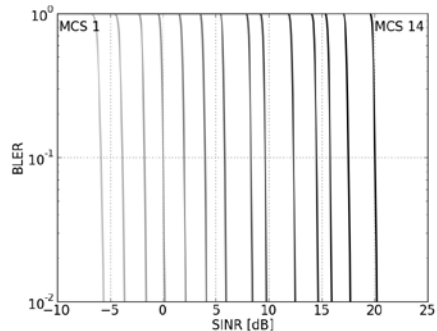


Figure 4.11: Block Error Rate for 14 MCSs based on [Olmos, 2010]

Figure 4.11 is a result of link level simulation [Olmos, 2010] with made assumptions listed in Table 4.4. Table 4.5 gives applied MCS and length of transport block sizes (bits). Figure 4.12 shows the throughput taking into account the BLER = 0.01 based on Eq. (4.20) [Bertsekas, 1992], where

$\gamma_{\text{Layer3}}$  is the throughput above the data link layer and  $\gamma_{\text{Layer2}}$  is the throughput at MAC layer.

$$\gamma_{\text{Layer3}} = \gamma_{\text{Layer2}}(1 - \text{BLER}) \quad (4.20)$$

In order to improve computational performance and reduce memory consumption of the evaluation software tool, the link capacity can be approximated in a compact formula instead, shown in Figure 4.12.

$$C(\text{SINR}) = \begin{cases} 0 & , \text{if } \text{SINR} < 5,6 \text{ dB} \\ \left(\frac{\text{SINR} + \alpha}{\beta}\right)^\gamma * 10^{-1} & , \text{if } 5,6 \text{ dB} < \text{SINR} < 21,5 \text{ dB} \\ C_{\text{max}} & , \text{if } \text{SINR} > 21,5 \text{ dB} \end{cases} \quad (4.21)$$

Where  $\alpha = 17.5415$ ,  $\beta = 10.0371$ ,  $\gamma = 2.5450$  and  $C_{\text{max}} = 3.17$  bit/s/Hz.

Table 4.4: basic assumptions made by iTeam in link level simulations within WINNER+ [Olmos, 2010]

Parameter	Comment
Transmission scheme	SIMO 1x2
fixed Transport Block Sizes	50 physical resource blocks
HARQ	Maximum 1 transmission
Receiver type	MRC
Control channel overhead	3 symbols plus reference signals
Channel model	AWGN

## 4 The Model of the Analytical Evaluation and the IMT-Advanced Channel

Table 4.5: Modulation and Coding Schemes for LTE based on [Olmos, 2010]]

Name	Modulation	Code Rate	Transport Block Size in bit
MCS 0		out of range	
MCS 1	QPSK	0.12	1384
MCS 2	QPSK	0.19	2216
MCS 3	QPSK	0.30	3624
MCS 4	QPSK	0.44	5160
MCS 5	QPSK	0.59	6968
MCS 6	16-QAM	0.37	8760
MCS 7	16-QAM	0.48	11448
MCS 8	16-QAM	0.60	14112
MCS 9	64-QAM	0.46	16416
MCS 10	64-QAM	0.55	19848
MCS 11	64-QAM	0.65	22920
MCS 12	64-QAM	0.75	27376
MCS 13	64-QAM	0.85	31704
MCS 14	64-QAM	0.93	31704

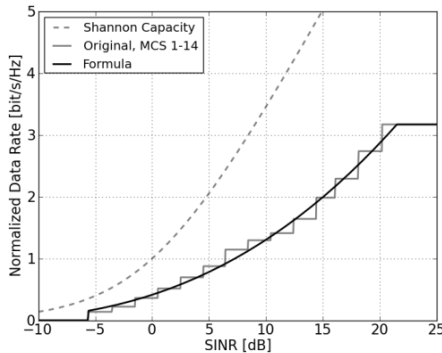


Figure 4.12: net spectral efficiency of LTE modulation and coding schemes taking BLER and ARQ account and Shannon bound

### 4.5.2 Mean Data Rate and Probability of Data Rate

The data rate  $r$  is calculated according Section 4.5.1 for a single permutation instance, considering a target PER, packet size, SINR and LTE overhead, see Section 2.3.7.3. It is worth noting that the calculation of the data rate and SINR distribution has to be done separately because their relationship is non-linear. Eq. (4.22) gives the mean data rate at position  $\vec{x}$  over all possible link and beam permutations, see Figure 4.13. The probability for a permutation  $j k$  is given by Eq. (4.23). The data rate probability in the entire cell is given by Eq. (4.24) considering  $n_A$  number of grid points in the evaluated cell area  $A_{cell}$  and all link and beam permutation instances ( $j \in J$  and  $k \in K$ ), compare to Eq. (4.17) - (4.19)

$$\bar{r}(\vec{x}) = \sum_{j \in J} p_{perm,j} \sum_{k \in K} p_{beam perm,k} r_{j,k}(\vec{x}) \quad (4.22)$$

$$P_{j,k,\vec{x}}(r) = 1, \text{ if } r = r_{j,k}(\vec{x}) \quad (4.23)$$

$$P_{cell}(r) = \frac{1}{n_A} \sum_{\vec{x} \in A_{eval}} \sum_{j \in J} p_{perm,j} \sum_{k \in K} p_{beam perm,k} P_{j,k,\vec{x}}(r) \quad (4.24)$$

$P_{cell}P_{cell}(r)$  can be input to the scheduling algorithm, see Section 4.5.4, which additionally considers resource allocation and the probability of number of MSs present in a cell (see Section 4.5.3). Output of the scheduling algorithm (see Table 4.3) is the probability of throughput of MSs,  $P_{cell}(\gamma)$ .

## 4 The Model of the Analytical Evaluation and the IMT-Advanced Channel

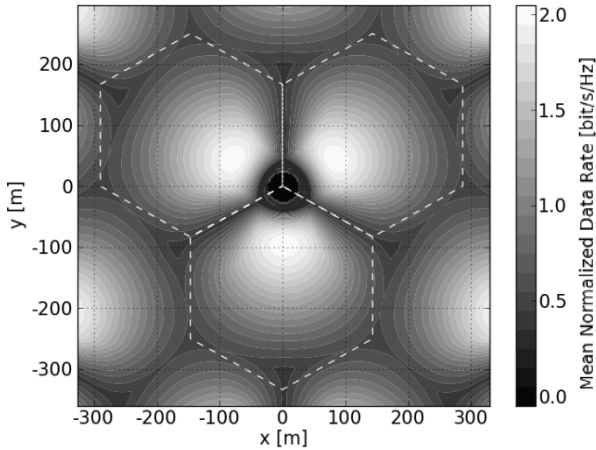


Figure 4.13: example of mean normalized data rate topography [bit/s/Hz]; UMa scenario with sectorised antennas

### 4.5.3 Distribution of Number of MSs per Cell

According to IMT-Advanced guidelines MSs shall be uniformly distributed over the scenario area with a mean density of 10 MSs per cell. Thereby, the number of MSs in a cell area can vary in different scenario instances as an outcome of the random process of dropping MSs. In the analytical model, probability of number of MSs per cell is shown in Figure 4.14, achieving the same MS density as specified by the IMT-Advanced guidelines. The probability of  $k$  MSs placed per cell area can be modelled as independent Bernoulli-Experiments resulting in a binomial distribution  $B(k|n, p)$ , where  $k$  is the number of MSs placed in a cell area in a sequence of  $n$  independent Bernoulli experiments, where  $n$  is the number of all MSs in the entire scenario and  $p$  ( $p = 1/\text{number of cells}$ ) is the probability of a MS to be placed within a given cell. Figure 4.14 shows the probability of  $k$  MSs served by one cell with 57 cells in the scenario and  $p = 1/57$ . The probabilities of the number of MSs per cell are used by the scheduler to weight the schedules for each number of MSs.

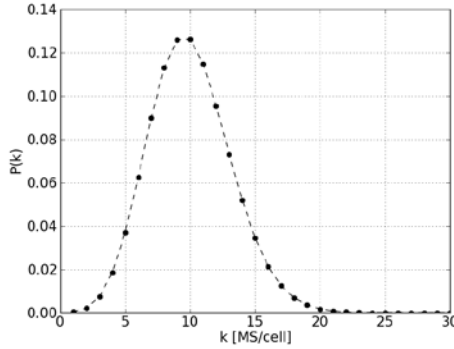


Figure 4.14: binomial distribution  $B(k|n,p)$ ; Probability of  $k$  MSs per cell, ;  $n = 570$ , and  $p = 1/57$

#### 4.5.4 Scheduling Strategies and Probability of MS Throughput

In this work following scheduling strategies are used: Round-Robin (RR) and Rate-Fair (RF) scheduling. The strategy RR allocates the same amount of radio resources to each MS, i.e., resource fair. The result of RR scheduling is a MS throughput proportional to the MS's SINR. The cell capacity is calculated by Eq. (4.25) where  $n_{PRB}$  is the number of Physical Resource Blocks (PRB) per second,  $n_A$  is the number of grid points in the cell area, and  $r$  is the normalized data rate (see Figure 4.13) at the position  $(x, y)$  which is calculated according to the link-to-system-level mapping depending on the SINR. Considering the probability  $P(k)$  (see Figure 4.14) for the number of MS per cell, Eq. (4.26) gives the probability of the normalized MS throughput, where  $P_{cell}(\gamma(r,k)) = P_{cell}(\gamma = \frac{r}{k})$  is given by Eq. (4.24), with data rate  $r$  scaled by the inverse of the number of MSs per cell  $1/k$ . Figure 4.15 exemplarily shows  $P_{cell,RR}(\gamma)$  for a sectorised system in a UMa scenario.

$$C_{cell,RR} = \frac{n_{PRB}}{n_A} * \sum_{\vec{x} \in A_{eval}} \sum_{j \in J} p_{perm,j} * r_j(\vec{x}) \quad , \text{ in [bit/s/Hz]} \quad (4.25)$$

$$P_{cell,RR}(\gamma) = \frac{n_{PRB}}{1} * \sum_k P(k) * P_{cell}(\gamma(r,k)) \quad , \text{ with } \gamma(r,k) = \frac{r}{k} \quad (4.26)$$

## 4 The Model of the Analytical Evaluation and the IMT-Advanced Channel

The RF strategy allocates radio resources in a manner that each MS has the same throughput. As a result, the number of resources allocated to a MS is proportional to the inverse of the SINR of a MS. The cell capacity is calculated by Eq. (4.27).  $\frac{1}{r_j(\vec{x})}$  is proportional to the average time required to transmit a bit to a MS at position  $\vec{x}$  and is also proportional to the required radio resources under RF scheduling. Eq. (4.28) calculates the distribution of normalized MS throughput under RF scheduling by summing up the common throughput for each MS  $\gamma = \frac{C_{cell,RF}}{k}$  weighted by  $P(k)$  the probability of  $k$  MSs per cell.

$$C_{cell,RF} = \left( \frac{\frac{1}{n_A} * \sum_{\vec{x} \in A_{eval}} \sum_{j \in J} P_{perm,j} * \frac{1}{r_j(\vec{x})}}{n_{PRB}} \right)^{-1}, \text{ in [bit/s/Hz]} \quad (4.27)$$

$$P_{Cell,RF}(\gamma) = \sum_k P(k) * \gamma(k), \text{ with } \gamma(k) = \frac{C_{cell,RF}}{k} \quad (4.28)$$

Another RR scheduling strategy called ‘‘RR Balanced’’ is later introduced with minor modifications to RR for Soft Frequency Reuse (SFR) resource partitioning, see end of Section 5.1.

### 4.5.5 Cell Spectral Efficiency (CSE)

Cell spectral efficiency  $\eta$  is defined as the aggregate throughput of all users normalized by the channel bandwidth per cell.

$$\eta = \frac{\sum_{i=1}^N \chi_i}{T \cdot \omega \cdot M} \text{ in [bit/s/Hz/cell]} \quad (4.29)$$

where  $\chi_i$  is the number of correctly received bits by user  $i$  (in downlink or uplink) in a system with  $N$  users and  $M$  cells.  $\omega$  is the bandwidth and  $T$  the time during which data bits are received. The bandwidth is defined as the effective bandwidth times the frequency reuse factor, where the effective bandwidth is the operating bandwidth normalized by the downlink/uplink ratio.

The number of correctly received bits corresponds to the number of bits contained in the service data units (SDUs) delivered to Layer 3. Accordingly, Layer 1 and Layer 2 overhead (e.g. common control channels, HARQ ACK/NACK signalling, channel feedback, random

access, packet headers and CRC) reduce the CSE. CSE is calculated as the mean normalized MS throughput using Eq. (4.26) or (4.28).

$$CSE = \bar{\gamma} = \sum_{\gamma} P_{Cell}(\gamma) * \gamma, \text{ in [bit/s/Hz]} \quad (4.30)$$

According to [ITU-R M.2134], the required cell spectral efficiency for the deployment scenario *Urban Macro-cell* (UMa), (see Chapter 6), is required to be at least 2.2 [bit/s/Hz/cell] in downlink and 1.4 [bit/s/Hz/cell] in uplink.

### 4.5.6 Cell Edge - User Spectral Efficiency (CE-USE)

The cell edge user spectral efficiency is defined as 5<sup>th</sup> percentile of the cumulative distribution function (CDF) of the normalized user throughput. The (normalized) user throughput for MS  $i$  is defined in Eq. (4.31).  $\chi_i$  is the number of correctly received bits of MS  $i$ ,  $T_i$  the time during which the data bits are received and  $\omega$  the channel bandwidth.

$$\gamma_i = \frac{\chi_i}{T_i \cdot \omega} \quad (4.31)$$

CE-USE can be calculated using Eq. (4.26) or (4.28).

$$CE-USE = \gamma_0, \text{ in [bit/s/Hz]}, \text{ if } P(\Gamma \leq \gamma_0) = \sum_{\gamma \leq \gamma_0} P_{Cell}(\gamma) = 5\% \quad (4.32)$$

The minimum cell edge user spectral efficiency required for UMa is 0.06 [bit/s/Hz] in downlink and 0.03 [bit/s/Hz] in uplink [ITU-R M.2134].

## 4.6 LTE-Advanced System-Level Validation

In this Section, a similar validation as in Section 4.4 is conducted but on system level assuming frequency reuse one, RR scheduling and sector antennas (without MIMO support). All aspects of the link-to-system model and the protocol implementation contribute to the normalized throughput results. Figure 4.15 compares the mean normalized user throughput CDFs for the UMa Scenario achieved by the analytic tool and the IMTaphy simulator [Ellenbeck, 2012a&c]. The analytical results achieve a slightly higher normalized user throughput than the IMTaphy simulator which may be caused by small deviations in the link-to-system model used.

#### 4 The Model of the Analytical Evaluation and the IMT-Advanced Channel

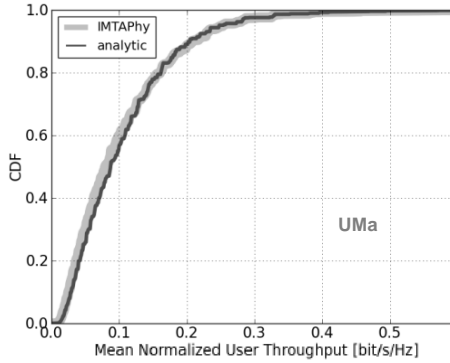


Figure 4.15: mean user throughput CDF normalized by the bandwidth (without small-scale fading)

In a real LTE-Advanced deployment higher normalized user throughput performance can be expected for example due to multi-antenna techniques and more sophisticated radio resource scheduler algorithms.

## CHAPTER 5

# Inter-cell Interference Coordination

Inter-cell interference limits system throughput capacity in cellular networks, especially for cell-edge MSs. Figure 5.1 shows qualitatively capacity per area unit and number of MS versus the distance to BS in cellular networks. Capacity per area unit is high close to the BS where only very few MSs reside however. With increasing distance of MSs to BS, capacity per area unit decreases rapidly while the number of MSs grows proportionally to the distance. Hence, desired ubiquitously perceived capacity cannot be provided. This goal can be better achieved by inter-cell interference coordination which can also increase mean spectral efficiency, see dashed curve in Figure 5.1.

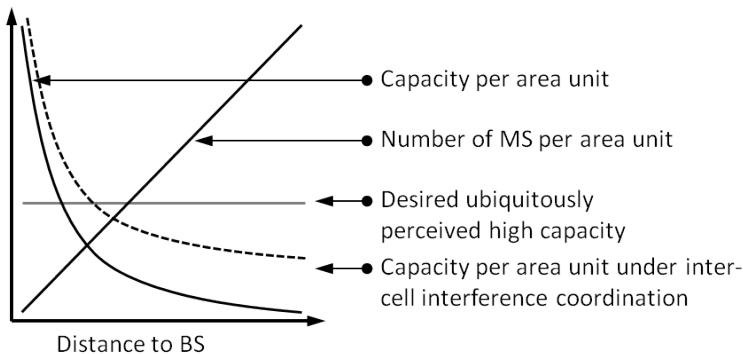


Figure 5.1: capacity per area unit and number of MS versus distance to BS in cellular networks

In order to limit inter-cell interference, frequency reuse schemes are used as discussed in the next Section. LTE-Advanced systems are designed to operate with frequency reuse one and need means to cope with inter-cell interference. For this purpose, LTE-Advanced as the first system can apply *Coordinated Multi-Point* (CoMP) transmission and reception as reviewed in Section 2.7. In this work, the algorithms of the CoMP type *coordinated beamforming* (CB) are discussed, see Section 5.2. CB schemes considering adaptive beamforming and SDMA are examined in Section 5.3. Section 5.4 presents a new CB scheme using fixed beams.

### 5.1 Frequency Reuse Schemes

The frequency reuse (FR) schemes applied in Chapter 6 are FR One (FR1), FR Three (FR3), and Soft FR (SFR) in order to compare CB based techniques to more conventional frequency reuse techniques. Both FR3 and SFR reduce inter-cell interference by increasing the reuse distance of radio resources, especially for MSs residing at the cell-edge. Figure 5.2 shows cells applying channel group  $c_i$  and the respective power masks which define the maximum transmit power a BS can use in a specific part of the spectrum. A network deployment of three cells per site is assumed. In all reuse schemes, the total transmit power of a BS is the same which allows a fair comparison. With **FR1**, the entire bandwidth can be exploited for transmissions in each cell with the same maximum transmit power but high inter-cell interference. With **FR3**, only a third of the entire system bandwidth can be used by a cell and inter-cell interference is reduced substantially. With **SFR** [Xiang, 2007], a frequency channels (called primary part) used to serve the cell edge MSs are assigned according to reuse 3 and apply high transmit power (defined by the parameter  $\alpha$ ). The parameter  $\alpha$  defines the transmit power of the primary part  $P_{Tx,primary}$  relative to the total transmit power  $P_{Tx}$ , where  $n_{FC}=3$  is the number of frequency channels.

$$P_{Tx,primary} = \frac{\alpha * P_{Tx}}{n_{FC}}, \text{ if } 1 \leq \alpha \leq n_{FC} \quad (5.1)$$

Two third of the bandwidth is assigned as secondary part for operation under reuse 1 with lower transmit power level  $\beta$

## 5.1 Frequency Reuse Schemes

$$\beta = (3 - \alpha)/2, \text{ if } 1 \leq \alpha \leq 3 \quad (5.2)$$

Parameter  $\alpha$  can be interpreted as the *effective reuse factor* applied which is between one and three, i.e., SFR includes FR1 for  $\alpha = 1$  and FR3 for  $\alpha = 3$ . The radio resource scheduler allocates resources to MSs from the three frequency channel parts. The resulting resource assignment is depicted in the left map of Figure 5.2 (c). In the comparative evaluation in Chapter 6, the classification of MSs to be cell centre or cell-edge users depends on their perceived SINR as well as the employed scheduling strategy. SINR of a MS served on secondary part is improved by allocating MSs to the best suited channel of the secondary part. In this manner, the distance to the strongest interferer is increased compared to frequency reuse one.

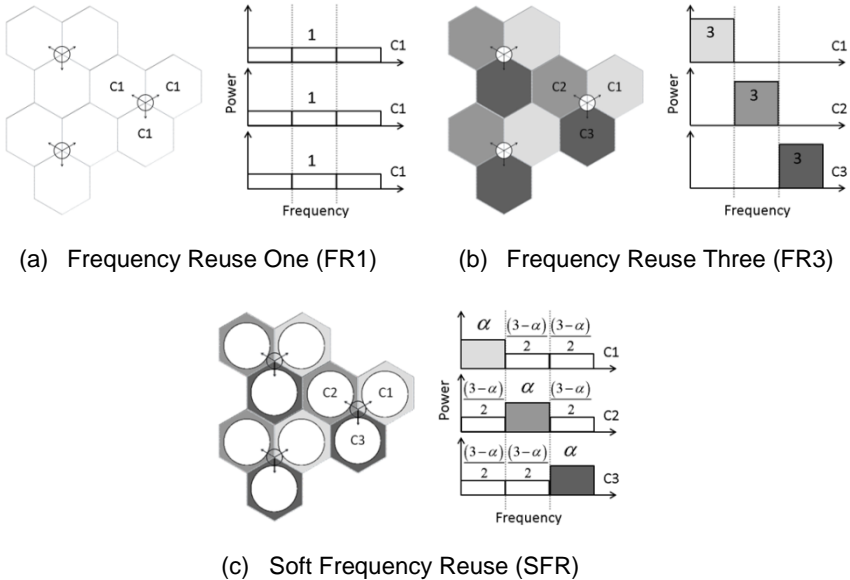


Figure 5.2: static frequency reuse schemes

With an increased  $\alpha$  value, the transmit power  $\beta$  in the secondary spectrum part decreases. MSs served on the secondary spectrum part

are disadvantaged by RR strictly allocating the same amount of radio resources to each MS (this strategy is referred to as RR *Strict* in the context of SFR in the following). Besides RF scheduling, a third scheduling strategy RR *Balanced* is introduced for SFR which overcomes this drawback by providing the same average throughput on each part by shifting MSs from spectrum parts with low to high average throughput but allocates the same amount of radio resources to each MS within each spectrum part.

### 5.2 Coordinated Beamforming Schemes

By applying smart antenna based beamforming and SDMA techniques, adaptive antennas increase cell capacity by reducing inter-cell interference and by supporting concurrent transmissions. As a downside, a beamforming enabled cell generates less predictable interference to other cells than a conventional cell, due to the so called *flash light* effect. It describes the phenomenon that a receiver perceives a reduced interference level in general but sometimes can reside in the main lobe of an interfering beam and is then interfered much more than in systems without beamforming. With SDMA enabled cells additional aspects contribute to the less predictable interference, e.g., the changing number of MSs sending uplink data in parallel and the changing transmitted power per beam<sup>19</sup> of multiple DL streams. The statistics of interference are affected by beamforming techniques in such a way that the mean interference level is decreased while the variance is increased. Thereby, the SINR estimation becomes less precise and the link adaptation sub optimal. CB targets for a more precise SINR estimation by creating predictable interference patterns and by mitigating inter-cell interference, especially by avoiding the flash light effect.

Interference coordination techniques can be classified with respect to the degree of distribution [Necker, 2008] and the time scale of operation [Ericsson, 2006]. Types of different degree of distribution are 1) Global-

---

<sup>19</sup> Assuming a constant total transmit power shared by the beams applied in parallel, the power per beam varies depending on the number of MSs served simultaneously in downlink.

2) Distributed-, 3) Decentralized-, and 4) Local interference coordination techniques. Global schemes (1) assume one omniscient central device and are usually not implementable in a real network but instead provide an upper limit for the potential gain of interference coordination. Distributed schemes (2) rely on one or more central components, which exchange information relevant for coordination among BSs in the network. Decentralized schemes (3) do not have a central entity but coordination is performed by information exchange among equally ranked BSs. Local schemes (4) purely base on local available information at a BS. Coordination is implicitly or explicitly performed by measuring interference or by running certain synchronised scheduling algorithms in every BS.

Besides the degree of distribution, the time scale of operation is an important characteristic of an interference coordination scheme. Three basic classes can be distinguished: a) static schemes, b) semi-static schemes, and c) dynamic schemes [Ericsson, 2006]. Static schemes (a) do not have a time variant component. Planning of the interference is conducted during the network planning process or with a time scale of operation in the order of days or longer (such as Fractional Frequency Reuse [WiMAX Forum, 2006]). Semi-static schemes (b) can handle uneven and variable load distributions among cells as well as uneven user distributions within a cell, operating with a time interval of several seconds or even minutes. Fully dynamic schemes (c) can instantly adapt to changing network conditions such as changing traffic load or user distributions. Their time scale of operation is in the order of a few MAC frames.

CB for mitigating inter-cell interference is well known from literature [Godara, 1997], [WINNER II D4.7.2, 2007], [Doettling, 2009] and mostly evaluated on physical and link level but rarely on system level for a few cells only, see [Hosein, 2008], [Hassanpour, 2008]. In general, antenna patterns are employed having high gains in the directions of desired MSs and signal suppression towards interfered MSs in downlink (or interfering MSs in uplink). This work focuses on CB and on its impact on system level performance considering the scenario shown in Figure 4.1.

## 5 Inter-cell Interference Coordination

As mentioned, CB targets first for a more precise SINR estimation by knowing the perceived interference, resulting from signalling or from a regular operation of beams, and second for an improved inter-cell interference mitigation. Fixed CB schemes [van Rensburg, 2009], [Hosein, 2009] basically assume that the perceived interference is known and thereby increase the precision of SINR estimations. [Hosein, 2009] also mitigates interference to a very limited extent by using local information in a semi-static manner. Fixed CB as presented by [Ellenbeck, 2010] mitigates interference in a decentralized and semi-static manner. This approach faces the issue that found resource allocation is instable over time and is suboptimal since scheduling bases only on local interference measurements of MSs. Similar problems are faced by the implicit coordination [Thiele, 2013] where also only local interference measurements for downlink are used as basis for scheduling decisions.

The three CB schemes proposed in [Wolz, 2009] and [Wolz, 2010] (see also Section 5.3) mitigate interference by basically applying zero forcing beamforming (see Section 3.3.2) to an SDMA enabled system and in addition directing zeros also towards MSs in neighbour cells. The dynamically exchanged coordination information affects only the shape of the employed adaptive beams and the resource allocation to users is only indirectly impacted. Hence, the flash light effect is not avoided but if a jammer is in the direction of a main lobe, the interference is at least known. These three coordination schemes are outlined in Section 5.3.

Section 5.4 presents a new scheme of fixed CB seeking for an optimal coordination of multiple cells by potentially considering all beam combinations<sup>20</sup> and thereby primarily mitigating interference in a global and static approach in a first step. The scheme can be adapted to a decentralized and dynamic coordination scheme being able to react on

---

<sup>20</sup> The number of beam combinations =  $n_{beams}^{n_{cells}}$ , where  $n_{cells}$  is the number of cells in the scenario and  $n_{beams}$  is the number of beams in each cell or the codebook size, see Section 4.3.6.

changing traffic load and user distribution, as discussed in Section 5.4.7. The scheme seeks to actively prevent the flash light effect, whereas for adaptive CB only implicit (i.e., decentralised) approaches of preventing this effect are known in literature, as mentioned. Advantages of fixed over adaptive beamforming have been described in Section 3.4. Beam coordination principles found in Section 5.4 are expected to be modifiable to adaptive beamforming as well.

### **5.3 Coordination for Adaptive Beamforming with SDMA**

Before presenting results of coordination of fixed beams in Chapter 6 investigation results by the author are presented focusing on coordination of adaptive beams. The parameter space of coordinated adaptive beamforming systems appeared to be such large that required simplifications of the model were necessary, still making impossible to gain analytical results. Therefore, the author decided to reduce complexity and consider coordination of fixed beam based systems for which optimal coordination turned out to be possible as shown in Chapter 6. Since the findings on systems with coordinated adaptive beamforming appear valuable they are enclosed in this work as Section 5.3 and Annex B and C.

Supporting adaptive beamforming and SDMA, the dynamic coordination approach presented in Section 5.3.1 provides a high system capacity at the cost of extensive signalling effort and delay requirements in order of a few frames on the backhaul due to forwarding all scheduling decisions including MS's position to all neighbour cells. Both schemes developed in Section 5.3.2 aim for solving the limitations of the scheme introduced in Section 5.3.1. One scheme reduces the number of bursts (or transmission blocks) and thereby the overhead by a factor of 2-3. The other scheme is designed for coping with variable bit rate (VBR) traffic by creating spatial regions and coordinating the interference of the set of MSs within a region, instead of predicting the traffic demand of a single MS. The coordination overhead as well as the backhaul delay requirement are dramatically

reduced thereby but with constant bit rate (CBR) traffic the system capacity as well.

### **5.3.1 Coordination for Adaptive Beamforming with SDMA - Scheme I**

This Section bases on [Wolz, 2009] and investigates the potential of coordination across BSs on MAC layer in an adaptive beamforming and SDMA enhanced system for mitigation of inter-cell interference and increasing precision of SINR estimation. The key finding of the evaluation results are discussed comparing the performance of a coordinated system (scheme I) versus a non-coordinated reference case.

#### 5.3.1.1 Introduction

Multiple antennas are utilized in the physical layer to form adaptive antenna patterns (see Section 3.3.2 ff) which have high gains in the direction of desired users and signal suppression (further referred to as directing zeros) in the directions of other users, e.g. inter-cell interferers. Inter-cell interferers can possibly be considered in the beamforming algorithm when BSs mutually exchange their scheduling decisions and positions of their MSs served. If its interferers are known, an SDMA enhanced BS can further mitigate inter-cell interference and improve SINR estimation. In the following, a system is assumed with multiple antenna elements at the BS and a single element antenna at the MS. Hence the uplink (UL) and downlink (DL) case differ. In uplink a BS increases its link quality by directing zeros towards interfering (jamming) MSs of adjacent cells. Whereas in downlink the link of interfered (disturbed) MSs can be improved if a neighbour BS puts zeros towards it.

#### 5.3.1.2 Coordination Scheme

Coordination of BSs relies on exchange of information about scheduling decisions and positions of MSs. The knowledge when interference will occur and from where is exploited. Here, a coordinated scheduling scheme with two iterations is proposed. First, a BS allocates its resource in conventional manner as in [Pabst, 2007] without coordination. Secondly, the received coordination information is utilized for adapting

the beamforming pattern accordingly. All scheduling decisions are also assumed to be exchanged.

A problem in coordination is the prediction of upcoming traffic. By assuming CBR traffic in the following, we are regarding a best case scenario. Nevertheless with MSs, the spatial separability of MS and thereby the SDMA groups change over time and hence resource allocation in the MAC frame slowly changes, see Section 5.3.1.4. Thus, a periodic update of the coordination information is required.

### 5.3.1.3 Information Exchanged

In a multi cell system a receiving station suffers from intra- and inter-cell interference. The optimal beamforming algorithm (see Section 3.3.3 and 3.3.4) and the SINR heuristic grouper [Hoymann, 2007] almost cancel the received intra-cell interference.

The following coordination approach mitigates inter-cell interference in uplink<sup>21</sup> by directing zeros towards all jamming MSs in neighbour cells, as depicted in Figure 5.3. In the downlink, zeros are directed towards all disturbed MSs. This is not possible if the jammer is in the direction of a main lobe. In this case the interference is at least known and hence the interference estimation is significantly improved. Below, for sake of simplicity, the concept is only explained for the uplink. The downlink case is similar.

For each transmission from a potentially interfering MS following information is forwarded to neighbour BSs: the position of the MS, transmit power, transmit antenna gain, transmission start- and end time, as well as the employed sub-channel. From the MS position, the BS is able to estimate path loss and directional Rx antenna gain ( $G_{RXAntenna}$ ). With information from adjacent cells, the BS estimates the inter-cell interference of each inter-cell MS using Eq. (5.3).

---

<sup>21</sup> In uplink, the optimal beam-former also mitigates inter-cell interference by maximizing SINR. It computes the array correlation matrix with the training sequence at the beginning of each burst, but does not account for changed interferers during the burst and hence is suboptimal.

$$I_{inter}[dBm] = Power + G_{RXAntenna} + G_{TXAntenna} - PathLoss_{BS-MS} \quad (5.3)$$

### 5.3.1.4 MAC Frame

This Section outlines the impact of coordination on the MAC frame. In the first scheduling iteration, groups of well separable MSs are generated and then resulting groups are scheduled in time domain to bursts of the same size, e.g., based on the fill level of the queues in downlink or based on bandwidth request in uplink. In the second iteration, inter-cell interfering MSs are suppressed in the receive beam pattern. If interferers change during a burst, a new pattern and thereby a new burst needs to be applied. Hence, one burst of the first iteration is subdivided into shorter bursts to be transmitted to the same spatial group consuming the same total allocated time as before.

Figure 5.4 depicts an example of uplink MAC sub-frames of three BSs: interfered BS1 and interfering BS2 & BS3. Group 9 of BS1 has three different sets of interferers: Group 1 & 5, Group 2 & 5, and Group 2 & 6. The initial single burst of Group 9 is divided into three bursts in order to apply three different patterns and to be able to direct zeros to the current interferers in each burst of Group 9. In this manner an increased number of information elements in the map is required indicating more shorter bursts.

In case of sufficient antenna elements ( $\geq 12$ ), one new pattern can be used directing zeros to all interferers occurring during the initial large burst. This approach prevents the scheduling from too many small bursts and is discussed in Section 5.3.2.

## 5.3 Coordination for Adaptive Beamforming with SDMA

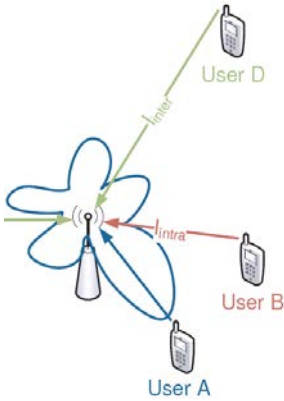


Figure 5.3: antenna pattern with zeros towards intra- and inter-cell interferers

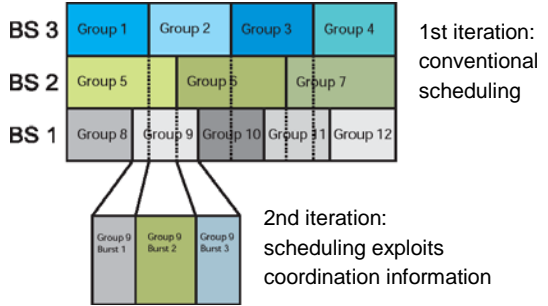


Figure 5.4: MAC frames of disturbed & jamming BSs

### 5.3.1.5 Decoupling

Coordination of a system requires decoupling of cells in order to prevent circular dependencies of cell schedules and to reduce the NP-hard complexity of the coordination problem [van Rensburg, 2009] to a feasible degree. In order to decouple the coordination process, BSs are sorted into three classes as shown in Figure 5.5. BSs of different classes update their coordination information asynchronously.

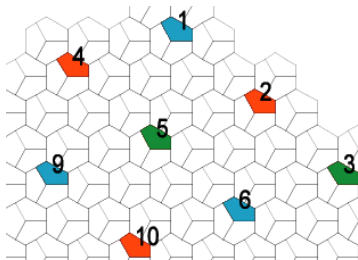


Figure 5.5: decoupling by classification of BS

## 5 Inter-cell Interference Coordination

Scheduling information is exchanged just before the start of each frame. The message sequence chart in Figure 5.6, for the example of coordination with three classes, shows that a BS forwards its scheduling decision every third frame, simultaneously with BSs of the same class. Hence, a BS uses the same information about an adjacent cell for three MAC frames. A coordination message comprises the MS's information for all transmitted bursts.

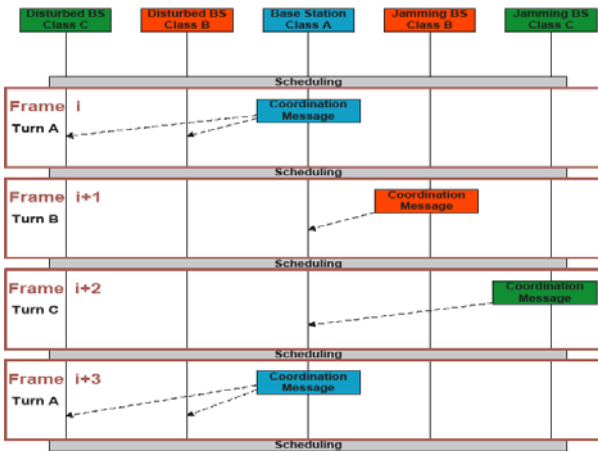


Figure 5.6: coordination message sequence chart

### 5.3.1.6 Summary of Results and Conclusion

Three key findings derived from performance evaluation results shown in Annex B are worth mentioning: the above CB scheme 1) mitigates inter-cell interference, 2) increases SINR predictability, and hence 3) improves system throughput capacity.

To 1), in a coordinated system, higher MCS can be used than in a non-coordinated system, the probability of the highest MCS 64QAM3/4 is increased by 16% from 75% to 86%, see Figure B.2.

To 2), the probability of employing the correct MCS scheme is improved from less than 70% in a non-coordinated system to 90% in the

coordinated system, see Figure B.3. Packet loss, due to too optimistic SINR estimation, approximately, does not occur in the coordinated system, see Figure B.3.

To 3), coordination increases the system throughput capacity from less than 10 Mbps for the non-coordinated system (see red circle) to 60 Mbps in uplink (see Figure B.4) and to 75 Mbps in downlink (see Figure B.5). For traffic load beyond the red circle the packet loss rate is such high that the service becomes useless.

In the studied interference limited scenario, coordination scheme I can be regarded as an enabling technology, given the poor performance of the non-coordinated system. The developed concept let a coordinated-outperform an uncoordinated system. The cost of coordination across BSs is the increase of system complexity (scheduler, grouper, beamformer) and of coordination overhead (exchanged messages, increased MAP size due to increased number of bursts).

Results presented in Annex B cannot meaningfully be compared to the results of Chapter 6 due to the different assumptions made - such as carrier frequency, number of antenna elements, down tilt, type of sector pattern, path loss model, and radio access technology. Hence results are summarized here only to demonstrate the potential of coordinated adaptive beamforming under SDMA operation. The detailed performance evaluation study including scenario description, traffic model, and all results is contained in Annex B.

#### **5.3.2 Region Coordination for Adaptive Beamforming with SDMA - Schemes II and III**

This Chapter presents and evaluates two schemes of CB on MAC layer for further mitigation of inter-cell interference and increasing precision of SINR estimation. Both new schemes aim for solving the limitations of scheme I, see Section 5.3.1 and Annex B. Coordination scheme II reduces coordination overhead by reducing the number of bursts (or transmission blocks). Coordination scheme III is designed for coping with variable bit rate (VBR) traffic by creating spatial regions and coordinating the interference of the set of MSs within a spatial region, instead of predicting the traffic of a single MS.

## 5 Inter-cell Interference Coordination

Schemes II and III in Section 5.3.2 can be classified as distributed- and dynamic interference coordination, which is “2c” according to the classification in Section 5.2. Here we assume ideal signalling which refers to zero delay and no message loss for any coordination signalling message.

### 5.3.2.1 Advanced Coordination Scheme

Common principles shared by all three coordination schemes (I, II, and III) are explained in Section 5.3.1.2 ff. Improvements of scheme II & III versus scheme I are presented in the following.

#### 5.3.2.1.1 Coordination Scheme II (one burst per group)

As described in the previous Section, the first scheduling iteration generates one burst per SDMA group. Scheme II preserves the single burst per group and thus is also called “*1 burst per group*” in the following. It calculates one new beamforming pattern that considers all interferers which occur during that burst. In this manner, scheme II prevents the scheduling from too many small bursts, see Figure 5.4. A sufficient number of antenna elements ( $\geq 12$ ) is required.

#### 5.3.2.1.2 Coordination Scheme III (regions)

Scheme III is designed for coping with variable bit rate (VBR) traffic such as MPEG4 (for high quality movie trace with a resolution for a small device) [Kim, 2005] which traffic up-come and related interference can be hardly forecasted. Instead of predicting the traffic of a single MS, scheme III creates spatial regions in a cell and coordinates interference to the set of MSs within a spatial region. A spatial region is assumed to approximately transmit the same number of packets per MAC frame (i.e. a constant-bit-rate (CBR)-like traffic characteristic resulting from multiple MSS contained in a set). Scheme III is called *regions coordination* and is first defined for the uplink case and then for downlink.

For uplink, Figure 5.7 (a)-(c) show how sectors are divided into spatial regions of the same size. BS A and B are interfered by a sector cell of BS C. BS C defines the spatial regions of its interfering cells. Only one MS per region is scheduled at the same time and thus a region is perceived as one MS. In this manner, scheme III simulates for the coordination

process a fixed number of sources of inter-cell interference each with CBR-like traffic. The number of regions equals the maximum number of concurrent beams. If a BS interferes more than one BS, sub-regions are created by the superposition of regions of the different interfered BSs as shown in Figure 5.7 (d). Each sub-region is labelled by a number, with as many digits as interfered BSs, each digit indicates the regions of one interfered BS. The SDMA grouper, deciding which set of MSs are served simultaneously by different beams, requires to be modified for the spatial regions scheme by introducing a spatial condition: *a group of currently served MSs is valid if it contains at most one station of each region.* In the example of Figure 5.7, valid groups can be built with MSs of sub-regions 11 and 22 or 12 and 21 fulfilling the spatial condition. The algorithm creating the spatial regions is explained at the example of sites with three cells each. The relative position between two BSs has to fulfill the following constraints also to allow for same size of regions, see Figure 5.8:

1.  $\alpha_a$  (angle between interfering BS and interfered BS)  $-30^\circ \leq \alpha_a \leq 90^\circ$
2.  $\psi_a \geq 0^\circ$  (angle between left point ( $P_l$ ) and interfered BS)
3.  $\xi_a \leq 60^\circ$  (angle between right point ( $P_r$ ) and interfered BS)

## 5 Inter-cell Interference Coordination

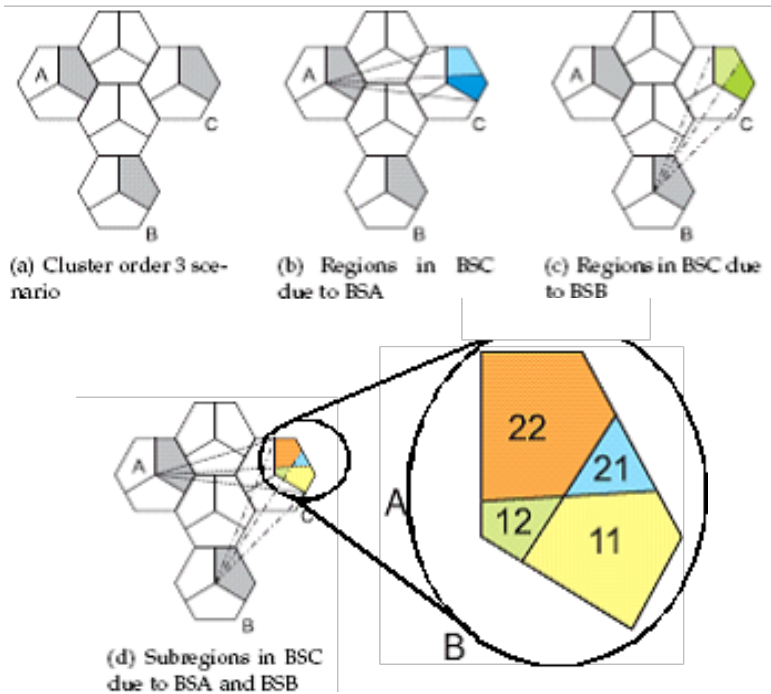


Figure 5.7: creation of spatial regions and sub-regions (example of two interfering BSs and two concurrent antenna beams)

For coordination and estimation of inter-cell interference, a region is modelled as a virtual MSs (vMS) at the centre of gravity of each region. A interfered BS directs zeros towards the directions of vMSs of each interfering region. The inter-cell interference at the interfered BS is estimated from the pathloss, see Eq. (5.3). The total inter-cell interference at a BS is estimated as the sum of the interference generated by its vMS.

In downlink, interference is fairly predictable because it is generated by BSs with known positions. Therefore same regions (represented by vMSs) as in uplink are considered in order to direct zeros towards it and to mitigate inter-cell interference. The introduced spatial condition of the SDMA Grouper is applied for grouping of MSs in each cell as in

uplink. As in uplink, one interfered MS is always assumed in each region and a zero is directed towards the region's centre of gravity.

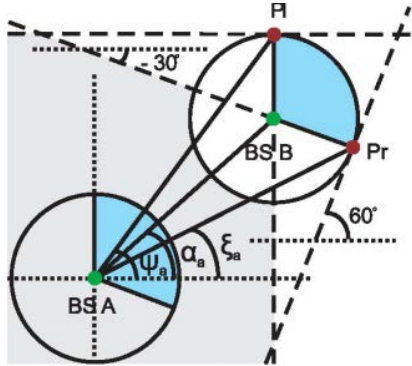


Figure 5.8: angular constraints

#### 5.3.2.1.3 Qualitative Coordination Cost

Signalling overhead with scheme I and II over the backhaul between a central coordination entity and the specific BSs is linear in number of MSs and linear in employed bandwidth. Scheme II has a reduced overhead by a factor of 2 to 3 linear in the reduced number of bursts. Coordination scheme III has a reduced signalling overhead which is constant and independent of the number of served MSs. Same information is exchanged as before but only for each region instead of for each MS. All Coordination schemes tend to require a higher number of antenna elements than the conventional beamforming system.

Scheme I and II have the same demand on the backhaul delay in the order of a few *ms* especially with variable traffic rate users. The requirement on the backhaul delay from scheme III can be relaxed since only regions are coordinated and detailed packet scheduling is conducted independently in each cell.

### 5.3.2.2 Summary of Results and Conclusions

Coordination scheme II (*one burst per group*) and scheme III (*region coordination*) are evaluated by means of system level simulations conducted in a cellular scenario with CBR downlink and VBR uplink traffic. Details of scenario description, traffic model, and all results are given in Annex C.

Comparing results of performance evaluation shown in Annex C for schemes I-III with the non-coordinated BF case, two key conclusions can be drawn: 1) scheme II (*one burst per group*) improves scheme I and remedies its limitation by decreasing the signalling overhead; but is limited in predicting interference under VBR traffic (see Figure C.5) and in efficiently coordinating a high number of MSs, 2) scheme III (*region coordination*) successfully predicts the interference under VBR traffic on uplink resulting in significant throughput gains compared to other schemes but throughput gains in the downlink are moderate only.

To 1), with CBR-traffic, scheme II improves scheme I, by 5Mbit/s from 69 to 74 Mbit/s (see Figure C.3), increases the burst size and thereby reduces overhead. This overcompensates the weakness of scheme II the lower precision of estimating the best suited MCS (see Figure C.2). SINR estimation under scheme II tends to be too pessimistic because interference is assumed to occur over the entire burst.

To 2), with VBR-Traffic in uplink, scheme III results in lowest probability of packet loss (i.e., 5% versus 25% without coordination) and highest probability for optimal MCS selection (80% versus 57% without coordination).

Scheme I, II, and III mitigate inter-cell interference and increase SINR predictability. All schemes improve system capacity compared an uncoordinated system in all scenarios studied. However, coordination across BSs increases both system complexity and overhead.

## 5.4 Synchronised Cycles of Coordinated Beams (CyBeamCo)

This Section introduces a new coordinated fixed beamforming algorithm that first targets for mitigating Inter-Cell Interference (ICI) by

providing beneficial beam selections in neighbour cells. Second, the algorithm also aims at making interference fluctuations predictable by introducing cyclic beam switching. Thereby, reported interference level and SINR estimation remain valid (at least for a certain time) since a MS keeps being interfered by the same beams applied in neighbour cells. Assuming fixed beamforming, a BS can choose beams from a codebook with limited number of entries as defined in [IEEE 802.16 D9], or [3GPP TS 36.211]. A beam is identified by a Precoding Matrix Index (PMI), as discussed in Section 4.2.3. The algorithm suggests that each cell cycles through a set of beams in a predefined order. In the presentation of the algorithm, the beam set and its order are first assumed to be constant for sake of intelligibility. Section 5.4.7 discusses how order and beam set can slowly change to account for variations in user location and traffic load. In the following the algorithm is referred to as Synchronised Cycles of Beam Coordination or as *CyBeamCo*.

The expected gain is caused by two effects: 1) improved SINR estimation due to creating predictable interference patterns through persistent use of beams (as described in Section 5.4.1) and 2) increased SINR due to the reduced interference level by applying beneficial beam combinations (as presented in Section 5.4.2.). Thereby, *CyBeamCo* aims for increasing cell spectral efficiency (CSE) as well as increasing cell edge user spectral efficiency (CE-USE). The concept is explained for the downlink but can be applied to the uplink as well.

### 5.4.1 Cell Type Specific Beam Coordination

Figure 5.9 (a) shows three types of cells (referred to as *A*, *B*, and *C*) to one of which a cell is associated to. Cell types are coordinated among each other with respect to interference instead of individually coordinating beams of every single cell with all its neighbour cells. Introducing cells types reduces the number of possible beam combinations to be considered from  $8^{57}$  to  $8^3$  (assuming a scenario with 57 cells, see Figure 4.1, and 8 beams<sup>22</sup> per cell). Thereby, cell types

---

<sup>22</sup> Even considering only the direct neighbours with a codebook size of 8 beams yields a number of  $8^7$  (> 2 million) different constellations of beams.

## 5 Inter-cell Interference Coordination

reduce the complexity of the beam coordination algorithm, which is NP-hard [van Rensburg, 2009]. Cells of the same type apply the same fixed beam in specific part of time-frequency radio resources. Radio resource parts are specified by the MAC scheduler and are initially of the same size in all coordinated cells. Figure 5.9 (b) depicts the *coordination matrix* of PMIs (each with N codebook entries) where a column relates to a specific radio resource part and a row relates to the cell type. With cell type specific beam coordination, each cell cycles through a set of PMIs in a predefined order. The assignment of MS to radio resources associated to a beam is independently conducted by each cell and is not coordinated across cells. The algorithm discussed in the next Section assures that beams applied at the same time in adjacent cells do not cause (mutual) harmful inter-cell interference preventing the flash light effect and providing at the same time that the entire cell is covered by network service.

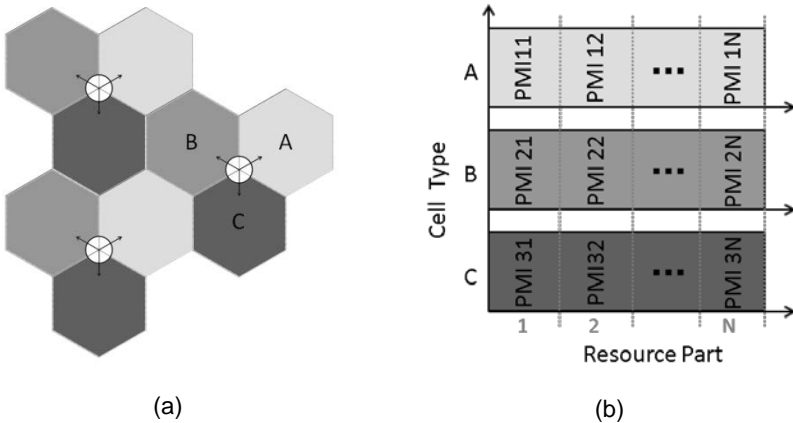


Figure 5.9: coordinated allocation of radio resource to cells and beams; (a) three cell types (b) coordination matrix for codebook subset with N entries

### 5.4.2 Algorithm for Seeking Beneficial Fixed Beam Combinations

This Section describes how to find a coordination matrix for assigning a PMI combination and thereby a fixed beam to each resource part of Figure 5.9 (b). The presented algorithm for beam coordination improves throughput performance of both cell edge and mean user. The optimal coordination matrix is found by first considering interference levels from measurement points at the cell edge, at least one point associated to each fixed beam of a given cell, and second by applying an appropriate cost function for comparing all beam combinations. The flow graph in Figure 5.10 depicts the algorithm. Input parameters are besides others the codebook (comprising  $N$  used beams), the reuse scheme, and the number of sites which cells are to be coordinated.

## 5 Inter-cell Interference Coordination

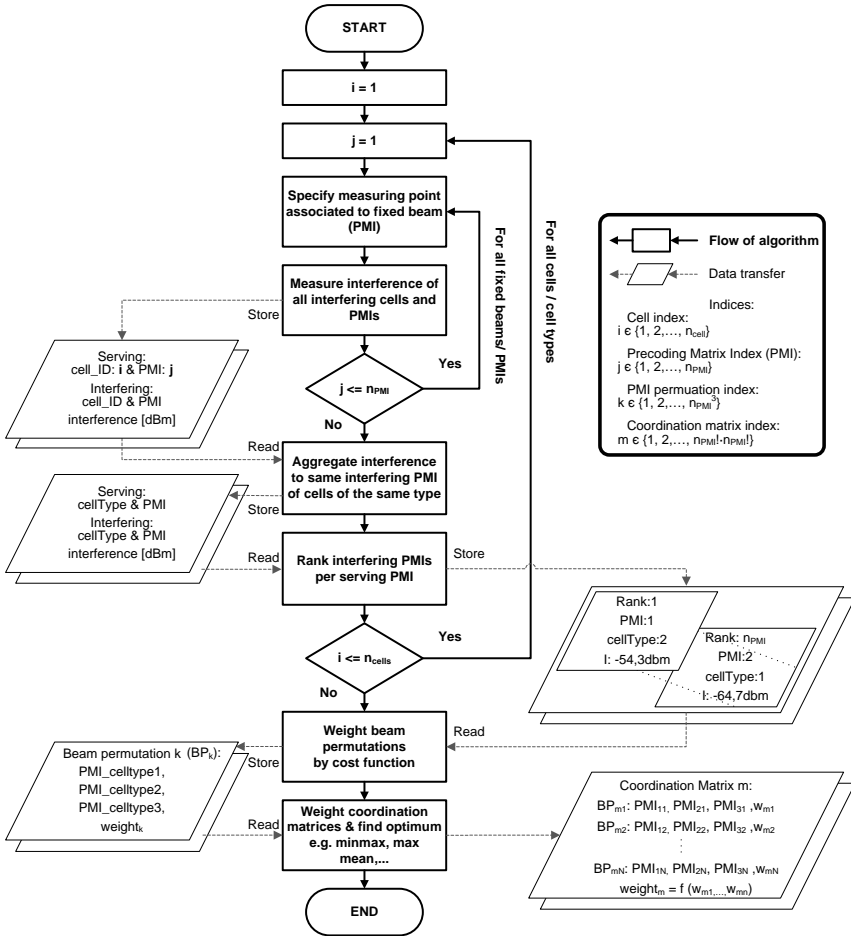


Figure 5.10: flow chart for algorithm defining a coordination matrix;  $n_{cell}$  = number of coordinated cells,  $n_{PMI}$  = number of beams in codebook subset

The algorithm starts with specifying measurements points at the cell edge at least one associated to each fixed beam of a chosen cell in order to be able to identify appropriate beam combinations that strengthen cell edge users. For all involved cell types, interference measurements and comparison of beam combinations are conducted. The beam combinations are defined by one serving beam (out of eight) of the

chosen cell and by the interfering beams (one out of eight per neighbour cell). For each serving beam, the individual interference is measured<sup>23</sup> resulting from each fixed beam of all neighbour cells. Since cell types instead of single cells are coordinated by the algorithm, interference from the same beam of cells of the same type is aggregated. Interfering beams for each serving beam are ranked by the degree of (aggregated) interference. After having performed these steps for the three cell types, each beam combination (described by three PMIs values, one for each cell type) are weighted by a cost function. The cost function in general assesses the amount of mutual interference caused by beams operated in parallel by neighbour cells. Different metrics can be utilized, for example the mean of the perceived interferences, or the minimum rank of the interfering beams, assuming the highest ranked beam interferes least.  $N$  selected beam permutations<sup>24</sup> establish a coordination matrix, where each beam is supposed to be applied in any cell type<sup>25</sup>. Based on the weighting of the beam permutations, each coordination matrix is weighted by an interference related cost function, e.g., the mean, the standard deviation, or the maximal minimum interference of beam combinations employed. With  $N^3$  different beam permutations, a number of  $N!/2$  ( $>10^9$  for  $N = 8$ ) different coordination matrices can be calculated. By considering only beam permutations with a weight above a certain threshold, search of the optimal coordination matrix can be sped up. Annex A.1 shows example coordination matrices for coordination of all neighbour cells and of cells belonging to one site only for 3, 5, and 7 beams.

In Chapter 6, beam coordination algorithms are evaluated and compared with coordination between all cells and with coordination

---

<sup>23</sup> In a real network this measurement procedure is rarely conducted, e.g., at network roll out. Challenges in a real system are discussed in Section 5.4.6

<sup>24</sup>  $N$  is size of the used codebook and so the number of beams.

<sup>25</sup> The constraint that all MSs (or positions) have to be served can be reformulated to “all beams have to be applied”, if a uniform user distribution is assumed and if the coverage areas of all beams is assumed to be of the same size, see Figure 4.6.

## 5 Inter-cell Interference Coordination

only between cells of one site using the minimum maximal interference as a cost function.

### 5.4.3 Beam Coordination under SFR

The CyBeamCo algorithm (see Section 5.4) can also be operated in an SFR scenario, because it only coordinates the association of beams to radio resources but leaves the assignment of a MS to radio resources and power control to each cell. Figure 5.11 shows an example RR radio resource schedule of a beam coordinated cell under SFR, where  $MS_{ij}$  is a MS served on the  $i^{\text{th}}$  radio resource part according to the SFR scheme (see Figure 5.2) and associated to the  $j^{\text{th}}$  PMI according to the beam coordination algorithm (see Figure 5.10).

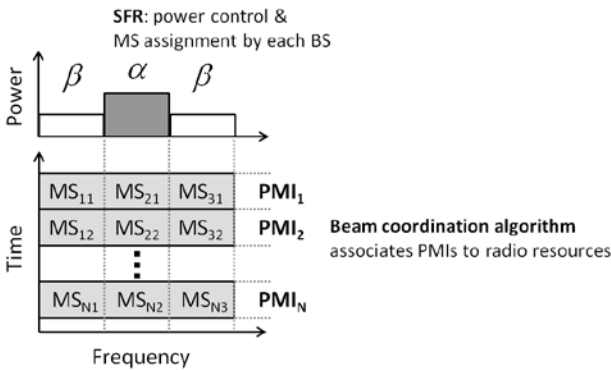


Figure 5.11: example RR radio resource schedule with beam coordination under SFR operation

### 5.4.4 Beam Coordination of Cells of the Same Site

The CyBeamCo algorithm can be simplified to only coordinate cells served by a given site. Only these cells and their beams are considered in finding the coordination matrix. Coordination of cells at one site can particularly impact the interference at cell edges common to cells of the site. In contrast, the algorithm designed in Section 5.4 aims for optimizing the entire cell edge including cell edges towards cells of

adjacent sites. Hence, one site coordination based on the CyBeamCo algorithm, as considered in chapter 6, reduces interference in a sub-optimal manner which is expected to be reflected by a reduced coordination gain.

### 5.4.5 Fair Evaluation of the Coordination Algorithm

The algorithmic complexity for beam coordination is so high that only one cell ring can be coordinated during a reasonable runtime duration. The model for the analytical evaluation introduced in Table 4.3 has been found to generate the same results when evaluating the capacity of one cell of the central site instead of the entire scenario. This statement is validated in terms of path loss (see Figure 4.8), SINR (see Figure 4.9), and mean user throughput distribution (see Figure 4.15). Evaluating beam coordination in one cell only has to assure that generated results are correct in a way that resources of neighbour cells are not “breathed in” and that cell gains are not created at cost of disregarded other cells. This kind of error can be definitively excluded. As described, the CyBeamCo algorithm equally treats cells of the same type by applying the same radio resources and beam cycles. Hence, resource breathing across cells of the same type cannot occur. Cells of different type employ the same resources but apply different beam cycles since they are represented by different columns of the coordination matrix. Unfair coordination gains can be detected by comparing evaluation results with switched matrix columns or results of different cell types. Both comparisons have been performed and have yielded no differences. Hence, the evaluation of the CyBeamCo algorithm in a single cell has been found to yield valid results which are not biased by the complexity reduction when limiting its application to one ring of cells and the evaluation to one centre cell.

Beamforming coordination gain occurs not only due to interference reduction but also due to known interference and the accordingly improved link adaptation as shown in [Wolz, 2009], [van Rensburg, 2009]. The coordination gain resulting from more predictable interference patterns and thereby improved link adaptation is up to 75% [Wolz, 2009] [van Rensburg, 2009] but is out of the scope of this work since the analytical evaluation model employed in Chapter 6 assumes

accurate SINR estimations already. Therefore, expected gains are only caused by interference mitigation and not by more reliable SINR estimations.

### 5.4.6 Creation of a Coordination Matrix in a Real System

The coordination matrix approximates the mutual interference characteristic of neighbour cells and their fixed beams. The respective interference measurements can be conducted in a real system after the roll-out of the network and need to be updated very rarely only to reflect changes in the environment or the network deployment. A central entity as a part of the network management system should gather the measurement results, calculate a coordination matrix, and distribute it to the BSs. Since this function is not supported by LTE/LTE-Advanced standard and updates are rarely required, a service residing in the Web can perform the role of the central entity. Identifying worst interfering beams of neighbour cells can result from measurements by MSs located at appropriate positions in each cell in two different manners. First, a MS may send a reference signal received at a neighbour BS. Then by spatial processing the neighbour BSs may identify their beams most interfering the respective MS. Second, the MS is forced to handover sequentially to all neighbour cells where it each time performs the procedure of selecting the best serving beam. The best serving beam of the neighbour cell is obviously the worst interfering beam if the MS is served by its initially associated cell. In order to gain interference measurements that are independent of capabilities of the individual receiver or which represent very local channel characteristics, several measurement cycles per beam should be conducted by different MSs at adequate positions in each cell. Because of the low update frequency of measurement results and the short duration of the handover procedure including association to a fixed beam, time overhead and spectrum resources consumption for providing measurement results can be assumed as negligible.

Calculated gains of the CyBeamCo algorithm can be lower in a real system as discussed later in Section 6 due to varying cell sizes, signal reflection and shadowing which might reduce efficiency of the found “optimized” beam coordination pattern. Also, in real networks

interference occurs between co-existing CoMP groups in which BSs are coordinated. This problem of uncoordinated “out of CoMP group” interference [Fang, 2011] may significantly reduce capacity gains but is ignored in this work. The introduced algorithm assumes synchronised cells. Failure of synchronisation would further reduce beam coordination gain.

### **5.4.7 Dynamic Beam Coordination – An Outlook**

The CyBeamCo algorithm is rather static and inflexible to adapt to non-uniformly distributed MS positions and to bursty MS traffic, since same amount of radio resources is dedicated to each beam. If no MSs reside in the area served by a beam, its resources remain unused. In order to reallocate unused resources, only minor modifications to the algorithms are required. Dynamic adaption is achieved by swapping unused resources from one beam to other beams serving higher load. Reallocation of resources can be conducted without producing destructive beam combinations of adjacent cells if a set of “good” beams (instead of a single one) is provided to the scheduler for each resource part of a cell. The set of good beams if well designed can help the scheduler to substitute beams on specific resources in a way that highly loaded beams can be provided more resources than without swapping unused resources. A ranking of the good beams would maintain interference mitigation. Both the set of “good” beams and their ranking are already provided by the CyBeamCo algorithm through the conducted weighting of all possible beam combinations by a cost function. Numerical results of dynamic beam coordination are not provided in Chapter 6



## CHAPTER 6

---

# Analytical Performance Evaluation Results for Systems with Coordinated Beamforming

In this Chapter, the CyBeamCo algorithm as defined in Chapter 5.4 is evaluated and compared to two reference systems, one with sectorised antennas and one with ordinary beamforming antennas, respectively. The impact of several parameters on the coordination performance is studied such as scheduling strategies (e.g., *RF* and *RR*) and frequency reuse schemes (e.g., *Frequency Reuse One* and *Soft Frequency Reuse*). Results presented in this Chapter are generated with the analytical tool presented in Chapter 4. The used metrics are defined in Section 4.5.2 ff. Table 6.1 presents main parameters applied for the performance evaluation. All calculations are conducted in the UMa scenario presented in Section 4.2.1. The default parameter set<sup>26</sup> characterizes a reference system which applies ordinary beamforming (BF) with 7 beams and uses RR scheduling with Frequency Reuse One (FR1).

This Chapter is organised as follows. Section 6.1 compares and characterises non-coordinated versus coordinated system types. Section 6.2 studies the impact of scheduling strategies on the coordination performance. Section 6.3 evaluates the Soft Frequency Reuse (SFR) scheme and derives an operating point in terms of the effective reuse factor. Section 6.4 assesses and compares the performance of the coordination algorithms in three different reuse schemes. Section 6.5

---

<sup>26</sup> Default values for variable parameters are shown bold face in Table 6.1

examines the impact of the size of the employed precoding codebook, which defines the number of available beams, on the coordination gain.

Table 6.1: main evaluation scenario parameters<sup>27</sup>

Parameter	Value
Environment	UMa, according to Table 4.2
Spatial Resolution	Equidistant 5m wide grid
eNB antenna	Sector antenna [Section 4.2.2] or antenna array with <b>4 elements</b> [Section 4.2.3]
Traffic model	Full buffer model [ITU-R M.2135, Annex 2]
System Type	Sector, <b>BF</b> , CBF 1, CBF
Scheduling strategy	Round Robin ( <b>RR</b> ) or Rate Fair (RF)
Frequency reuse schemes	Frequency Reuse 1 ( <b>FR1</b> ) and 3 (FR3), and Soft Frequency Reuse (SFR) with $\alpha = 2.6$
Number of fixed beams	Sector pattern, 3, 5, or <b>7</b> beams

## 6.1 Beam Coordination Performance versus other System Types

This Section compares and characterises four system types which are studied throughout this evaluation chapter. The systems are 1) using sector antennas (referred to as *Sector*), 2) performing ordinary beamforming (*BF*), 3) conducting Coordinated Beamforming only in cells of the same site (*CBF 1*), and 4) carrying out system wide Coordinated Beamforming (*CBF*). The coordination gain of system types is compared to the reference system BF. The second reference system *Sector* allows for relating these gains to the beamforming gain itself.

Figure 6.1 shows the Cumulative Distribution Function (CDF) of SINR for four system types. Table 6.2 completes Figure 6.1 by providing the corresponding mean and standard deviation. BF increases the SINR

<sup>27</sup> Bold values define the default parameter set.

## 6.1 Beam Coordination Performance versus other System Types

level by approximately 8 dB on average compared to the Sector reference system but increases standard deviation by 27% decreasing precision of CQI prediction. SINR gain of BF results from an increased receive power provided by beamforming. The higher standard deviation is caused by the mentioned flash light effect which increases variance of interference.

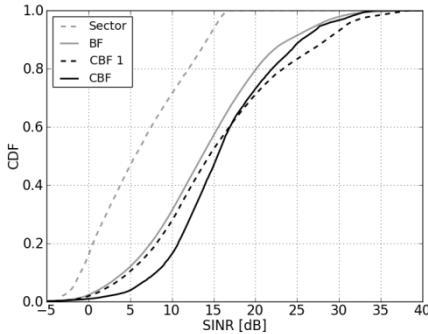


Figure 6.1: SINR CDF of four system types: sector antennas (Sector), Beamforming (BF), Coordinated BF of cells of one BS (CBF 1), and full Coordinated BF (CBF); (RR, FR1, 7 beams)

Table 6.2: Mean and Standard Deviation (STD) of SINR shown in Figure 6.1

System Type	Mean	STD
	in [dB]	
Sector	6.17	4.78
BF	13.97	6.05
CBF 1	15.60	7.06
CBF	16.16	5.39

Figure 6.1 and Table 6.2 show that CBF 1 further improves mean SINR by 1.6 dB but increases standard deviation by 17% compared to BF. Especially the probability of high SINR values is significantly increased compared to BF. Both, increased SINR variance and more high SINR values, are unexpected for one site coordination, which is supposed to only reduce interference of MS residing at common cell-edges of the site considered. Clearly, coordination in system CBF 1 is suboptimal. The relative low gain of CBF 1 has to be put in relation to the low beam coordination cost.

Coordination in a system wide manner as performed in system type CBF increases mean SINR compared to BF by 2.2 dB and reduces

## 6 Analytical Performance Evaluation

standard deviation by 11%. Clearly, CBF succeeds in avoiding strong interfering beams used in neighbour cells and thereby reduces probability of low SINR compared to BF, substantially. A reduced standard deviation of SINR supports more reliable SINR prediction and best possible link adaptation decisions.

Figure 6.2 depicts the CDF of the normalized data rate in bit/s/Hz according to Eq. (4.24) including the link adaptation introduced in Section 4.5. The rate does not exceed 3.2 bit/s/Hz achieved by the highest MCS (64-QAM-0.926) at SINR values  $\geq 20$  dB. Clearly, more efficient MCSs would result in a higher normalized data rate with a probability of approximately 15% for BF and 25% for coordinated systems. The Sector system would not benefit from more efficient MCS because  $\text{SINR} \leq 17$  dB. Hence, even higher beamforming gains and especially higher coordination gains would occur and can be expected in LTE-Advanced Release 11 systems also providing 128-QAM.

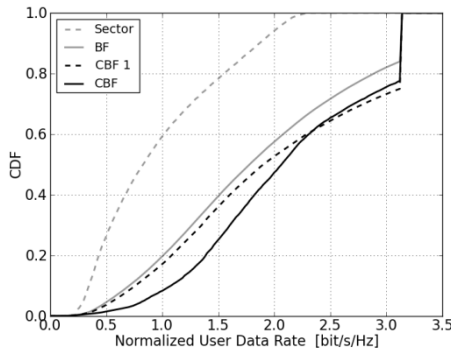


Figure 6.2: CDF of normalized data rate (before resource allocation) in [bit/s/Hz]; of the four system types; (RR, FR1, 7 beams)

## 6.1 Beam Coordination Performance versus other System Types

For each of the four system types, Figure 6.3 shows a map of the mean normalized data rate<sup>28</sup> for each grid point of the service area, according to Eq. (4.22)<sup>29</sup>, whereas Figure 6.2 shows the CDF of the normalized data rate of each permutation at all grid points. The centre BS in Figure 4.1 resides at the origin ( $x=0$  m,  $y=0$  m)<sup>30</sup> and serves the highlighted cell. Figure 6.3 generally supports the findings of Figure 6.1 and Figure 6.2. BF compared to Sector increases the normalized data rate level, with increased probability of high data rate values, see Figure 6.3 (b). Figure 6.3 (c) shows that CBF 1 further increases the normalized data rate compared to BF, but only slightly at the cell edge common to cells of one site and mainly locations having already a good SINR. Figure 6.3 (d) depicts that CBF can improve normalized data rate performance in the whole cell also at the cell edges between BSs but areas served by the two outer beams are slightly neglected.

---

<sup>28</sup> Mean data rate is over all permutations at a grid point.

<sup>29</sup> At a grid point with a normalized mean data rate  $\leq 0$  bit/s/Hz still service may be provided by the network due to possible higher data rate within several beneficial permutations.

<sup>30</sup> Data rate inside the small circular area with radius 25m around the BS is set to zero according to ITU-R guidelines.

## 6 Analytical Performance Evaluation

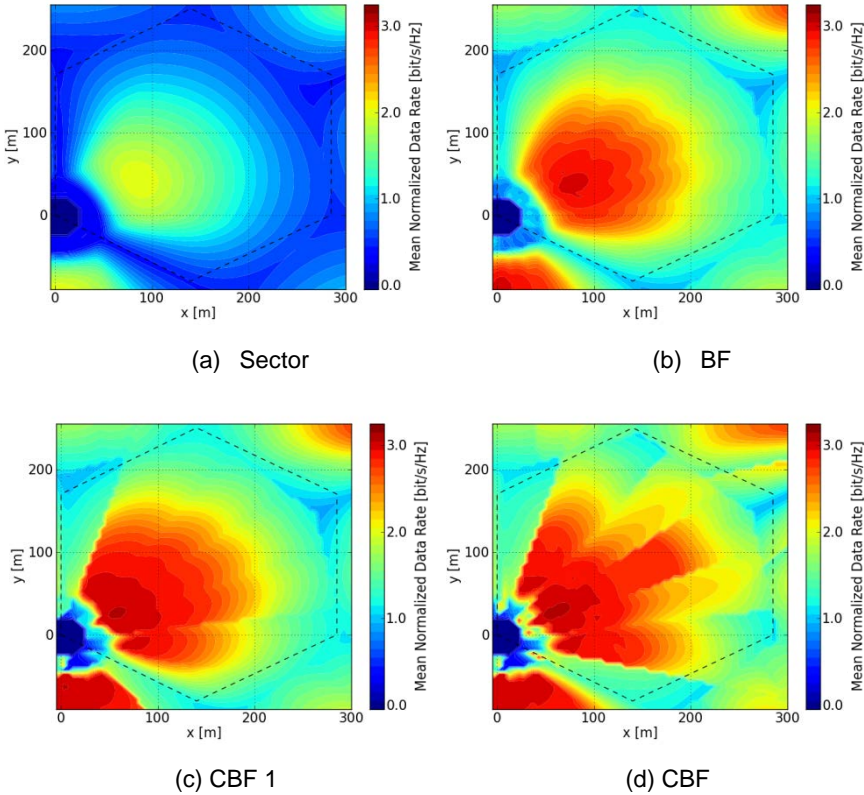


Figure 6.3: topography of mean normalized data rate [bit/s/Hz]; of the four system types; (RR, FR1, 7 beams)

Figure 6.4 shows the absolute coordination gain in terms of the mean normalized data rate compared to the non-coordinated BF for system type CBF 1 and for CBF, respectively. Figure 6.4 (a) reveals that with CBF 1 primarily two regions suffer from beam coordination and perceive lower data rate than with BF, namely a vertical stripe starting at  $x = 30$  m,  $y = 90$  m and a horizontal stripe starting at  $x = 130$  m,  $y = 0$  m. Figure 6.4 (b) reveals that with CBF mainly six regions in the cell are served with lower data rate than with BF. The worse served regions result from beams of adjacent cells colliding there giving evidence that

## 6.2 Impact of Scheduling Strategies on Beam Coordination Performance

still potential exists for further SINR improvement by further improved beam coordination.

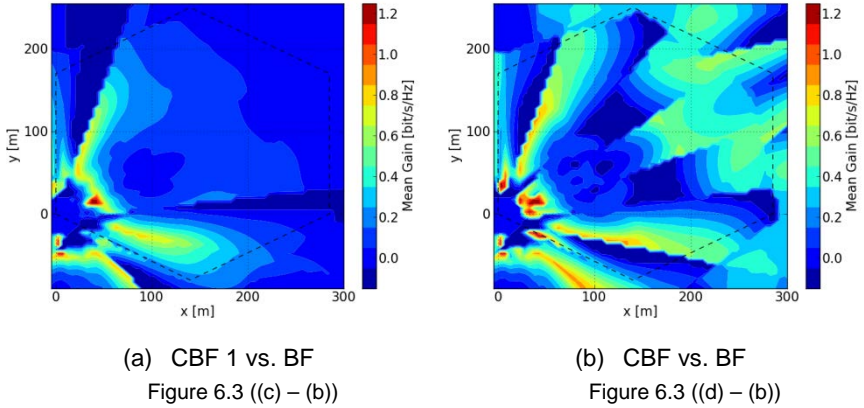


Figure 6.4: topography of absolute coordination gain in terms of mean normalized data rate [bit/s/Hz]<sup>31</sup>

## 6.2 Impact of Scheduling Strategies on Beam Coordination Performance

This Section compares the impact on beam coordination of two scheduling strategies for radio resource allocation, namely RR and RF (as defined in Section 4.5.4). The scheduling considers a discrete radio resource allocation to a random number of MSs per cell<sup>32</sup>. For evaluating the coordination gain, the performance metrics Cell-Edge User Spectral Efficiency (CE-USE) and Cell Spectral Efficiency (CSE) are

---

<sup>31</sup> Depicted gains are cut off for values beyond the range between -0.1 and 1.2 bit/s/Hz due to the rare occurrence and for sake of significance.

<sup>32</sup> See discussion in Section 4.5.3.

used<sup>33</sup> (see Eq. (4.30) and (4.32), respectively). CE-USE is an indicator for fairness of the scheduling algorithm whereas the CSE gives the total cell capacity per bandwidth unit.

Figure 6.5 plots CE-USE over CSE for both RR and RF scheduling strategies and for all system types considered. RR yields approximately 40% higher CSE than RF whereas RF yields approximately 70% higher CE-USE than RR for all system types, except CBF. For the CBF, system RR gains 20% CSE versus RF and RF gains 40% CE-USE versus RR. The trade off between fairness and CSE is obvious, a strategy can optimize one at the expense of the other, only. Figure 6.6 completes the comparison of scheduling strategies by depicting the CDF of the mean MS throughput exemplarily for a BF system (see Figure A.1 for other system types). RF scheduling provides the same throughput to MSs in a cell. The variable number of MSs per cell sharing the radio resources available per cell result in variance of the MS throughput in Figure 6.6: with few MSs, each MS gains a higher throughput than with many MSs per cell. Figure 6.6 shows results of multiple samples each with another number of MSs per cell according to the probability distribution in Figure 4.14. RR scheduling grants the same amount of resources to all MSs. Since SINR has a high variance and so the chosen MCS has, since MS throughput is proportional to MSs SINR also has a high variance. While RF scheduling obviously maximises fairness and RR scheduling favours MSs with high SINR and thereby cell capacity.

Table 6.3 completes Figure 6.5 by listing coordination gain compared to the BF system. It shows that beam coordination significantly improves CSE and CE-USE with both scheduling strategies. The gain of both metrics is substantially under CBF whereas gains are much lower under CBF 1.

---

<sup>33</sup> Cell-Edge User Spectral Efficiency (CE-USE) is the 5<sup>th</sup> percentile of the mean user throughput CDF and the Cell Spectral Efficiency (CSE) is the mean of this CDF.

## 6.2 Impact of Scheduling Strategies on Beam Coordination Performance

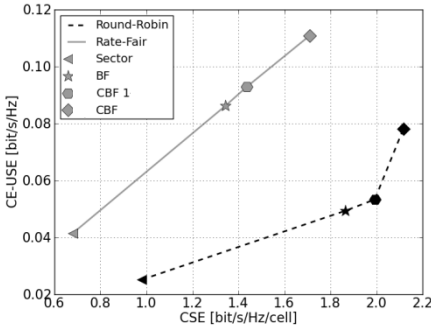


Figure 6.5: CE-USE versus CSE with both RR and RF scheduling; (FR1, 7 beams)

Table 6.3: coordination gain vs. beamforming in Figure 6.5

	CSE	CE-USE
System Type		
CBF 1		
RR	7%	8%
RF	7%	8%
CBF		
RR	13%	48%
RF	27%	29%

The results under RR prove that CBF boosts especially CE-USE, i.e., primarily the performance of MSs with low SINR. Although CBF under RF scheduling also prefers MSs with low SINR, as depicted in Figure 6.5, MSs in the whole cell profit more from the mitigated interference in terms of spectral efficiency than with RR. Hence, beam coordination gain is exploited differently depending on the scheduling strategy which decides how the SINR gain is translated into CSE or fairness.

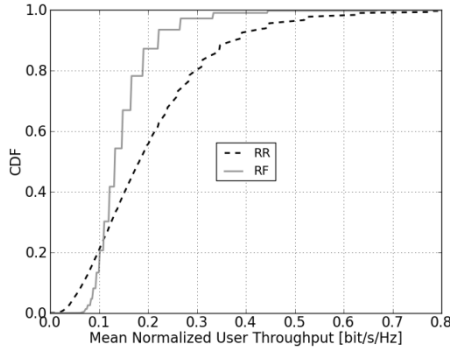


Figure 6.6: CDF of Mean Normalized MS Throughput for RR and RF scheduling; (BF, FR1, 7 beams)

### 6.3 SFR - Derivation of an Operating Point

This Section studies the SFR scheme, as discussed in Section 5.1, with scheduling strategies RR and RF and derives an operating point in terms of effective reuse factor  $\alpha$ . The derived operating point is shown to be a reasonable choice for both studied scheduling strategies and for all system types, coordinated as well as non-coordinated systems. How a system can employ Beam Coordination under SFR is described in Section 5.4.3.

#### 6.3.1 Different Scheduling Strategies Operated under SFR

SFR has the parameter of effective frequency reuse  $\alpha$  see Eq. (5.1). Assuming fixed total transmit power, the power level of the secondary spectrum parts is  $\beta = 3 - \alpha/2$ .  $\alpha$  can vary between one corresponding to FR1 and three corresponding to FR3. The best operating point for  $\alpha$  should yield both high cell capacity and fairness independent of the scheduling strategy. For sake of fair comparison of scheduling strategies under SFR, one operating point of  $\alpha$  for all scheduling strategies is sought. In the following, performance results are presented, a recommended operating point is identified, and results are interpreted.

Figure 6.7 (a) shows CSE versus  $\alpha$  with three scheduling strategies. RR Strict, as the most unfair strategy, outperforms both other scheduling strategies in terms of CSE for  $\alpha < 2.3$ , with a maximum of 1.78 bit/s/Hz/cell at  $\alpha = 1.8$ . For  $\alpha > 2.3$ , RR Balanced performs best in terms of CSE, with a maximum of 1.75 bit/s/Hz/cell at  $\alpha = 2.6$ . RF scheduling owing to its fair service to all MSs achieves its CSE maximum of 1.46 bit/s/Hz/cell at  $\alpha = 2.4$ . For  $\alpha > 2.6$ , CSE declines significantly for all strategies, since FR3 is more and more approximated.

Figure 6.7 (b) plots the CE-USE versus  $\alpha$  for varying scheduling strategies. RF scheduling nearly independent of  $\alpha$  yields the best CE-USE, as expected. Both RR scheduling strategies achieve much lower CE-USE than RF with a small advantage for RR balanced since CE-USE is for a wide range of  $\alpha$  independent of the value of  $\alpha$ .

The optimal operating point for RF scheduling in SFR scheme is at  $\alpha \approx 2.4$ . For  $\alpha > 2.3$ , RR Balanced appears in general to be superior over RR Strict owing to much higher CSE and CE-USE that is less sensitive to  $\alpha$ . Hence RR Balanced besides RF scheduling is only considered in the following to be used with SFR. From the result shown an operation at  $\alpha = 2.4$  to 2.6 appears optimal. Anticipating later shown results for system Sector, SFR scheme is assumed to operate at  $\alpha = 2.6$ .<sup>34</sup> It is worth noting that optimal  $\alpha$  would decrease if higher valued MCS were available for SINR > 20 dB. With link adaptation as standardized in 3GPP LTE(-Advanced), strong MSs perceiving SINR > 20dB do not benefit from this since no appropriate MCS is available to exploit such good receive condition.

---

<sup>34</sup> An operating point at  $\alpha = 2$  with RR Strict scheduling seems to be a feasible option but this choice would decline the performance of the system Sector and BF under SFR over proportionally, as depicted in the Annex, Figure A.1.

## 6 Analytical Performance Evaluation

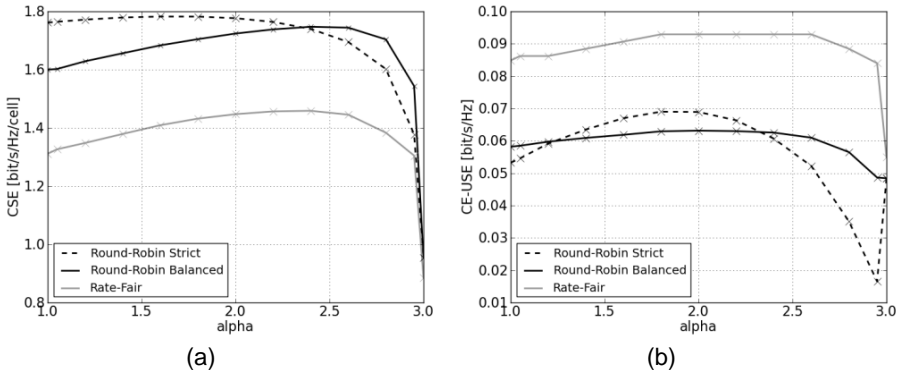


Figure 6.7: (a) CSE and (b) CE-USE versus  $\alpha$  under SFR with RR vs. RF scheduling; (BF, SFR, 3 beams<sup>35</sup><sup>36</sup>)

Figure A.4 completes the comparison of scheduling strategies by depicting the CDF of the mean MS throughput exemplarily for a Sector and a BF system for  $\alpha = 1.8$ .

### 6.3.2 Different System Types Operated under SFR

Figure 6.8 depicts (a) CSE and (b) CE-USE versus  $\alpha$  for various system types under RR scheduling. For all values of  $\alpha$ , both coordinated system CBF 1 and CBF show significant coordination gains (except for  $\alpha \approx 3$ ) versus the BF system. The CSE optimal  $\alpha$  for Sector and BF system is at  $\alpha = 2.6$ , where for Sector system also the CE-USE maximum resides and where for the BF system CE-USE is only 2-3% lower to its maximum at

<sup>35</sup> In Section 6.3, 3 beams are employed instead of 7 beams because of major reduction of computational effort and time consumption and marginal impact on findings as derived later.

<sup>36</sup> Results with SFR at poles of  $\alpha$  with beamforming can slightly deviate from the ones with FR1 and FR3 (< 5%) because they are generated differently. With SFR, allocation to spectrum parts requires to use mean values over all beam permutations (similar to Figure 6.3) instead of exact values of each beam permutation with FR1 and FR3, see Figure 6.2.

$\alpha = 2.2$ . For the coordinated systems,  $\alpha = 2.6$  results in CSE values of 1-2% lower than the own maximum (at  $\alpha = 2.2$ ) and in CE-USE values of 9% for CBF (and of 4% for CBF 1) lower than own maximum. Hence  $\alpha = 2.6$  as operating point is a reasonable choice.

Figure 6.9 correspond to Figure 6.8 but shows results for RF scheduling. It shows that  $\alpha = 2.6$  yields maximal (or very close to maximal) CSE and CE-USE for both Sector and BF system. For the coordinated system CBF 1 and CBF, this is an acceptable  $\alpha$  with less than 5% loss for both metrics CSE and CE-USE versus its maximum at  $\alpha = 2.0$ .

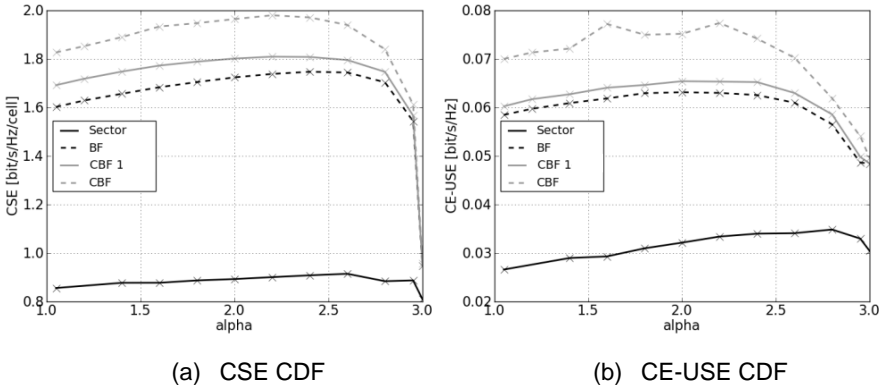


Figure 6.8: (a) CSE and (b) CE-USE versus  $\alpha$  under SFR with RR-Balanced Scheduling; (BF, SFR, 3 beams)

## 6 Analytical Performance Evaluation

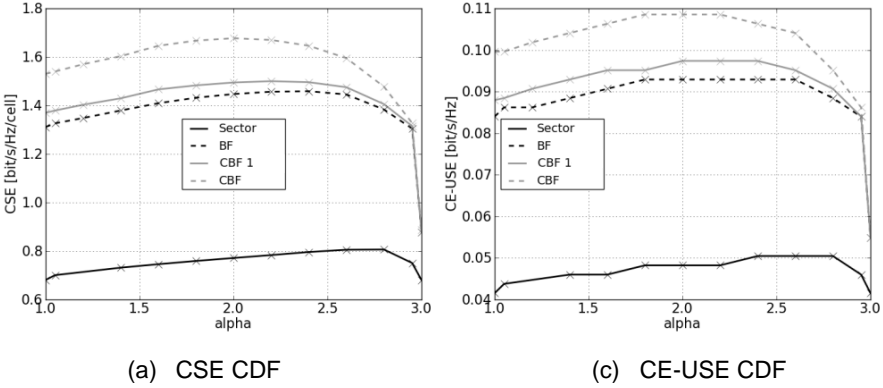


Figure 6.9: (a) CSE and (b) CE-USE versus  $\alpha$  under SFR with RF Scheduling; (BF, SFR, 3 beams)

For sake of fair comparison of scheduling strategies and system types under SFR, one operating point of  $\alpha$  is sought. Summarizing, the operating point at  $\alpha=2.6$  yields optimal (or very close to optimal) results with SFR for non-coordinated systems and allows still for significant coordination gains. Hence, in Figure 6.10 to Figure 6.12, the SFR scheme is used with  $\alpha = 2.6$ .

### 6.4 Impact of Frequency Reuse Schemes on Beam Coordination Performance

In this Section, the impact of different frequency reuse schemes on the spectral efficiency under beam coordination is studied. The studied schemes are FR1, SFR and FR3, as discussed in Section 5.1.

Figure 6.10 shows CE-USE versus CSE for various reuse schemes and four systems types. Table 6.4 complements Figure 6.10 by listing coordination gain compared to a BF system in terms of CSE and CE-USE. Under SFR, CBF 1 increases CSE (cell capacity) by 12% and CE-USE (fairness) by 8% whereas CBF achieves CSE of 17% and CE-USE of 72%. Under FR1 gains are smaller than under SFR, CBF 1 improves CSE by 7% and CE-USE by 8% whereas CBF lifts CSE by 13% and CE-USE

## 6.4 Impact of Frequency Reuse Schemes on Beam Coordination Performance

by 58%. Under FR3, no or almost no coordination gain occurs. In FR3, where distances to most interfering BSs is approximately doubled compared to FR1, beams do not well focus their transmit power making beam coordination ineffective. Summarising, both CBF 1 and CBF significantly increase CSE and CE-USE in FR1 and SFR scenarios, with higher gains in SFR.

CBF in both SFR and FR1 scenarios improves cell capacity but particularly increases cell edge performance which is the design goal of CBF. The coordination gain in SFR scenario is higher than in FR1. This is a result of coordinated transmission of MSs served on the secondary spectrum part. These MSs perceive low signal strength (with  $\beta = 0.2$ ) and high interference (with  $\alpha = 2.6$ ) and thus profit more from interference mitigation than a MS in FR1. Transmit power of the (serving) secondary spectrum is 13 times lower than that of the (interfering) primary spectrum, see Eq. (5.2).

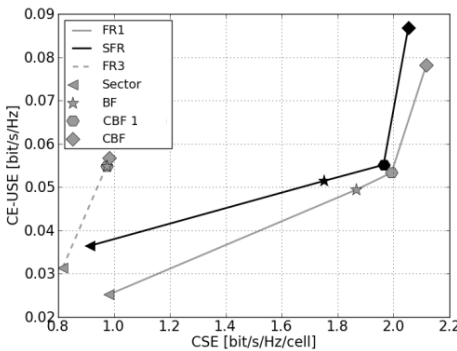


Figure 6.10: CE-USE versus CSE in various frequency reuse schemes; (RR, 7 beams)

Table 6.4: coordination gain vs. beamforming in Figure 6.10

System Type	CSE	CE-USE
<b>CBF 1</b>		
FR1	7%	8%
SFR	12%	8%
FR3	0%	0%
<b>CBF</b>		
FR1	13%	58%
SFR	17%	72%
FR3	1%	3%

Figure 6.10 shows frequency reuse schemes differ in fairness and cell performance. For example in the BF system (plotted as stars), FR1 has the highest CSE of 1.85 bps/Hz/cell, 7% higher than in SFR and 92% higher than in FR3; but cell edge MSs suffer from high interference. FR3

## 6 Analytical Performance Evaluation

yields the highest fairness indicated by CE-USE = 0.055 bit/s/Hz which is 7% higher than in SFR and 11% higher than in FR1. In FR3, the large reuse factor provides improved SINR to cell edge MSs but achieves only half the CSE compared to SFR owing to small system bandwidth available per cell. Reuse schemes, similar to scheduling strategies, tend to trade capacity versus fairness.

Figure 6.11 depicts SINR CDFs for the frequency reuse schemes considered for a BF system. FR3 cannot transfer its SINR advantages into high data rate due to missing appropriate MCSs in LTE-Advanced standard translating SINR > 20 dB into higher data rate. If higher MCSs were available, more than 70% of the MSs in FR3 could be served with much higher data rate than possible at SINR = 20 dB. In FR1 and SFR, only 20% of the MSs perceive higher SINR values than 20 dB. SFR increases SINR of cell edge MS at the cost of slightly reducing SINRs of centre cell MSs. Even lower SINR results of systems operating with three beams instead of seven as above (see Figure A.5 to Figure A.7) show only a marginally reduced percentage of SINR > 20 dB and hence emphasise that higher MCSs are required.

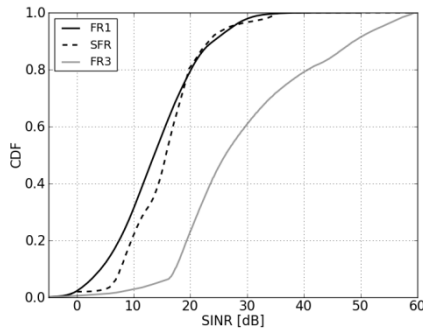


Figure 6.11: SINR CDF of varying frequency reuse schemes, (BF, RR, 7 beams)

Figure 6.12 plots CE-USE versus CSE under RF scheduling. Table 6.5 complements Figure 6.12 by listing coordination gain compared to BF

## 6.4 Impact of Frequency Reuse Schemes on Beam Coordination Performance

case. The trend of the results is similar to that under RR scheduling shown in Figure 6.10. Under RF, the gain is shared between all MSs. With RF scheduling, CBF generates slightly higher gain when applied in FR1 system than in an SFR system for both metrics CSE and CE-USE. The reason is that with SFR, more MSs are scheduled on the primary spectrum part than under RR. In an FR1 system, more interference occurs with BF that can be mitigated by CBF than in an SFR system which already operates with reduced interference in the primary spectrum part. SFR under RF scheduling is superior to the other frequency reuse schemes considered.

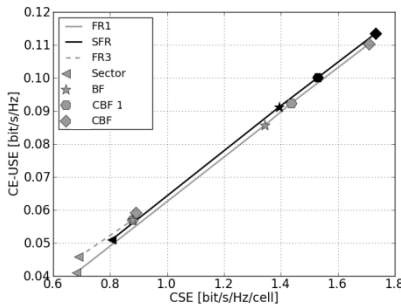


Figure 6.12: CE-USE versus CSE for various reuse schemes; (RF<sup>37</sup>, 7 beams),

Table 6.5: coordination gain vs. beamforming in Figure 6.12

System Type	CSE	CE-USE
<b>CBF 1</b>		
FR1	7%	8%
SFR	10%	10%
FR3	0%	0%
<b>CBF</b>		
FR1	27%	29%
SFR	24%	25%
FR3	1%	4%

Summarizing for both scheduling strategies RR and RF:

- 1) Gain from CBF 1/CBF under FR3 operation is marginal and not worth the effort.
- 2) With CBF 1 under SFR operation the gain is up to 12% in CSE and 10% in CE-USE.

<sup>37</sup> All points appear to be approximately on the same axis. For sake of better visibility, results for FR3 and FR1 scheme are shifted by +/-0.001 bit/s/Hz on the y-axis, respectively.

- 3) Under SFR and FR1 operation, CBF systems outperform significantly a BF system in terms of CSE by up to 27% as well as CE-USE by up to 72%. Clearly CBF is worth the effort.

### **6.5 Impact of the Codebook Size on Beam Coordination Performance**

This Section studies the impact of the number of applied fixed beams on the achieved coordination gain. Figure 6.13 shows three different beam sets being a subset of the 3GPP codebook [3GPP TS 36.211] depicted in Figure 4.3. The sector pattern (see Figure 4.2 (a)) is which the MS associates to but data transmission is performed on beams only if available in the studied system.<sup>38</sup>

---

<sup>38</sup> except the *Sector* system employing its sector pattern.

## 6.5 Impact of the Codebook Size on Beam Coordination Performance

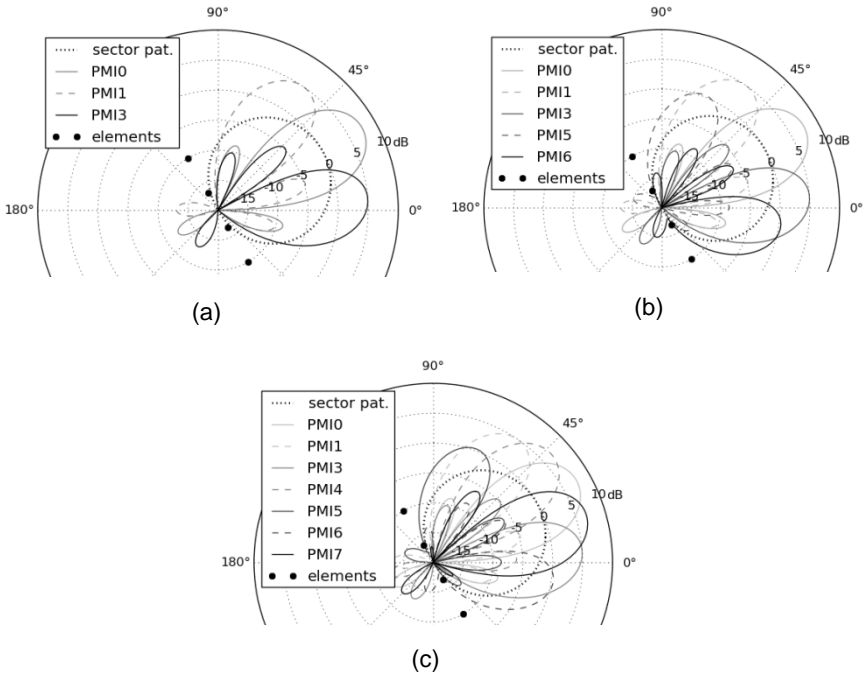


Figure 6.13: studied subsets of codebook in [3GPP TS 36.211] and Section 4.2.3, (a) 3 beams (b) 5 beams (c) 7 beams; all sets include the sector pattern for MS association.

Figure 6.14 shows CE-USE versus CSE for RF and RR scheduling with the number of beams as parameter. For each number of beams, results are shown for all system types. It becomes evident that an increasing number of beams improves both CSE and CE-USE. One exception is CBF under RR scheduling where an increased number of beams from 3 to 5 only impacts CE-USE.<sup>39</sup>

---

<sup>39</sup> Spectral efficiency values are derived from graphs in Figure A.8 accordingly to Eq. (4.30) and (4.32).

## 6 Analytical Performance Evaluation

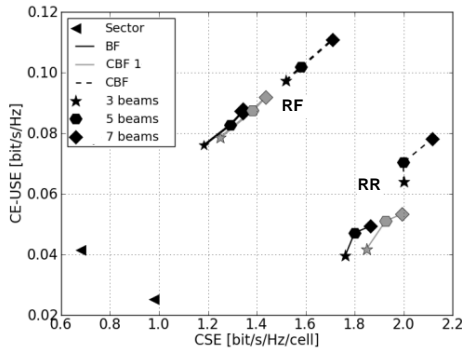


Figure 6.14: fairness versus capacity under various number of beams for both RR and RF scheduling; FR1

These results are also plotted as a bar-diagram in Figure 6.15 for RR and Figure 6.16 for RF scheduling in order to improve the visibility of the coordination gain. The percentage values plotted next to bars give the coordination gain compared to BF case. Figure 6.15 shows that CBF 1 improves the CSE between 5-7% and the CE-USE between 6-8%. CBF increases the CSE between 11-14% and the CE-USE between 49-62%. The high gain of CE-USE under CBF emphasises that system wide beam coordination is especially beneficial for MSs at the cell edge.

## 6.5 Impact of the Codebook Size on Beam Coordination Performance

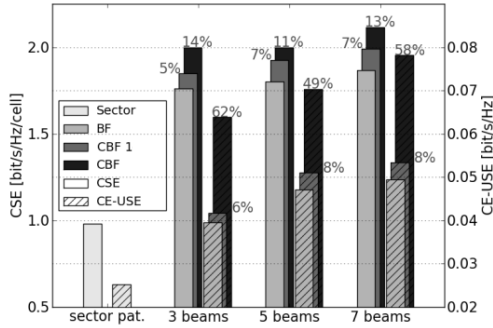


Figure 6.15: CSE and CE-USE versus number of beams; coordination gain in [%] is compared to BF case; RR scheduling; FR1

Figure 6.16 shows for RF scheduling spectral efficiency versus number of beams, as in Figure 6.15. CBF 1 improves CSE by 6-7% and CE-USE by 6-8%. CBF increases CSE by 22-28% and CE-USE by 25-30%.

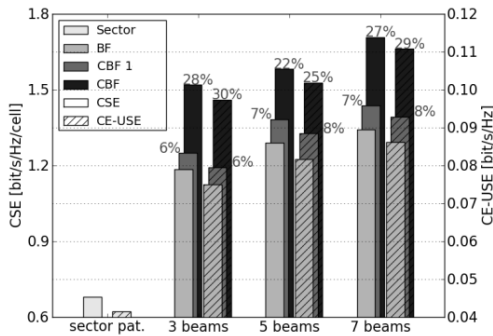


Figure 6.16: CSE and CE-USE versus number of beams; coordination gain in [%] is compared to BF case; RF scheduling; FR1

The relative coordination gain over BF in terms of CSE and CE-USE seems to be approximately independent of the number of beams. Due to

an increasing gain of BF versus a sectorized system, the absolute CSE and CE-USE values increase with the number of beams. Coordination gain results from two reasons, 1) improved efficiency of link adaptation by knowing interferers and SINR, and 2) mitigating interference by avoiding harmful collisions of beams from neighbour cells. As mentioned, 1) is not included in the model applied in this work since correct SINR estimation is assumed. 2) may lead to the assumption that increasing number of beams would improve capacity owing to improved flexibility of beam coordination steering interference away from receiving MSs. An increasing number of beams, however, does not result in sharper beams but basically in more overlapping beam patterns, see Figure 6.13. An increasing average signal strength is visible there with an increased number of beams. For example, with 7 beams antenna gain at an angle of  $45^\circ$  is higher compared to 5 beams only. Hence, higher number of beams increases coverage (signal strength) for both BF and CBF systems - but the total interference perceived in neighbour cells remains unchanged. An antenna array with increased number of elements, say eight, can form sharper beams and hence is supposed to increase coordination gain, similar as in implicit beam coordination [Thiele, 2013], where CSE is tripled if the number of antennas is quadrupled, whereas the CE-USE scales almost linearly. Another reason, for the coordination gain to be independent of the number of beams, might result from characteristics of CBF 1/CBF focusing on cell edge interference mitigation which might result in not fully exploiting the potential of higher number of beams to improve CSE. The CyBeamCo can easily be modified to also explicitly mitigate interference in the centre cell.

## CHAPTER 7

---

### **Conclusion and Outlook**

Coordinated beamforming (CBF) as introduced in this work for instance by means of the CyBeamCo-algorithm significantly outperforms ordinary beamforming (BF) for all studied parameters such as scheduling strategy, frequency reuse scheme, or number of beams, independent of whether beams of all cells or cells only of one site are coordinated. With frequency reuse three beamforming gains are marginal. Beam coordination increases mean SINR by 2.2 dB and reducing variance of the SINR by 11%. Both scheduling strategies such as Round-Robin (RR) and Rate-Fair (RF) and reuse schemes such as FR1 and SFR are shown to trade off fairness to MSs against cell capacity. Beam coordination improves both Cell Spectral Efficiency (CSE) and Cell Edge-User Spectral Efficiency (CE-USE).

Interference mitigation under FR1 is shown to boost CE-USE by up to 58% while improving at the same time CSE of the entire cell by up to 29% compared to BF. Under soft frequency reuse (SFR), cell edge performance is further improved by up to 72% compared to ordinary BF. The derived relative coordination gain found is only due to interference mitigation since the possible contribution of an improved link adaptation resulting from better predictable interferers through coordination is not considered in the studied model.

For an SFR based system an operating point in terms of effective reuse factor is derived in this work yielding optimal results for ordinary BF systems and allowing significant beam coordination gain. The optimal operating point is shown to be dependent on the scheduling strategy and the peak data rate available from the link-adaptation algorithm.

## 7 Conclusion and Outlook

A higher number of beams (with constant number of antenna elements) does not significantly improve coordination gain compared to ordinary BF but increases the CSE of all beamforming based systems due to a resulting improved cell coverage.

Coordination of cells of one BS (CBF 1) (compared to ordinary BF) yields gains of up to 12% in cell capacity and up to 10% in fairness which are much lower than under beam coordination of all cells of a system, but a simple software update of BSs should be sufficient to enable this type of coordination. Possible improvements to CBF 1 based beam coordination is introduced in this work such as only coordinating cell edges common to cells of one BS, which could be an issue for future work.

The two-dimensional coordination gain calculated shows regions in a cell which even suffer from beam coordination. Hence promising extension to the developed beam coordination scheme could be to explicitly mitigate interference in the centre cell as well.

Results shown for beam coordination should be considered as an upper bound since a central coordination might be not feasible in a real system and unsteady geometry of cells as well as bursty traffic might further reduce beam coordination gains of real systems. On the other hand, coordination gains in a real system are improved by the resulting reduction of SINR estimation error and by exploiting future MCS with higher data rate for high SINR conditions.

The beam coordination algorithm developed is especially beneficial in sparse multipath scenarios with medium to large cell size and high LOS probability of the radio path such as urban macro, rural macro scenarios, or scenarios with direct wireless communication between an aircraft and the ground [ETSI, 2010]. The developed beam coordination algorithm could be adapted to this scenario in future work which might also include multiple beams (SDMA) or consider adaptive beamforming.

# A Additional Results

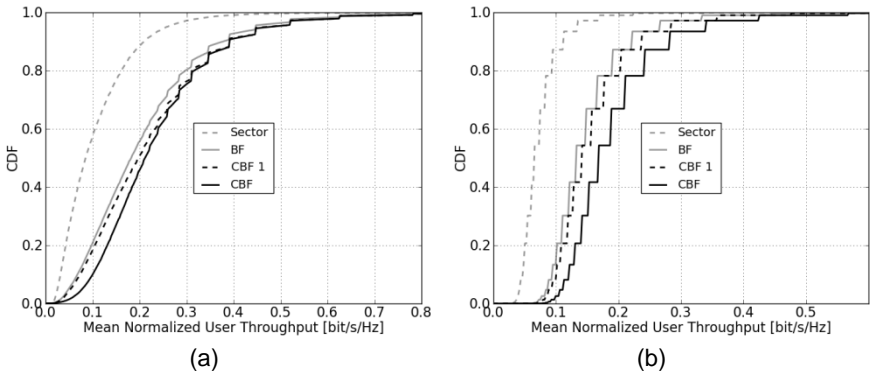


Figure A.1: CDF of Mean Normalized MS Throughput for (a) RR and (b) RF scheduling; (FR1, 7 beams)

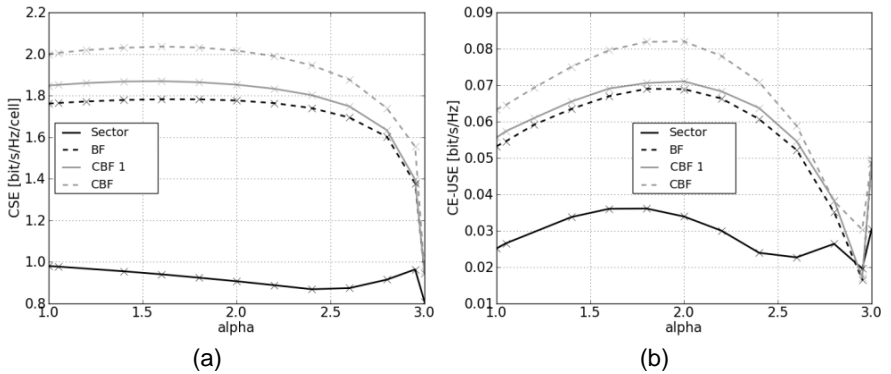


Figure A.2: spectral efficiency (a) CSE (b) CE-USE of the SFR system versus alpha; RR Strict Scheduling; (3 beams)

## A Additional Results

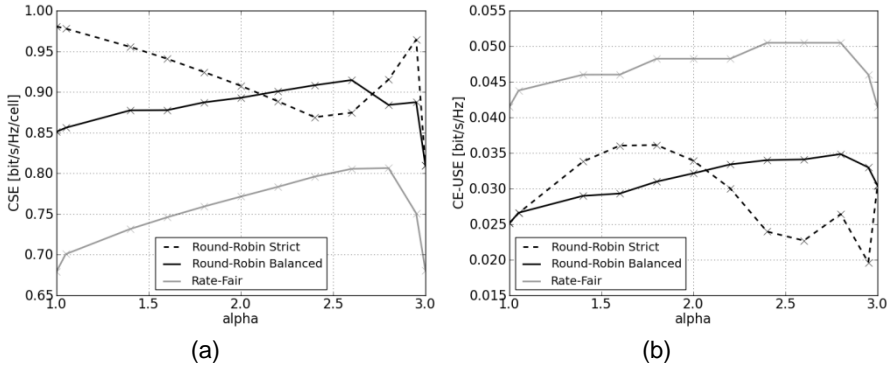


Figure A.3: spectral efficiency (a) CSE (b) CE-USE of the SFR system versus  $\alpha$ ; RR vs. RF scheduling; (Sector)

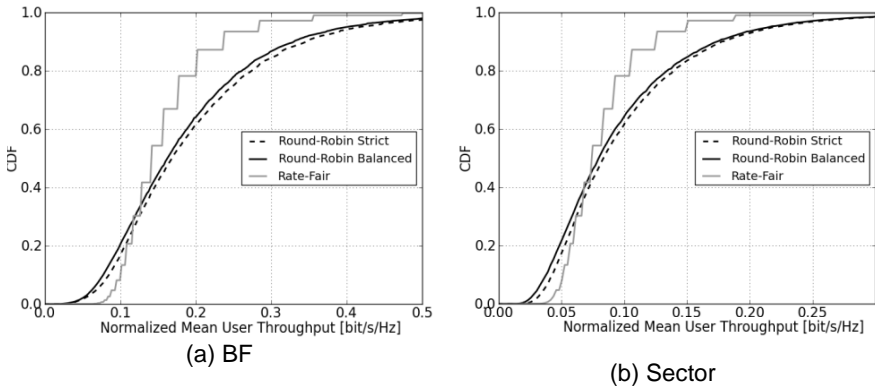


Figure A.4: CDF of Normalized Mean MS Throughput in SFR with varying scheduling strategy at  $\alpha = 1.8$ ; (a) Beamforming system with 3 beams and (b) Sector system

## 6.5 Impact of the Codebook Size on Beam Coordination Performance

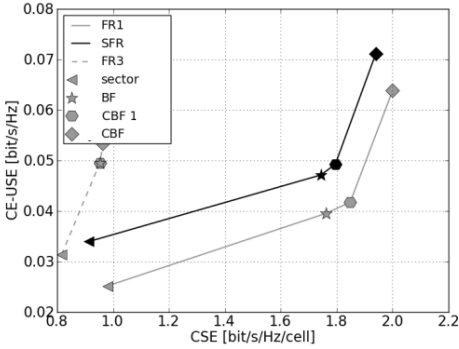


Figure A.5: CE-USE versus CSE with different reuse schemes; (RR, 3 beams)

Table A.1: coordination gain vs. beamforming of Figure A.5

System Type	CSE	CE-USE
CBF 1		
FR1	5%	6%
SFR	3%	5%
FR3	0%	0%
CBF		
FR1	14%	62%
SFR	11%	51%
FR3	1%	8%

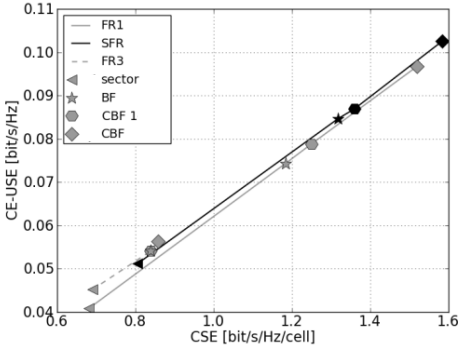


Figure A.6: CE-USE versus CSE with different reuse schemes; (RF, 3 beams)

Table A.2: coordination gain vs. beamforming of Figure A.6

System Type	CSE	CE-USE
CBF 1		
FR1	6%	6%
SFR	3%	3%
FR3	0%	0%
CBF		
FR1	28%	30%
SFR	20%	21%
FR3	2%	4%

## A.1 Example Coordination Matrices

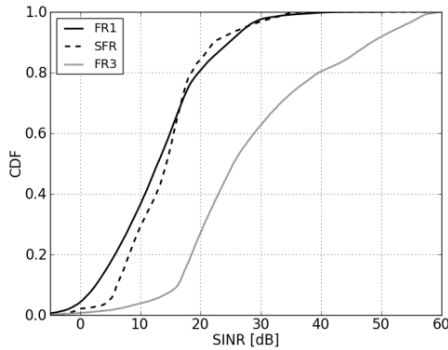


Figure A.7: SINR CDF of varying frequency reuse schemes; (BF, RR, 3 beams)

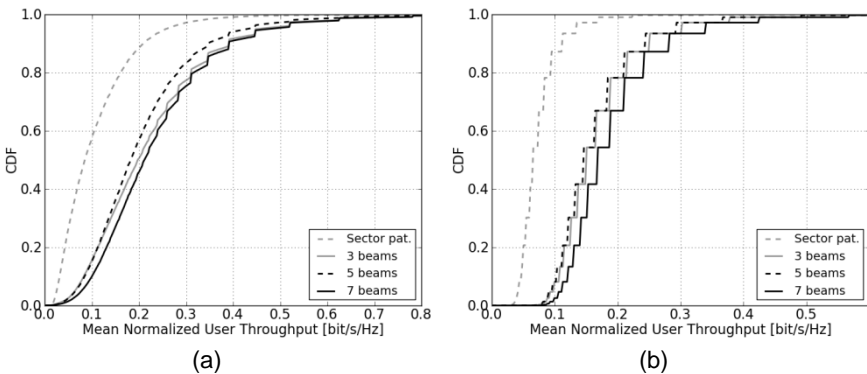


Figure A.8: CDF of Mean Normalized MS Throughput for CBF with various number of beams under (a) RR and (b) RF scheduling; (FR1)

## A.1 Example Coordination Matrices

Following coordination matrices utilize PMIs of Figure 4.3 and subsets of Figure 6.13 assuming the scenario of Figure 4.1. A line of a matrix defines simultaneously employed PMIs in different cells and a column defines sequentially employed PMIs for a cell (type):

## 6.5 Impact of the Codebook Size on Beam Coordination Performance

$$M_{3\text{Beams}} = \begin{bmatrix} 0 & 3 & 1 \\ 1 & 0 & 3 \\ 3 & 1 & 0 \end{bmatrix} \quad M_{3\text{Beams},1\text{Site}} = \begin{bmatrix} 0 & 0 & 0 \\ 1 & 1 & 1 \\ 3 & 3 & 3 \end{bmatrix}$$

$$M_{5\text{Beams}} = \begin{bmatrix} 0 & 3 & 5 \\ 1 & 0 & 6 \\ 3 & 6 & 1 \\ 5 & 1 & 3 \\ 6 & 5 & 0 \end{bmatrix} \quad M_{5\text{Beams},1\text{Site}} = \begin{bmatrix} 0 & 0 & 0 \\ 1 & 3 & 5 \\ 3 & 5 & 1 \\ 5 & 1 & 3 \\ 6 & 6 & 6 \end{bmatrix}$$

$$M_{7\text{Beams}} = \begin{bmatrix} 1 & 4 & 3 \\ 3 & 1 & 4 \\ 4 & 3 & 1 \\ 6 & 6 & 6 \\ 7 & 7 & 7 \\ 0 & 0 & 0 \\ 5 & 5 & 5 \end{bmatrix} \quad M_{7\text{Beams},1\text{Site}} = \begin{bmatrix} 0 & 0 & 0 \\ 1 & 3 & 4 \\ 3 & 4 & 1 \\ 4 & 1 & 3 \\ 5 & 5 & 5 \\ 6 & 6 & 6 \\ 7 & 7 & 7 \end{bmatrix}$$



## B Performance Evaluation of CB for adaptive BF with SDMA (Scheme I) - Assumptions and Results

### B.1 Simulation Scenario

The evaluated scenario consists of 7 BSs serving  $120^\circ$  (sector) cells, each with 10 MSs, as shown in Figure B.1. Measurements are only performed in the central cell (black) for the corresponding BS and MSs. The stations in the surrounding 6 cells only produce interference and are not evaluated. Nevertheless, the same event driven stochastic simulation, with identical average traffic loads, and with the same degree of detail, is conducted at all 66 stations. The cells have a radius of  $R = 333\text{m}$  and an  $N = 3$  cell cluster order is used as shown in Figure B.1. Cells that are not shown are assumed to operate on different frequency bands, which means their interference can be ignored. The nearest interfering cells (red) have a distance of  $D = \sqrt{3NR} = 1000\text{m}$ . Scenario parameters such as the cluster order and cell radius are selected according to the Urban Macro cell scenario in [IEEE 802.16m EMD]. In the TDD system cells are synchronized and all BSs transmit their DL and UL MAPs at the same time. In the broadcasting phase, BF patterns must not be used which means that MSs experience worst case SINR levels during these times.

Simulation parameters that are still not available in the IEEE.16m draft [IEEE 802.16m SDD] are taken from [IEEE 802.16 D8].

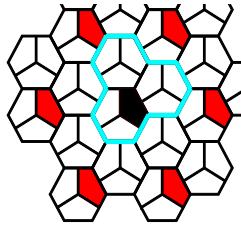


Figure B.1: positions of sectors in central (black) and co-channel (red) cells of evaluated clustered cellular deployment

### B.1.1 Simulator and Traffic Model

The open Wireless Network Simulator (openWNS) developed at ComNets [Buelmann, 2009] is a time discrete, event driven simulator. The load generator of each station generates IP data packets according to a specified arrival process and feeds them into the WiMAX data link layer (DLL) via the suitable Service Access Point (SAP). When a packet is scheduled, it is forwarded to the physical layer (PHY) module that adds the packet's transmission to the set of currently active transmissions in the scenario. Until the transmission is over, all other packets transmitted at the same time on the same frequency band experience the interference generated by the transmission, taking into account pathloss and antenna characteristics in form of the beam pattern and sectorization. For all MSs we apply symmetric traffic loads in DL and UL direction to and from all MSs, respectively. For each run, the following performance values are derived and evaluated:

**Modulation and Coding Scheme (MCS):** the MCS used for the packet transmission. Six MCS are employed and namely given e.g. by "QPSK 3/4". MCS is selected accordingly to the SINR thresholds of Table 1.

**Delta MCS:** Here MCS (namely ["Not Valid", QPSK1/2, ..., 64QAM3/4]) are mapped to integer numbers [0-6]. Delta MCS indicates the deviation of the MCS estimation. It is the difference between the optimal and the estimated MCS. Negative values indicate a too optimistic MCS choice, i.e., packet loss.

**Throughput:** Measured in Bit/s as the total bits of all packets successfully arriving at the WiMAX SAP of the destination station during a fixed time window. Separate values are measured for packets travelling to/from every MS in UL and DL direction.

### B.1.2 Link Adaptation and Error Modelling

The scheduling strategy performs link adaptation based on the SINR estimations provided by the spatial grouper. For each packet that is scheduled for transmission to a MSs, a MCS (also referred to as PHY-mode) with the respective PHY data rate is chosen according to the SINR threshold values shown in table 1. The SINR threshold values aim at a target residual bit error rate (BER) of  $10^{-6}$ .

Table B.1: MCS Switching Threshold and PHY Data Rates  
[IEEE P802.16Rev2/D8]

No.	Modulation	Code rate	Min. SINR [dB]	PHY data rate [MBit/s]
1	QPSK	1/2	5.0	14.93
2	QPSK	3/4	8.0	22.4
3	16 QAM	1/2	10.5	29.87
4	16 QAM	3/4	14.0	44.80
5	64 QAM	2/3	18.0	59.73
6	64 QAM	3/4	20.0	67.20

### B.1.3 WiMAX Frame Structure and Overhead

In our simulations the total frame duration is assumed to be 5 ms. We divide this time equally between DL and UL data transmission phases. UL and DL MAPs are always transmitted using an omnidirectional antenna pattern. Beamforming for concurrent SDMA transmissions are only used for the DL and UL bursts. When operating in SDMA mode, the BS can schedule multiple concurrent bursts and has to set beam patterns accordingly to separate the co-scheduled users' signals. Of course, individual map entries (information elements, IEs) for parallel bursts have to be signalled. OFDMA parameters are chosen accordingly to IEEE 802.16m documents [IEEE 802.16m EMD], [IEEE 802.16m SDD] with a nominal channel bandwidth of 20 MHz and a cyclic prefix factor

## B Performance Evaluation of CB for adaptive BF with SDMA (Scheme I) - Assumptions and Results

of 1/8. The OFDMA symbol length is 102,857  $\mu\text{s}$ , making for a total of 47 OFDMA symbols in each 5 ms frame (excluding 165.714  $\mu\text{s}$  dedicated to transition gaps). Each map is transmitted using QPSK 1/2 as the modulation and coding scheme. Using 1536 subcarriers, 1536 bits can be transmitted with one symbol. Thus, an UL MAP holding 25 information elements is 7 full OFDM symbols long (0.97% of the frame). A DL MAP holding 75 information elements needs 19 symbols (2.7% of the frame). 4 OFDM symbols are deducted from the frame capacity to account for the different phases of the preamble. In total, the organizational overhead for the whole frame is around 4.3%.

### B.1.4 Other Simulation Parameters

In order to rule out other influencing factors when evaluating the performance of the coordination scheme, neither Segmentation and Reassembly (SAR) nor Automatic Repeat Request (ARQ) mechanisms are used. Each BS is equipped with a 12-element linear antenna array used to serve one sector. The sector is modeled by a superimposed antenna pattern with the gain factor of one for the 120° (sector) cell width and zeros for the other 240°.

MSs are equipped with standard omnidirectional antennas. The transmit power is 49 dBm for a BS, i.e., 44.23 dBm for a cell, and 23 dBm for a MS. No further power control / adaption is performed. A mid frequency of 2.5 GHz is used. MSs are moving with a speed of 30 km/h inside their sector with a Brownian motion. Handovers do not occur. As a roof-top deployment is envisioned for the MS's antenna, the pathloss model presumes LOS conditions. The "LOS C2" path loss model for the urban environment [IEEE 802.16m SDD] is used in the following. Shadowing or fading effects are not considered. Table II gives an overview of all relevant simulation parameters.

Table B.2: overview of simulation parameters

Parameter	Value
Cluster Order	3
Cell radius	333 m
Number of sectors	3
MS velocity	Brownian motion 30 km/h
Height BS/MS	32 m / 1.5 m
Tx Power BS(per cell) / SS	44.23 (49dBm) / 23 dBm
Mid frequency	2.5 GHz
Pathloss	WINNER „LOS C2”
Shadowing & Fast Fading	No
Antenna array/elements	ULA / 12
Max. number of beams	4
Channel bandwidth	20 MHz
Traffic type	Symmetric CBR
packet size	190 Bytes (fixed)
MAC Frame length	5 ms (47 OFDM symbols)
Number of subchannels	32
Data subcarriers	1536
Nominal OFDMA symbol duration	102.857 $\mu$ s
SAR & ARQ	None
Scheduling strategy:	Proportional Fair
No coordination	Round Robin
Spatial grouper:	Tree-based SINR heuristic [Hoymann, 2007]

## B.2 Simulation Results

In this Section, we present and discuss the results of the performed simulations. First, we discuss the link adaptation by regarding the probability of used MCS and the MCS estimation error for a conventional and a coordinated system. The impact on cell throughput and packet delay is studied as well.

In UL, the coordinated system outperforms the uncoordinated system in terms of link adaptation. Figure B.2 depicts the probability density function of the MCS used for transmission in a conventional (black) and a coordinated system (blue) at an offered traffic of 10Mbps. The highest MCS, i.e., 64QAM3/4, is used for 75% of the transmissions in a conventional system. Coordination increases the use of 64QAM3/4 by 15% to a value of 86%. With coordination higher MCS are used than in a conventional system because inter-cell inference is mitigated.

## B Performance Evaluation of CB for adaptive BF with SDMA (Scheme I) - Assumptions and Results

Figure B.3 shows the density of the delta MCSs metric [Section B.1.1] at 10 Mbps offered traffic. The conventional system (black) uses the correct MCS scheme in less than 70%. The other transmissions use incorrect MCSs based on SINR estimation which are either too optimistic or too conservative. The first causes packet losses whereas the second wastes resources by choosing too robust PHY modes. With coordination (blue) correct MCSs are employed for 90% of the transmissions and packet loss does approximately not occur. Coordination improves precision of the estimation of the suitable MCS. Inter-cell interference is more predictable with coordination because inter-cell interferers are mostly known.

In the Figure B.4 the mean UL MAC throughput is presented. Coordination increases saturation throughput from less than 10 Mbps for the conventional system to 60 Mbps. Packet loss occurs for almost 20% of the conventional system at an offered traffic of 10 Mbps. This indicates the lack of precision in the SINR estimation. In this interference limited scenario coordination can be regarded as enabling technology given the poor performance of the conventional system.

Figure B.5 depicts the mean DL MAC throughput. Saturation throughput increases from less than 10 Mbps for the conventional system (black) to 75 Mbps for the coordinated system (blue). The imprecise SINR and MCS estimation in the conventional system causes packet loss even in low load (< 10 Mbps) and hence the offered traffic cannot be carried. Coordination in DL also allows for higher MCS by decreasing inter-cell interference and decreases estimation errors in link adaptation (not shown); similar to uplink case shown in Figure B.2 and Figure B.3.

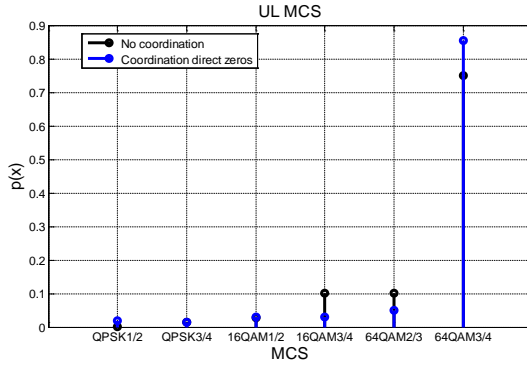


Figure B.2: Probability Density Function (PDF) of used MCS at 10Mbps offered traffic

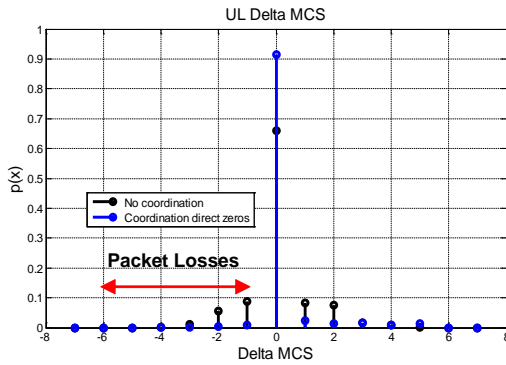


Figure B.3: Delta MCS between MCS used for Tx and MCS based on measured SINR during Rx, at 10Mbps offered traffic

## B Performance Evaluation of CB for adaptive BF with SDMA (Scheme I) - Assumptions and Results

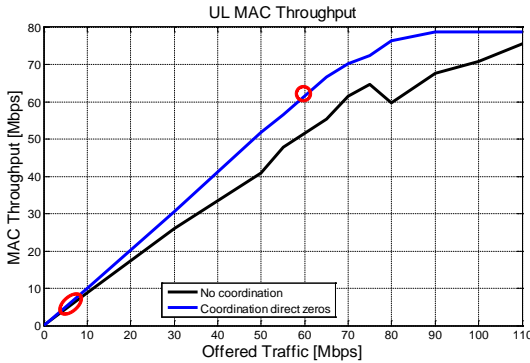


Figure B.4: mean cell throughput in UL

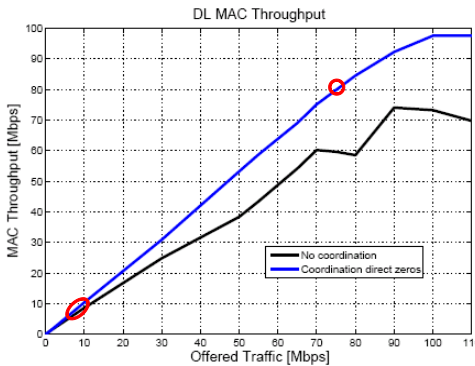


Figure B.5: mean cell throughput in DL

### B.3 Conclusion

Shown results proved that coordination mitigates inter-cell interference and increases its predictability. Hence the developed concept improves system capacity and let a coordinated- outperform an uncoordinated system. The cost of coordination across BSs is the increase of system complexity (scheduler, grouper, beamformer) and of coordination overhead (exchanged messages, increased MAP size due to increased number of bursts).

Future work will quantitatively investigate the costs of coordination. Also, the impact on variable traffic models on coordination is in the interest of further studies.



# C Performance Evaluation of Region Coordination for Adaptive BF with SDMA (Scheme II and III) - Assumptions and Results

## C.1 Simulation Results

In this Section, we present and discuss the results of the performed simulations for a conventional reference system and three systems enhanced by different coordination algorithms I, II and III; I) a coordinated system according to Section 5.3.1; II) *one burst per group* coordination (see Section 5.3.2.1.1); and III) *spatial region coordination* (see Section 5.3.2.1.2). First, the link adaptation is discussed by regarding the probability of used MCS and the MCS estimation error. The relative impact of different coordination algorithms on cell throughput is studied as well. Simulations are conducted first with constant-bit-rate (CBR) - and second with variable-bit-rate (VBR) traffic [Section B.1.1].

### C.1.1 Constant Bit Rate Downlink Traffic with 30 MSs

Figure C.1 depicts the probability density function of the MCS used for transmission in a conventional (black), a system with coordination I (blue points), with coordination II (blue cross) and coordination III (green) at an offered DL traffic of 10 Mbps. The coordinated systems select higher MCS with higher probability than the uncoordinated system because inter-cell inference can be mitigated. Coordination I performs best and for instance increases the use of highest MCS (i.e. 64QAM3/4) by 21% to a value of 84% compared to a conventional system.

Figure C.2 shows the density of the delta MCS metric [Section B.1.1] at 10 Mbps offered traffic. The conventional system (black) employs the optimal MCS scheme in 50%. The Coordinated systems improve the precision of the SINR estimation and select the optimal MCS in 68%-87% of the transmissions with highest gains for scheme I. The other transmissions use incorrect MCSs based on inexact SINR estimation which are either too optimistic or too conservative. The first causes

## C Performance Evaluation of Region Coordination for Adaptive BF with SDMA (Scheme II and III) - Assumptions and Results

packet losses whereas the second wastes resources by choosing too robust PHY modes. Coordination II chooses MCSs too pessimistically in 30% of its transmissions. This occurs because interferers, which are only interfering parts of the burst, are assumed for a whole burst. With coordination, packet losses do only occur with scheme III (green). These too optimistic estimations arise because interference is suppressed towards the direction of the weight point of a region which is several degrees beside the actual position of the interfering station. Inter-cell interference is more predictable with all coordination schemes because inter-cell interferers are known (or better known with scheme II and III).

In Figure C.3 the mean DL MAC throughput is presented. The reference system (black) saturates at less than 10 Mbps. Packet losses occur for almost 30% in the uncoordinated system at an offered traffic of 10 Mbps [Figure C.2]. This indicates the imprecise SINR estimation (or too low capacity for specific MSs) of the uncoordinated SDMA enhanced system. Coordination increases the saturation throughput to more than 50 Mbps with scheme I and II. A higher maximum throughput is reached with coordination II (73Mbps) than with coordination I (69Mbps). The gain by 4Mbps accounts for the reduced number of bursts and thereby reduced padding. The MAP is simulated with constant resource consumption. An increased MAP overhead of approximately 1MB/s due to the increased number of bursts is not considered in the results of Figure C.3. Coordination III (green) outperforms the uncoordinated system in terms of throughput but is not able to serve all MSs below 10 Mbps and thereby cannot achieve the performance of the other coordination schemes due to the less precise link adaptation (as shown in Figure C.1 and Figure C.2).

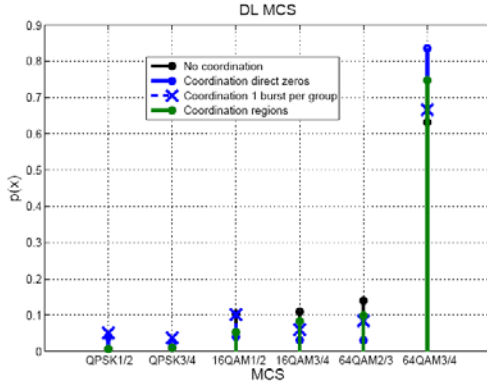


Figure C.1: Probability Density Function (PDF) of used MCS at 10Mbps offered traffic - CBR

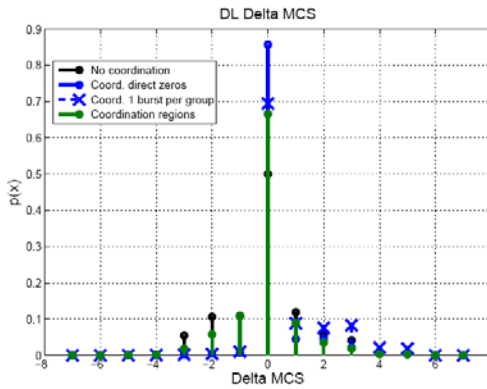


Figure C.2: Delta MCS between MCS used for Tx and MCS based on measured SINR during Rx, at 10Mbps offered traffic – CBR

## C Performance Evaluation of Region Coordination for Adaptive BF with SDMA (Scheme II and III) - Assumptions and Results

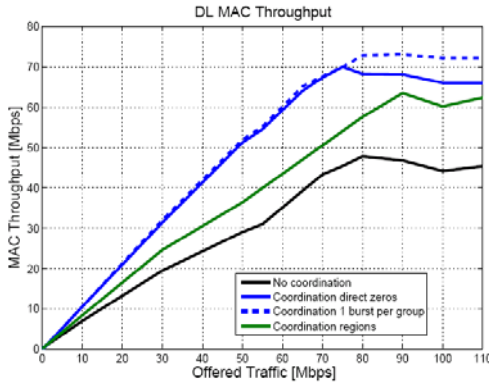


Figure C.3: mean cell throughput in DL – CBR

### C.1.2 Variable Bit Rate Uplink Traffic

In following results, the offered traffic is stimulated by the number of MSs each having a MPEG4 uplink stream with a mean rate of 0.55 Mbps.

Figure C.4 depicts the probability density function of the MCS used for uplink transmission at an offered VBR traffic of 10 Mbps [in a conventional system (black), a system with scheme I (blue points), with scheme II (blue cross) and with scheme III (green)]. As with CBR downlink traffic Figure C.1, the coordinated systems tend to select higher MCS than the uncoordinated system because inter-cell inference can be still mitigated. Still, scheme I performs best and for instance increases the use of highest MCS (i.e. 64QAM3/4) by 12% to a value of 84% compared to a conventional system.

Figure C.5 shows the distribution of the delta MCS metric [Section B.1.1] at 10 Mbps offered traffic. The conventional system (black) employs the optimal MCS scheme (Delta MCS = 0) in 57% of the transmission (50% in CBR downlink). The SDMA system in the UL case has a more predictable interference level than in downlink. All coordination schemes improve the precision of the estimation of the suitable MCS. A system with Coordination III employs the correct MCS 80% of the transmissions and only 5% of the packets are lost (compared to packet losses of 25% in an uncoordinated system, 13% with scheme I, 6% with scheme II). Scheme III (green) shows the most precise link adaptation by

coordinating the interference of regions and set of MSs instead of single users.

In Figure C.6 the mean UL MAC throughput is presented. The uncoordinated reference system (black) can never properly carry the offered traffic. At less than 10 Mbps packet losses occur for 25% [Figure C.5]. The coordinated systems with scheme I (blue solid) or II (blue dashed) saturate at an offered traffic of more than 25 Mbps. They are limited due to their lack of predicting the interference with VBR traffic and efficiently coordinating a high number of MSs with the given RR scheduling. Coordination III (green) significantly increases the throughput to more than 40 Mbps compared to all other systems due to its ability to predict the interference even with VBR traffic.

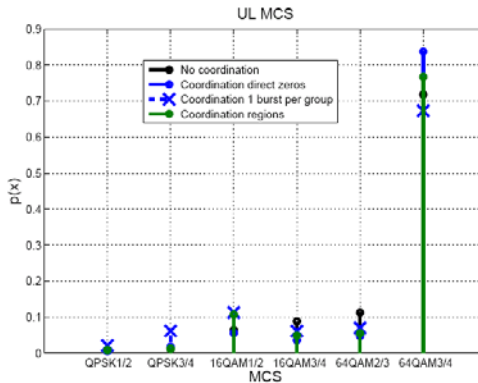


Figure C.4: Probability Density Function (PDF) of used MCS at 10Mbps offered traffic – VBR

## C Performance Evaluation of Region Coordination for Adaptive BF with SDMA (Scheme II and III) - Assumptions and Results

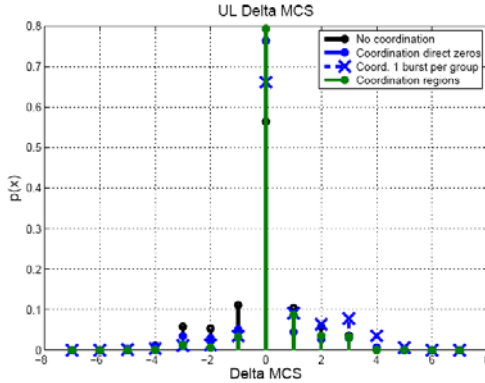


Figure C.5: Delta MCS between MCS used for Tx and MCS based on measured SINR during Rx, at 10Mbps offered traffic - VBR

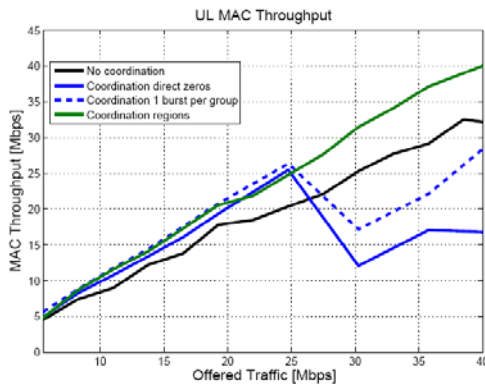


Figure C.6: mean cell throughput in UL - VBR

## C.2 Conclusion

Two coordination schemes (scheme II, *one burst per group*, and scheme III, *region coordination*) for coordination of SDMA enhanced BSs and inter-cell interference mitigation are developed and evaluated in this Chapter. The performance evaluation by means of system level simulations is conducted in a cellular scenario with CBR downlink and VBR uplink traffic. The developed coordination *one burst per group* further improves the scheme from previous Chapter and overcomes its limitation by

decreasing the number of bursts. But both schemes (I and II) are limited due to their lack of predicting the interference with VBR traffic and efficiently coordinating a high number of MSs with the given RR scheduling. Shown results proved that *region coordination* successfully predicts the interference with VBR uplink traffic with significant throughput gains towards all other systems by the cost of moderate gains in the downlink. All coordination schemes mitigate inter-cell interference and increase its predictability. Hence the developed concepts improve system capacity and let a coordinated- outperform an uncoordinated system. The cost of coordination across BSs is the increase of system complexity and of coordination overhead.

In future work, thresholds will be studied for an optimal coordination combining scheme 1-3 in a problem space spanned by the dimensions CBR/VBR, UL/DL traffic as well as low/high number of MSs.



# List of Figures

---

Figure 2.1: approximated timeline of mobile communication standards [Sesia, 2010].....	19
Figure 2.2: 3GPP working group structure .....	20
Figure 2.3: functional split between E-UTRAN and EPC; and the EPS network elements relevant for radio evaluation [3GPP 36.300].....	22
Figure 2.4: user plane protocol stack [3GPP TS 36.300].....	25
Figure 2.5: control plane protocol stack [3GPP TS 36.300] .....	26
Figure 2.6: MAC structure overview, UE side [3GPP TS 36.321] .....	31
Figure 2.7: channel mapping (a) in downlink (b) in uplink [3GPP TS 36.321].....	32
Figure 2.8: Transport Channel processing for DL-SCH, PCH and MCH. ....	34
Figure 2.9: Physical Channel processing .....	34
Figure 2.10: frame structure and downlink resource grid (normal cyclic prefix) [3GPP TS 36.211] .....	37
Figure 3.1: fundamental benefits of multiple antennas: (a) diversity gain; (b) spatial multiplexing gain; (c) array gain [Sesia, 2011].....	48
Figure 3.2: definition of coordinate system.....	52
Figure 3.3: linear array with plane wave incident [Mailloux, 2005] .....	52
Figure 3.4: structure of a narrow-band beamformer using a reference signal [Godara, 1997].....	57

## List of Figures

Figure 3.5: sector pattern and example beam patterns defined by the Precoding Matrix Index (PMI) from codebook of (a) [3GPP TS36.211] $\lambda/2$ and (b) [IEEE802.16m] $\lambda/4$ ; both with antenna array of four elements with $30^\circ$ boresight.....	58
Figure 3.6: beamforming system supporting N parallel beams [Liberti and Rappaport, 1999].....	59
Figure 4.1: hexagonal cell layout, Figure 1 in [ITU-R M.2135].....	64
Figure 4.2: antenna gain pattern.....	66
Figure 4.3: beam pattern of codebook in [3GPP TS 36.211] for four antenna elements, calculated by Eq. (3.5). Sector antenna characteristic (see Figure 4.2 (a)) is already included in the diagram. ....	68
Figure 4.4: pathloss and LOS probability in UMa.....	69
Figure 4.5: link permutation instances of two BSs as binominal words, where $i^{\text{th}}$ bit defines $i^{\text{th}}$ link characteristic, with 1 = LOS, 0 = NLOS .....	74
Figure 4.6: map of most likely applied beams; indentified by Precoding Matrix Index (PMI), UMa scenario with LOS; centre site in origin (0m,0m).....	76
Figure 4.7: example of mean SINR topography [dB]; UMa scenario with sectorised antennas .....	77
Figure 4.8: Feeder Pathgain CDF.....	79
Figure 4.9: Wideband SINR CDF .....	79
Figure 4.10: Mutual Information per bit depending on the SINR and the modulation [Schoenen, 2007].....	80
Figure 4.11: Block Error Rate for 14 MCSs based on [Olmos, 2010] .....	80
Figure 4.12: net spectral efficiency of LTE modulation and coding schemes taking BLER and ARQ account and Shannon bound.....	82
Figure 4.13: example of mean normalized data rate topography [bit/s/Hz]; UMa scenario with sectorised antennas .....	84
Figure 4.14: binomial distribution $Bk n, p$ ; Probability of $k$ MSs per cell, ; $n = 570$ , and $p = 1/57$ .....	85

Figure 4.15: mean user throughput CDF normalized by the bandwidth (without small-scale fading).....	88
Figure 5.1: capacity per area unit and number of MS versus distance to BS in cellular networks.....	89
Figure 5.2: static frequency reuse schemes.....	91
Figure 5.3: antenna pattern with zeros towards intra- and inter-cell interferes .....	99
Figure 5.4: MAC frames of disturbed & jamming BSs.....	99
Figure 5.5: decoupling by classification of BS.....	99
Figure 5.6: coordination message sequence chart .....	100
Figure 5.7: creation of spatial regions and sub-regions (example of two interfering BSs and two concurrent antenna beams) .....	104
Figure 5.8: angular constraints.....	105
Figure 5.9: coordinated allocation of radio resource to cells and beams; (a) three cell types(b) coordination matrix for codebook subset with N entries .....	108
Figure 5.10: flow chart for algorithm defining a coordination matrix; $n_{cell}$ = number of coordinated cells, $n_{PMI}$ = number of beams in codebook subset.....	110
Figure 5.11: example RR radio resource schedule with beam coordination under SFR operation .....	112
Figure 6.1: SINR CDF of four system types: sector antennas (Sector), Beamforming (BF), Coordinated BF of cells of one BS (CBF 1), and full Coordinated BF (CBF); (RR, FR1, 7 beams) .....	119
Figure 6.2: CDF of normalized data rate (before resource allocation) in [bit/s/Hz]; of the four system types; (RR, FR1, 7 beams) .....	120
Figure 6.3: topography of mean normalized data rate [bit/s/Hz]; of the four system types; (RR, FR1, 7 beams).....	122
Figure 6.4: topography of absolute coordination gain in terms of mean normalized data rate [bit/s/Hz].....	123

## List of Figures

Figure 6.5: CE-USE versus CSE with both RR and RF scheduling; (FR1, 7 beams) .....	125
Figure 6.6: CDF of Mean Normalized MS Throughput for RR and RF scheduling; (BF, FR1, 7 beams) .....	126
Figure 6.7: (a) CSE and (b) CE-USE versus $\alpha$ under SFR with RR vs. RF scheduling; (BF, SFR, 3 beams) .....	128
Figure 6.8: (a) CSE and (b) CE-USE versus $\alpha$ under SFR with RR-Balanced Scheduling; (BF, SFR, 3 beams) .....	129
Figure 6.9: (a) CSE and (b) CE-USE versus $\alpha$ under SFR with RF Scheduling; (BF, SFR, 3 beams) .....	130
Figure 6.10: CE-USE versus CSE in various frequency reuse schemes; (RR, 7 beams) .....	131
Figure 6.11: SINR CDF of varying frequency reuse schemes, (BF, RR, 7 beams) .....	132
Figure 6.12: CE-USE versus CSE for various reuse schemes; (RF, 7 beams), .....	133
Figure 6.13: studied subsets of codebook in [3GPP TS 36.211] and Section 4.2.3, (a) 3 beams (b) 5 beams (c) 7 beams; all sets include the sector pattern for MS association. ....	135
Figure 6.14: fairness versus capacity under various number of beams for both RR and RF scheduling; FR1 .....	136
Figure 6.15: CSE and CE-USE versus number of beams; coordination gain in [%] is compared to BF case; RR scheduling; FR1 .....	137
Figure 6.16: CSE and CE-USE versus number of beams; coordination gain in [%] is compared to BF case; RF scheduling; FR1 .....	137
Figure A.1: CDF of Mean Normalized MS Throughput for (a) RR and (b) RF scheduling; (FR1, 7 beams) .....	141
Figure A.2: spectral efficiency (a) CSE (b) CE-USE of the SFR system versus alpha; RR Strict Scheduling; (3 beams) .....	141

Figure A.3: spectral efficiency (a) CSE (b) CE-USE of the SFR system versus alpha; RR vs. RF scheduling; (Sector).....	142
Figure A.4: CDF of Normalized Mean MS Throughput in SFR with varying scheduling strategy at $\alpha = 1.8$ ; (a) Beamforming system with 3 beams and (b) Sector system .....	142
Figure A.5: CE-USE versus CSE with different reuse schemes; (RR, 3 beams) .....	143
Figure A.6: CE-USE versus CSE with different reuse schemes; (RF, 3 beams) .....	143
Figure A.7: SINR CDF of varying frequency reuse schemes; (BF, RR, 3 beams) .....	144
Figure A.8: CDF of Mean Normalized MS Throughput for CBF with various number of beams under (a) RR and (b) RF scheduling; (FR1).144	144
Figure B.1: positions of sectors in central (black) and co-channel (red) cells of evaluated clustered cellular deployment .....	148
Figure B.2: Probability Density Function (PDF) of used MCS at 10Mbps offered traffic.....	153
Figure B.3: Delta MCS between MCS used for Tx and MCS based on measured SINR during Rx, at 10Mbps offered traffic .....	153
Figure B.4: mean cell throughput in UL .....	154
Figure B.5: mean cell throughput in DL .....	154
Figure C.1: Probability Density Function (PDF) of used MCS at 10Mbps offered traffic - CBR.....	159
Figure C.2: Delta MCS between MCS used for Tx and MCS based on measured SINR during Rx, at 10Mbps offered traffic – CBR .....	159
Figure C.3: mean cell throughput in DL – CBR.....	160
Figure C.4: Probability Density Function (PDF) of used MCS at 10Mbps offered traffic – VBR.....	161
Figure C.5: Delta MCS between MCS used for Tx and MCS based on measured SINR during Rx, at 10Mbps offered traffic - VBR.....	162

## List of Figures

Figure C.6: mean cell throughput in UL - VBR ..... 162

# List of Tables

---

Table 2.1: TDD uplink-downlink configurations. ....	38
Table 4.1: deployment scenarios and related channel models [ITU-R M.2135, Table A1-1] .....	63
Table 4.2: UMa scenario and configuration parameters.....	65
Table 4.3: analytical system model in pseudo code .....	72
Table 4.4: basic assumptions made by iTeam in link level simulations within WINNER+ [Olmos, 2010] .....	81
Table 4.5: Modulation and Coding Schemes for LTE based on [Olmos, 2010]] .....	82
Table 6.1: main evaluation scenario parameters.....	118
Table 6.2: Mean and Standard Deviation (STD) of SINR shown in Figure 6.1 .....	119
Table 6.3: coordination gain vs. beamforming in Figure 6.5.....	125
Table 6.4: coordination gain vs. beamforming in Figure 6.10.....	131
Table 6.5: coordination gain vs. beamforming in Figure 6.12.....	133
Table A.1: coordination gain vs. beamforming of Figure A.5.....	143
Table A.2: coordination gain vs. beamforming of Figure A.6.....	143
Table B.1: MCS Switching Threshold and PHY Data Rates [IEEE P802.16Rev2/D8] .....	149
Table B.2: overview of simulation parameters.....	151



# List of Abbreviations

---

<b>3GPP</b>	The Third Generation Partnership		Efficiency
<b>AM</b>	Acknowledged Mode	<b>CoMP</b>	Coordinated Multi-Point
<b>AS</b>	Access Stratum	<b>CRC</b>	Cyclic Redundancy Check
<b>BCCH</b>	Broadcast Control Channel	<b>CS</b>	Coordinated Scheduling
<b>BCH</b>	Broadcast CHannel	<b>CSE</b>	Cell Spectral Efficiency
<b>BER</b>	Bit Error Rate	<b>CT</b>	Core Network & Terminals
<b>BF</b>	Beamforming (System)	<b>CyBeamCo</b>	Cyclic Beam Coordination
<b>BLER</b>	Block Error Rate	<b>DCCH</b>	Dedicated Control Channel
<b>CAPEX</b>	Capital Expenditure	<b>DCS</b>	Dynamic Cell Selection
<b>CB</b>	Coordinated Beamforming	<b>DL-SCH</b>	Downlink Shared CHannel
<b>CBF</b>	Coordinated BF (System)	<b>DPS</b>	Dynamic Point Selection
<b>CBF 1</b>	CBF only of cells at one site	<b>DRB</b>	Data Radio Bearer
<b>CCCH</b>	Common Control Channel	<b>DTCH</b>	Dedicated Traffic Channel
<b>CDF</b>	Cumulative Distribution Function	<b>eICIC</b>	enhanced ICIC
<b>CDMA</b>	Code Division Multiple Access	<b>eNB</b>	Evolved Node B
<b>CE-USE</b>	Cell Edge -User Spectral	<b>EPC</b>	Evolved Packet Core
		<b>EPS</b>	Evolved Packet System
		<b>E-SMLC</b>	Evolved Serving Mobile

## List of Abbreviations

	Location Centre	<b>MCH</b>	Multicast CHannel
<b>E-UTRAN</b>	Evolved-UTRAN	<b>MCS</b>	Modulation and Coding Scheme
<b>FR1</b>	Frequency Reuse One	<b>MCS</b>	Modulation and Coding Scheme
<b>FR3</b>	Frequency Reuse Three	<b>MME</b>	Mobility Management Entity
<b>GERAN</b>	GSM EDGE Radio Access Networks	<b>MMSE</b>	Minimum Mean Square Error
<b>GMLC</b>	Gateway Mobile Location Centre	<b>MSE</b>	Mean Square Error
<b>GPRS</b>	General Packet Radio Service	<b>MTCH</b>	Multicast Traffic Channel
<b>HSS</b>	Home Subscriber Server	<b>MVDR</b>	Minimum Variance Distortionless Response
<b>ICI</b>	Inter-Cell Interference	<b>NAS</b>	Non-Access Stratum
<b>ICIC</b>	ICI Coordination	<b>NLoS</b>	Non-Line-of-Sight
<b>IMS</b>	The IP Multimedia Subsystem	<b>OFDMA</b>	Orthogonal Frequency Division Multiple Access
<b>IMT</b>	International Mobile Telecommunications	<b>OPEX</b>	Operational Expenditure
<b>IP</b>	Internet Protocol	<b>PBCH</b>	Physical Broadcast Channel
<b>ITU</b>	The International Telecommunication Union	<b>PCCH</b>	Paging Control Channel
<b>ITU-R</b>	ITU Radio Communication Sector	<b>PCFICH</b>	Physical Control Format Indicator Channel
<b>JP</b>	Joint Processing	<b>PCH</b>	Paging CHannel
<b>JT</b>	Joint Transmission	<b>PCRF</b>	Policy Control and Charging Rules Function
<b>LoS</b>	Line-of-Sight	<b>PCRF</b>	Policy Control and
<b>LTE</b>	Long Term Evolution		
<b>MAC</b>	Medium Access Control		
<b>MCCH</b>	Multicast Control Channel		

	Charging Rules Function	<b>QPSK</b>	Quadrature Phase Shift Keying
<b>PDCCH</b>	Physical Downlink Control Channel	<b>RACH</b>	Random Access Channel
<b>PDCP</b>	The Packet Data Convergence Protocol	<b>RAN</b>	Radio Access Networks
<b>PDN</b>	Packet Data Network	<b>RE</b>	Resource Element
<b>PDSCH</b>	Physical Downlink Shared Channel	<b>RLC</b>	Radio Link Control
<b>PER</b>	Packet Error Rate	<b>RMa</b>	Rural Macro-cell
<b>P-GW</b>	Packet Data Network Gateway	<b>RRC</b>	Radio Resource Control
<b>PHICH</b>	Physical Hybrid ARQ Indicator Channel	<b>RSRP</b>	Reference Signal Received Power
<b>PHY</b>	Physical Layer	<b>SA</b>	Service & Systems Aspects
<b>PLMN</b>	Public Land Mobile Network	<b>SAE</b>	System Architecture Evolution
<b>PMCH</b>	Physical Multicast Channel	<b>SDMA</b>	Spatial Division Multiple Access
<b>PMI</b>	Precoding Matrix Index	<b>SDU</b>	Service Data Unit
<b>PRACH</b>	Physical Random Access Channel	<b>SINR</b>	Signal-to-Interference Plus Noise Ratio
<b>PRB</b>	Physical Resource Block	<b>SFR</b>	Soft Frequency Reuse
<b>PUCCH</b>	Physical Uplink Control Channel	<b>S-GW</b>	Service-Gateway
<b>PUSCH</b>	Physical Uplink Shared Channel	<b>SRB</b>	Signalling Radio Bearer
<b>QAM</b>	Quadrature Amplitude Modulation	<b>STD</b>	Standard Deviation
<b>QCI</b>	QoS Class Identifier	<b>TB</b>	Transport Blocks
<b>QoS</b>	Quality of Service	<b>TM</b>	Transparent Mode
		<b>TSGs</b>	Technical Specification Groups
		<b>UE</b>	User Equipment

## List of Abbreviations

<b>UL-SCH</b>	Uplink Shared CHannel	<b>UTRAN</b>	Universal Terrestrial Radio Access
<b>UM</b>	Unacknowledged Mode	<b>VBR</b>	Variable Bit Rate
<b>UMa</b>	Urban Macro-cell	<b>VoIP</b>	Voice over IP
<b>UMi</b>	Urban Micro-cell	<b>WGs</b>	Working Groups
<b>UMTS</b>	Universal Mobile Telecommunications System		

# Bibliography

---

- 3G Americas: MIMO and Smart5 Antennas for 3G and 4G Wireless Systems – Practical Aspects and Deployment Considerations. URL: <http://lteworld.org/whitepaper>, May 2010.
- 3GPP TR 36.814 V 9.0.0: Further advancements for E-UTRA physical layer aspects. Mar. 2010.
- 3GPP TR 36.819 V 11.1.0: Coordinated multi-point operation for LTE physical layer aspects. Dec. 2011.
- 3GPP TS 36.211 V 9.1.0: Physical Channels and Modulation. Mar. 2010.
- 3GPP TS 36.300 V 9.9.0: Evolved Universal Terrestrial Radio Access (E-UTRA) and Evolved Universal Terrestrial Radio Access Network (E-UTRAN); Overall description. Dec. 2011.
- 3GPP TS 36.321 V 9.6.0: Medium Access Control (MAC) Protocol Specification. Mar. 2012.
- 3GPP TS 36.322 V 9.3.0: Radio Link Control (RLC) Protocol Specification. Sep. 2010.
- 3GPP TS 36.323 V 9.0.0: Packet Data Convergence Protocol (PDCP) Specification. Dec. 2009.
- 3GPP TS 36.331 V 9.11.0: Radio Resource Control (RRC); Protocol specification. June 2012.
- 3GPP TS 36.420 V 10.2.0: X2 general aspects and principles. Sep. 2011.
- 3GPP TS 36.423 V 9.6.0: X2 application protocol (X2AP). Mar. 2011
- Andre, T.: Cell Spectral Efficiency of a 3GPP LTE-Advanced System. Diploma thesis, RWTH Aachen University, Chair of Communication Networks, Dec. 2012.

## Bibliography

- Bertsekas, D. P. and Gallager, R. G. (1992). *Data Networks*, Prentice Hall, 2nd edition, 1992
- Bong Ho Kim.: Text Modification for Draft 802.16m Evaluation Methodology: 11.4 Near Real Time Video Streaming. Proceedings of 14th WWRF Meeting, San Diego, CA, USA, July 2005.
- Brueninghaus, K. and Astely, D. and Saelzer, T. and Visuri, S. and and Alexiou, A. and Karger, S. and Seraji, G.: Link performance models for system level simulations of broadband radio access systems. Proceedings of IEEE 16th Personal, Indoor and Mobile Radio Communications Conference (PIMRC 2005), Berlin, Germany, Sep. 2005.
- Bueltmann, D. and Andre, T. and Schoenen, R.: Analysis of 3GPP LTE-Advanced Cell Spectral Efficiency. Proceedings of IEEE 21st International Symposium on Personal, Indoor and Mobile Radio Communications (PIMRC), Istanbul, Turkey, Sep. 2010.
- Bueltmann, D. and Muhleisen, M. and Klagges, K. and Schinnenburg, M.: openWNS - open Wireless Network Simulator. European Wireless Conference, EW 2009, Aalborg, Denmark, May 2009.
- Doettling, M. and Mohr, W. and Osseiran, A.: *Radio Technologies and Concepts for IMT-Advanced*. ISBN: 978-0470747636, John Wiley & Sons Dec. 2009.
- Einhaus, M.: Dynamic resource allocation in OFDMA systems. Ph. D. Dissertation, RWTH Aachen University, Faculty 6, Chair of Communication Networks (ComNets), ISBN:3-86130-941-3, ABMT 61, Wissenschaftsverlag Mainz, Feb. 2009.
- Ellenbeck, J. (2012a): IMTAphy source code hosted on launchpad.net. URL: <http://launchpad.net/imtaphy>, Jan. 2012.
- Ellenbeck, J. (2012b): IMTAphy channel model and LTE simulator documentation website. URL: <http://www.lkn.ei.tum.de/personen/jan/imtaphy/index.html>, Jan.2012.

- Ellenbeck, J. (2012c): System-Level Simulations with the IMT-Advanced Channel Model, LTE-Advanced and Next Generation Networks: Channel Modelling and Propagation. Book Chapter, ISBN: 978-1119976707, John Wiley & Sons, Nov. 2012.
- Ellenbeck, J. and Hammoud, M. and Lazarov, B. and Hartmann, C.: Autonomous beam coordination for the downlink of an IMT-Advanced cellular system. European Wireless Conference, EW 2010, Apr. 2010.
- Ericsson, NTT DoCoMo; 3GPP TSG RAN WG1#44 R1-060586: Downlink and uplink inter-cell interference co-ordination/avoidance – impact on the specifications. Technical document, Denver, CO, USA, Feb. 2006.
- ETSI TR 103 054 V1.1.1. Electromagnetic compatibility and Radio spectrum Matters (ERM); Broadband Direct-Air-to-Ground Communications. Technical Report, July 2010.
- Fang, Y. and Thompson, J.: Out of group interference aware precoding for CoMP: An ergodic search based approach. 14th International Symposium on Wireless Personal Multimedia Communications (WPMC), Oct. 2011.
- Finland: Guidelines for using IMT-Advanced channel models. Tech. Rep. URL: <http://www.itu.int/oth/R0A06000021/en>.
- Godara, L.: Application of antenna arrays to mobile communications. II. Beamforming and direction-of-arrival considerations. Proceedings of the IEEE, vol. 85, no. 8, pp. 1195–1245, Aug. 1997.
- Hassanpur, N. and Smee, J. E. And Hou, J. And Soriaga, J. B.: Distribute Beamforming based on Signal-to-Caused-Interference Ratio. Proceedings of 10th IEEE ISSSTA, Bologna, Italy, Aug. 2008.
- Hosein, P. and Van Rensburg, C.: On the Performance of Downlink Beamforming with Synchronized Beam Cycles. Proceedings of IEEE 69th Vehicular Technology Conference, VTC Spring 2009, Barcelona, Spain, Apr. 2009.
- Hosein, P.: Cooperative scheduling of downlink beam transmissions in a cellular network. Proceedings of IEEE Globecom Workshops 2008, San Diego, USA, Dec. 2008.

## Bibliography

- Hoymann, C. and Ellenbeck, J. and Pabst, R. and Schinnenburg, M: Evaluation of Grouping Strategies for an Hierarchical SDMA/TDMA Scheduling Process. Proceedings of IEEE International Conference on Communications, ICC2007, Glasgow, United Kingdom, June 2007.
- Hoymann, C.: IEEE 802.16 Metropolitan Area Network with SDMA Enhancement. Ph. D. Dissertation, RWTH Aachen University, Faculty 6, Chair of Communication Networks (ComNets), ISBN: 3-86130-936-X, ABMT 57, Wissenschaftsverlag Mainz, July 2008.
- Hoymann, C.: MAC Layer Concepts to Support Space Division Multiple Access in OFDM based IEEE 802.16s. Wireless Personal Communications, URL: <http://www.comnets.rwth-aachen.de>, May 2006.
- Ibing, A. and Manolakis, K.: MMSE Channel Estimation and Time Synchronization Tracking for Cooperative MIMO-OFDM with Propagation Delay Differences. The IEEE 6th International Symposium on Wireless Communication Systems 2009, ISWCS'08, Reykjavik, Iceland, Oct. 2009
- IEEE 802.16m EMD: Evaluation Methodology Document : IEEE 802.16m-08/004r5. Jan. 2009.
- IEEE 802.16m SDD: System Description Document [Draft]: IEEE 802.16m-08/003r6. Dec. 2008.
- IEEE 802.16Rev2/D8: IEEE DRAFT standard for local and metropolitan area networks part 16: Air interface for fixed broadband wireless access systems. Dec. 2008.
- IEEE 802.16Rev2/D9: IEEE standard for local and metropolitan area networks part 16: Air interface for fixed broadband wireless access systems. May 2009.
- ITU-R M.2134: Requirements related to technical performance for IMT-Advanced radio interface(s). Report, Nov. 2008.
- ITU-R M.2135: Guidelines for evaluation of radio interface technologies for IMT-Advanced. Nov. 2008.

- ITU-R M.2135-1: Guidelines for evaluation of radio interface technologies for IMT-Advanced. Report, Dec. 2009.
- Kim, B. H.: Text Modification for Draft 802.16m Evaluation Methodology: 11.4 Near Real Time Video Streaming. Proceedings of the 14th WWRF Meeting, San Diego, CA, USA, July 2005.
- Lee, D. and Seo, H. and Clerckx, B. and Hardouin, E. and Mazzaresse, D. and Nagata, S. and Sayana, K.: Coordinated multipoint transmission and reception in LTE-advanced: deployment scenarios and operational challenges. IEEE Communications Magazine, p.148-155, Feb. 2012.
- Lee, Y.-S. and Chung S.-Y., "Analysis and Design of Dirty Paper Coding by Transformation of Noise," IEEE 65th Vehicular Technology Conference, VTC2007-Spring, Dublin, Ireland, Apr. 2007.
- Liberti, J. and Rappaport, T.: Smart Antennas for Wireless Communications: IS-95 and Third Generation CDMA Applications. ISBN: 978-0137192878, Prentice Hall, Apr. 1999.
- Mailloux, R. J.: Phased Array Antenna Handbook, Second Edition. ISBN: 1-58053-689-1, Artech House Antennas and Propagation Library, Mar. 2005.
- Marsch, P. and Grieger, M. and Fettweis, G.: Field Trial Results on Different Uplink Coordinated Multi-Point (CoMP) Concepts in Cellular Systems. Proceedings of the IEEE Global Communications Conference (GLOBECOM'10), Miami, FL, USA, Dec. 2010.
- Muehleisen, M. and Wolz, B. and Siddique, M.M. and Gorg, C.: Capacity Analysis and Improvement for Coexisting IEEE 802.16 Systems in Unlicensed Spectrum. Proceedings of IEEE 20th International Symposium on Personal Indoor and Mobile Radio Communications, PIMRC 2009, Tokyo, Japan, Sep. 2009
- Myung, H. G. and Lim, J. and Goodman, D. J.: Single carrier FDMA for uplink wireless transmission. IEEE Vehicular Technology Magazine, vol.1, no.3, pp.30-38, Sep. 2006.
- Necker, M. C. "Interference coordination in cellular OFDMA networks", IEEE Network, 22(6), Nov. 2008.

## Bibliography

- Olmos, J. and Ruiz, S. and Garcia-Lozano, M. and Martin-Sacristan, D.: Link Abstraction Models Based on Mutual Information for LTE Downlink. COST 2100, Tech. Rep. TD(10)11052, June 2010.
- Pabst, R. and Ellenbeck, J. and Schinnenburg, M. and Hoymann, C.: System Level Performance of Cellular WiMAX IEEE 802.16 with SDMA-enhanced Medium Access. IEEE Wireless Communications and Networking Conference, WCNC2007, Hong Kong, China, Mar. 2007.
- Schoenen, R. and Walke, B.: On PHY and MAC Performance of 3G-LTE in a Multi-Hop Cellular Environment. International Conference on Wireless Communications, Networking and Mobile Computing, WiCom 2007, Sep. 2007
- Sesia, S. and Toufik, I. and Baker, M.: LTE – The UMTS Long Term Evolution From Theory to Practice, 2nd Edition. ISBN: 9780470660256, John Wiley & Sons, 2011.
- Thiele, L. and Kurras, M. and Olbrich M. and Haustein, T.: Boosting 4G Networks with Spatial Interference Management Under Feedback Constraints – A Noncooperative Downlink Transmission Scheme, IEEE Vehicular Technology Magazine, vol.8, pp.40-48, Feb. 2013
- Van Rensburg, C.; Hosein, P.: Interference Coordination through Network-Synchronized Cyclic Beamforming. IEEE 70th Vehicular Technology Conference Fall, VTC 2009-Fall, Anchorage, Alaska, USA, Sep. 2009.
- Walke, B.: Mobile Radio Networks. ISBN: 978-0471499022, John Wiley & Sons, Nov. 2001.
- WiMAX Forum: Mobile WiMAX – Part I: A Technical Overview and Performance Evaluation. Section 4.2, Aug. 2006.
- WINNER II D 1.1.2: Part I channel models. WINNER II Channel Models, IST-4-027756 WINNER II, Deliverable, URL: <http://www.ist-winner.org/deliverables.html>, Feb. 2008
- WINNER II D4.7.2: Interference avoidance concepts. Deliverable, IST-4-027756, June 2007

- Wolz, B. and Muehleisen, M. and Klagges, K. and Einhaus, M.: Region Coordination Across Space Division Multiple Access Enhanced Base Stations in IEEE 802.16m Systems. Proceedings of IEEE Wireless Communications and Networking Conference Workshops, WCNCW 2010, Sydney, Australia, Apr. 2010.
- Wolz, B. and Muehleisen, M. and Klagges, K.: Coordination Across Base Stations for Effective Control of Space Division Multiple Access Enhanced IEEE 802.16m Systems. Proceedings of IEEE 20th International Symposium on Personal, Indoor and Mobile Radio Communications, PIMRC 2009, Tokyo, Japan, Sep. 2009.
- Xiang, Y. and Luo, J. and Hartmann, C.: Inter-cell Interference Mitigation through Flexible Resource Reuse in OFDMA based Communication Networks. Proceedings of European Wireless, EW 2007, Paris, France, Apr. 2007.



# Acknowledgement

---

This work has been elaborated during my time as research assistant at the Department of Communication Networks (ComNets) at RWTH Aachen University.

I particularly thank my advisor, Prof. Dr.-Ing. Bernhard Walke, for his support, detailed guidance, fruitful discussions, and experienced freedom in research. I am grateful to Prof. Dr.-Ing. Christian Wietfeld from the Institute of Communication Networks at Dortmund University of Technology for his support as second examiner.

Special thanks go to all members and great colleagues at the Department of Communication Networks for supporting this work and the inspiring work environment. For correcting this work special thanks to Michael Einhaus, Daniel Bültmann, Klaus Sambale, and friends. Many thanks go to all students that contributed to my research at ComNets, especially to, Benjamin Strang, Francesco Nino Alvarez, Afroditi Kyrilgitzi, Christoph Spiegolski, Izabella Gocza, Sebastian Albrink, Siying Wang, Haoqing Zhang.

I like to thank my friends and family for having them on my side. Special thanks go to my parents for their support. Finally, I like to thank Esther for her love, support and patience during the preparation of this thesis.

Aachen, February 2014

Benedikt Wolz